Characterization of Changes in the Kidney, Liver, and Adipose Tissue of RTSAKO Mice

by

Iman M'Hiri

A thesis
presented to the University of Waterloo
in fulfillment of the
thesis requirement for the degree of
Master of Science
in
Kinesiology

Waterloo, Ontario, Canada, 2018

Author's Declaration

This thesis consists of material all of which I authored or co-authored: see Statement of Contributions included in the thesis. This is a true copy of the thesis, including any required final revisions, as accepted by my examiners. I understand that my thesis may be made electronically available to the public.

Iman M'Hiri

Statement of Contributions

Parts of this thesis refer to published materials from the MSc thesis of Phillip Marvyn. I would like to acknowledge those who contributed to the research described in this dissertation:

- Phillip Marvyn
- Dr. Maria Fernanda Fernandes
- Daniel Scarr
- Dr. Robin E. Duncan
- Juan J. Aristizabal Henao
- Dr. Ken D. Stark
- Dr. Andre Marette

Abstract

Our laboratory has developed a novel genetic mouse model with kidney-specific lipid accumulation called *RTSAKOs*. The principle aim of my thesis was to study differences in the expression of genes and proteins related to fat and glucose metabolism in the kidneys, liver, and adipose of these mice before (9-12wks), during (16-18wks), and after (23-25wks) the onset of glucose intolerance, and compare their expression profiles to age-matched *control* littermates.

At 9-12 weeks of age, few significant differences in the expression of glucose and lipid regulators were evident in the kidneys or livers of *knockouts*. *RTSAKO* kidneys had significantly lower *Dgat1* expression, and the livers showed significantly lower *G6Pase*, *Hk2*, *Hk3*, and *Cd36* expression. Interestingly, all *RTSAKO* adipose depots studied at this time point had reduced expression of adipogenic marker gene expression, coupled with low lipolysis and lipogenesis gene expression, which indicates that preadipocyte differentiation was likely inhibited.

At 16-18 weeks, male *RTSAKO* mice had significantly more activated pro-lipolytic PHSL S660, and lower renal lipogenic gene expression, as observed by 35% lower *Fas* and *Lipin1* expression relative to *controls*. Furthermore, *RTSAKO* livers had significantly higher *Hk2* expression, as well as lower *Dgat1, Dgat2,* and *Fas* expression in *knockouts* relative to *controls*. Interestingly, adipose depots assessed at this time point showed no significant differences in lipid regulating gene expression in any of the four depots analyzed.

At age 23-25 weeks, *RTSAKO* mice had higher renal *Sglt2* gene expression relative to *control* littermates, and *knockout* livers had significantly higher *G6Pase* and significantly lower *Gck* gene expression in comparison to *controls*. Subcutaneous depots in the gluteal and gluteofemoral regions showed higher expression of *Fabp4* and *Pparγ*.

Expression comparisons between *knockouts* and *controls* will aid in the characterization of this mouse model and are important for understanding renal steatosis.

Acknowledgements

First and foremost, I would like to extend my sincerest appreciation to my supervisor, Dr. Robin Duncan for allowing me to contribute to such impactful work. Thank you for believing in my abilities and being a constant support throughout this process. You are truly a visionary, and it is an incredible privilege to have been under your tutelage. I am sincerely thankful for all your patience during these two years. Your feedback has helped improve my ability to communicate, think critically, and develop as a scientist. Finally, I would like to express my appreciation for all the positive energy and understanding you exude; Robin, you are as amazing a person as you are an academic.

I would also like to thank my lab members, both past and present, for their role in supporting this work and nurturing my development. Ryan Bradley, thank you for taking on the responsibility of training me and being patient through my incessant questioning. I wish you all the best in your post-doctoral endeavors. Dr. Maria Fernanda Fernandez, thank you for the support you provided during our work on this project. I appreciate the insight and encouragement you have given me, especially during difficult days.

To Ash Hashemi, Meghan Weins, Esther Lee, and our 499 students Kalsha, Michelle, Callum, Saloni, and Daniel: thank you for putting up with my outrageous stories and for being some of the most kind and supportive people I have ever met. Your companionship has been a highlight of this experience. I would like to extend a special thanks to Daniel Scar for aiding me in some of the characterization of the liver in this mouse model. Daniel LK, thank you for being a supportive companion throughout this journey. To Alaa, Amna, and Maha, thank you for being the most supportive roommates; I have life-long sisters in the three of you.

Juan Henao and Dr. Ken Stark, thank you for contributing your time, equipment, and expertise towards helping this project progress. Dr. Stark and Dr. Mourtzakis, thank you for taking the time to review and evaluate my thesis work. Your expertise and feedback are so appreciated.

I want to dedicate this thesis to my beautiful family. I want to thank my parents, Mourad and Lamia, for encouraging me to pursue my passion for science, and for always reminding me to approach every task with my 100%. Thank you for dedicating your lives for our betterment and being role models for myself and my brothers through your own academic achievements. To my brothers, Mohammed, Omar, and Ibrahim, I am so proud of your achievements, as I know you are proud of mine. Finally, I want to thank my fiancé Abdurrahman Muni for being my constant throughout this process. I could not have asked for a more supportive and nurturing companion.

Table of Contents

List of Figures and Tables

Figures:

Tables:

List of Abbreviations

18S: 18S Ribosomal Subunit
ACC: Acetyl-CoA Carboxylase
AcCoA: Acetyl-CoA
AGK: Acylglycerol Kinase
AGPAT: 1-Acylglycerol-3-Phosphate-O-Acyltransferase
AMPK: Adenosine Monophosphate-Activated Protein Kinase
ATGL: Adipose-Triglyceride Lipase
ATX: Autotaxin
BACTIN: β-actin
BAT: Brown Adipose Tissue
BSA: Bovine Serum Albumin
C/EBP: Ccaat/Enhancer-Binding Proteins (variants α, β, γ)
cAMP: Cyclic Adenosine Monophosphate
CD36: Cluster of Differentition 36/ Fatty Acid Translocase
CDS: Coding Region
CDS1: Phosphatidate cytidylyltransferase 1
CKD: Chronic Kidney Disease
CoA: Coenzyme A
DAG: Diacylglycerol
DGAT: Diacyglycerol Acyltransferase (variants Dgat1 and Dgat2)
DGK: Diacylglycerol Kinase (variants α, β, γ, θ, ε)
DKD: Diabetic Kidney Disease
DM: Diabetes Mellitus
DN: Diabetic Nephropathy
Ewat: Epididymal white adipose tissue
F6P: Fructose-6-Phosphate
FABP4: Fatty Acid Binding Protein 4
FATX: Adipose Specific Autotaxin
FAS: Fatty Acid Synthase
G3P: Glycerol-3-Phosphate
G6P: Glucose-6-Phosphate
G6Pase/G6PC: Glucose-6-Phosphatase
GAPDH: Glyceraldehyde phosphodehydrogenase
GCK: Glucokinase (also known as HK4)
GLUT: Glucose Transporter (GLUT1, GLUT2, GLUT4)
GPAT: Glycerophosphate Acyltransferase
GPDH: Glycerol-3-Phosphate Dehydrogenase
HK: Hexokinase (variants HK1, HK2, HK3, HK4)
HSL: Hormone-Sensitive Lipase
IGF: Insulin Growth Factor
IRS: Insulin Receptor Substrate
Iwat: Inguinal white adipose tissue
KI67: KI67 or MKI67 Cellular Proliferation Protein

Ksp-cadherin: Kidney-specific promoter
LPA: Lysophosphatidic Acid
LPAAT: Lysophosphatidic Acid Acyltransferase
LPC: Lysophosphatidylcholine
MAG: Monoacylglyceride
MAPK: Mitogen-Activated Protein Kinase
MCoA: Malonyl CoA
MGK: Monoacylglycerol Kinase
MGL: Monoglycerol Lipase
MPGN: Membranoproliferative Glomerulonephritis
NAFLD: Non-Alcoholic Fatty Liver Disease
NCBI: National Center for Biotechnology Information
NEFAs: Non-Esterified Fatty Acids
PA: Phosphatidic Acid
PAP/LIPIN: Lipin (also known as Phosphatidic Acid Phosphohydrolase)
PC: Phosphatidylcholine
PCNA: Proliferating Cell Nuclear Antigen
PHSL: Phosphorylated Hormone Sensitive Lipase (at serine residues S563, S565, S660)
PKA: Protein Kinase A
PLA1: Phospholipase A1 (Sn-1 Specific)
PLA2: Phospholipase A2 (Sn-2 Specific)
PLIN: Perilipin
PPARγ: Peroxisome Proliferator-Activated Receptor Gamma
PREF1: Preadipocyte Factor 1
Pwat: Perirenal white adipose tissue
QPCR: Quantitative Polymerase Chain Reaction
RTSAKO: Renal-Tubule Specific *ATGL* Knockout
Rwat: Retroperitoneal white adipose tissue
SGLT: Sodium-Glucose Co-Transporter (variants SGLT1 and SGLT2)
SREBP: Sterol Response Element-Binding Protein
STAT: Single Transducers and Activators Of Transcription
Subc: Subcutaneous gluteal-femoral white adipose tisse
T2DM: Type II Diabetes Mellitus
TAE: Tris-acetate-EDTA
TAG: Triacylglycerol
TLC: Thin Layer Chromatography
WAT: White Adipose Tissue

Chapter 1: Introduction

Chronic Kidney Disease (CKD) is a global epidemic and rates increase in close parallel with the aging population [1]. Senescence is strongly correlated with kidney disease, with diagnostic rates of 25% in those aged 65-74 years and 50% in people over the age of 75yrs [1]. Aging kidneys are susceptible to damage from various risk factors, chiefly chronic hyperglycemia and obesity, the rates of which continue to climb [2]. CKD is often comorbid with other age-related metabolic syndromes, most notably Type II Diabetes Mellitus (T2DM) [1,2]. Diabetes is also a progressive disease that is closely correlated with aging and obesity [1]. Elderly patients who have prolonged exposure to hyperglycemia are at an increased risk of developing CKD secondary to their diabetes, a complication described extensively in the literature as diabetic kidney disease (DKD) or diabetic nephropathy (DN)[1,3,4]. Diabetics are an overwhelmingly at-risk population for kidney damage, with about 40% of new cases of CKD stemming from diabetes [5]. In a reciprocal nature, however, kidney damage has been implicated in new-onset T2DM [6–8]. The mechanisms that mediate this bidirectional relationship are poorly understood (Figure 1).

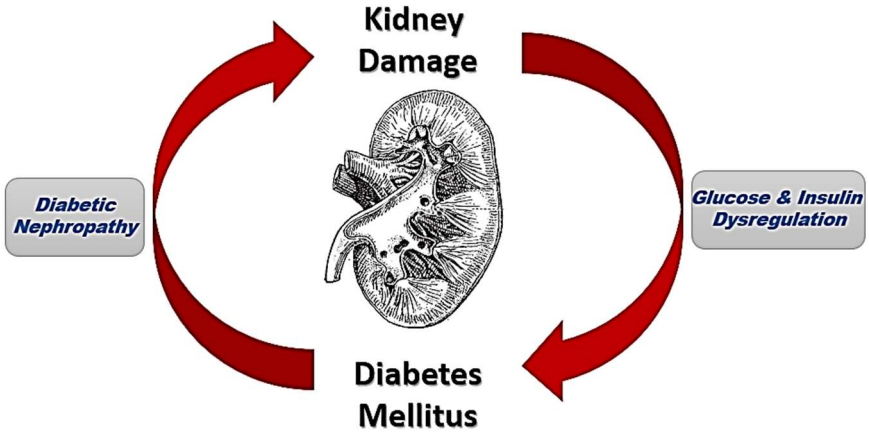

Figure 1: The reciprocal relationship between renal disease and glucose metabolic dysregulation.

Renal disease of any etiology often leads to insulin resistance, which is nearly universal in CKD [9], as well as glucose intolerance, suggesting that renal dysfunction plays a role in insulin action and glucose regulation [9–12]. This appears to occur both as a direct effect of changes in kidney metabolism of glucose and insulin, and through cross-talk between the kidneys and other

metabolic tissues, including the liver, adipose tissue, pancreas, and skeletal muscle [9]. The manner through which this occurs is not entirely understood. However, the kidneys are known to influence systemic glucose regulation through a variety of mechanisms [9–12]. For example, the kidneys play a significant role in the regulation of circulating insulin levels by filtration through the glomerulus and into the proximal tubules where insulin is subsequently degraded [9]. Therefore, patients with kidney damage may have impaired ability to dispose of insulin, contributing to irregular insulin signaling, secretion, and degradation. Furthermore, the kidneys are a major contributor to systemic glucose regulation [9–12]. Urinary excretion of glucose helps to reduce blood levels during hyperglycemia, and the recent development of inhibitors that prevent glucose reuptake by sodium-glucose cotransporter 2 (SGLT2) from filtrate has led to new pharmacological strategies for diabetes [12]. The kidneys also perform gluconeogenesis, the process by which non-carbohydrate substrates like glycerol and amino acids are converted into glucose [9–12]. It was previously believed that the liver was the sole organ capable of undertaking this task, but recent studies show that the kidneys may contribute anywhere from 5- 40%[10] of total systemic glucose, whereas some papers suggest they can release glucose at a rate equal to the liver, by mass[9,10,13].

With advances in treatments for various metabolic disorders, lifespans have become longer despite increasing rates of obesity and metabolic syndromes[14,15]. As a result, the population of elderly suffering from metabolic impairments is increasing, globally expanding the cohort of people who are at a high-risk of developing kidney disease, and by extension diabetes[1,14,15]. Globally, more than half a billion people are at risk of developing diabetes secondary to kidney disease. In Canada, 1 in 10 individuals are at risk of, or have, chronic kidney disease, and the number of people requiring treatment for CKD has more than tripled in the past 20 yrs[5]. Although diabetes management options are available, the only treatments for kidney damage are dialysis or renal transplant[5]. Dialysis is expensive, at up to $107, 000 per patient annually, creating a considerable financial burden on the health care system[5]. About 75% of CKD patients await kidney transplantation, with 1/3 of these patients not surviving the wait for a healthy kidney[5]. Elderly individuals suffering from kidney disease have the worst prognosis, with the highest mortality rates in comparison to other groups[14]. These mortality rates double when kidney disease coincides with diabetes, a comorbidity that is common[14]. Therefore, understanding the damaging cycle between renal dysfunction and impaired glucose regulation,

with the goal of correcting both, is incredibly important. Strategies to disrupt this vicious cycle would reduce the strain on the healthcare system, and significantly improve the quality of life for millions of at-risk individuals worldwide.

Renal lipid retention is a hallmark of damaged kidneys, and is also present in the kidneys of patients with diabetes[16–18], and in the kidneys of older adults[19]. This suggests that renal steatosis may play a role in the pathological development of both kidney disease and diabetes[7,8,14,20–23]. Previous studies have investigated renal steatosis using murine overfeeding or aging rodent models[20,21,24]. However, it is not possible to distinguish the direct effects of renal steatosis on glucose regulation from systemic influences confounded by other obesity/age-associated diseases and risk factors[1,20–22,24–26]. Therefore, a more targeted model is required to isolate the direct effect of renal steatosis on diabetes.

Attaining renal steatosis without the accumulation of lipids or damage in other organs was made possible by kidney-specific gene targeting[27]. Total gene *knockout* of *Adipose triglyceride lipase* (*Atgl*), the rate limiting enzyme in the breakdown of triacylglycerol (TAG), has been shown to cause excess lipid accumulation in virtually all tissues[28]. Our laboratory therefore developed a kidney-specific model of *Atgl* gene ablation. Initial investigation of kidney ATGL by immunohistology indicated an enrichment in renal-tubules, specifically at the apical membrane, where albumin complexed to non-esterified fatty acids (NEFAs) is reabsorbed from the urinary filtrate[29]. Our kidney-specific *Atgl knockout* was therefore developed using Cre-recombinase that restricts gene ablation primarily to the renal-tubules, and does not affect glomeruli or podocytes [27]. This model is thus referred to as Renal-Tubule Specific *Atgl-Knockout* (*RTSAKO*).

The contents of this dissertation describe the initial characterization of the expression of genes involved in lipid and glucose metabolism in kidneys, liver, and adipose tissue from *RTSAKO* mice. All assessments were completed in male *RTSAKO* mice in three age cohorts, 9-12wks old, 16-18wks old, and 23-25wks old. All analyses in *RTSAKO* mice were made by comparison to age-matched littermate *controls*. The study of females in this strain of mice are of interest, but falls outside the scope of this thesis and will be completed by others.

Chapter 2: The *RTSAKO* Mouse Model

2.1 Overview

Lipids are important in the maintenance of cell metabolism and energy. In times of energy surplus, excess glucose is converted into glucose-6-phosphate (G6P), followed by acetyl-CoA, then shunted into *de novo* lipogenesis to produce increases in TAG by esterification of three consecutive fatty acids onto a glycerol backbone[30]. The TAG is then stored for future use in the cytoplasm of the cell in the form of a lipid droplet. These lipid droplets are dynamic, and fatty acids can be cleaved from the glycerol backbone and released as NEFAs for mobilization and energy use[29–31]. The liberation of these NEFAs occurs through the action of droplet-associated lipases that breakdown TAG. These enzymes, ATGL and hormone sensitive lipase (HSL), act on the glycerol backbone to liberate NEFAs for energy use, especially in a fasted state[29–31].

Adipose tissue is unique in that adipocytes are the major cell type and have the capacity to store substantial amounts of excess fat in the form of lipid droplets. In contrast, non-adipose tissues, like the liver and kidney, are primarily comprised of parenchymal and stromal cells that carry out specific functions and have limited space and resources for lipid storage[30,32]. Therefore, an excess of fat in these tissues can cause damage and interfere with primary functions. Cellular dysfunction and death resulting from excessive lipid accumulation is termed lipotoxicity[18,30,32].

A pathological role for hyperglycemia in kidney disease is well-established, and even has its own name (*i.e.* diabetic nephropathy)[4,16]. Because of this common association, studies on kidney disease in the absence of diabetes as a co-morbidity are rare, and it is only recently that kidney disease has become recognized as an independent risk factor for diabetes[7,8,33]. The mechanism(s) responsible for this association are poorly understood. Rudolf Virchow first suggested an association between renal lipid accumulation and kidney disease 150 years ago[34]. Kidney lipid overstorage is associated with kidney dysfunction in a variety of models of renal and metabolic disease, including diabetic nephropathy, obesity, chronic kidney disease, and cases of acute renal injury[16,18,35–38]. The presence of lipid retention as a common element in a range of conditions characterized by kidney dysfunction, including diabetes, suggests they are causally related[16,18,35–38].

2.2 The Development of the RTSAKO Model

The study of the direct effect of renal steatosis on glucose metabolism was made possible by the development of a kidney-specific *knockout* model with impaired lipid breakdown (lipolysis). The enzyme targeted for *knockout* was *Atgl*, the rate-limiting enzyme in the breakdown of TAG. The study of renal ATGL indicated highest expression in the renal-tubules[29]. Therefore, the attenuation of this enzyme in the renal-tubules was expected to induce TAG accumulation and allow for the direct study of the impact on system-wide metabolism. Mice transgenic for *Cre*-recombinase under control of the Ksp16-promoter were mated with mice that had the entire 1st exon of *Atgl* flanked by LoxP sites (Figure 2). The presence of LoxP sites, notably, does not disrupt normal function and expression of the *Atgl* gene[39–41]. The 1st exon of *Atgl* contains the coding sequence for the active site serine/aspartate catalytic dyad, and so, Cre-mediated recombination across this exon would result in the excision and joining of the two LoxP sites. Therefore, mating between mice homozygous for floxed *Atgl*, but lacking the *Cre*-transgene, with mice homozygous with floxed *Atgl* and heterozygous for kidney-specific Ksp16-Cre-recombinase, would result in 50% offspring lacking renal-tubule *Atgl* (*RTSAKO*), and 50% unaltered *control* mice that are indistinguishable from *wildtype* (with floxed *Atgl*, but no gene deletion) (Figure 3). Both strains of mice were extensively (>10 generations) backcrossed onto a C57Bl/6J background, and therefore are essentially congenic with this strain. All analyses of *RTSAKO* mice conducted are relative to littermate *controls*.

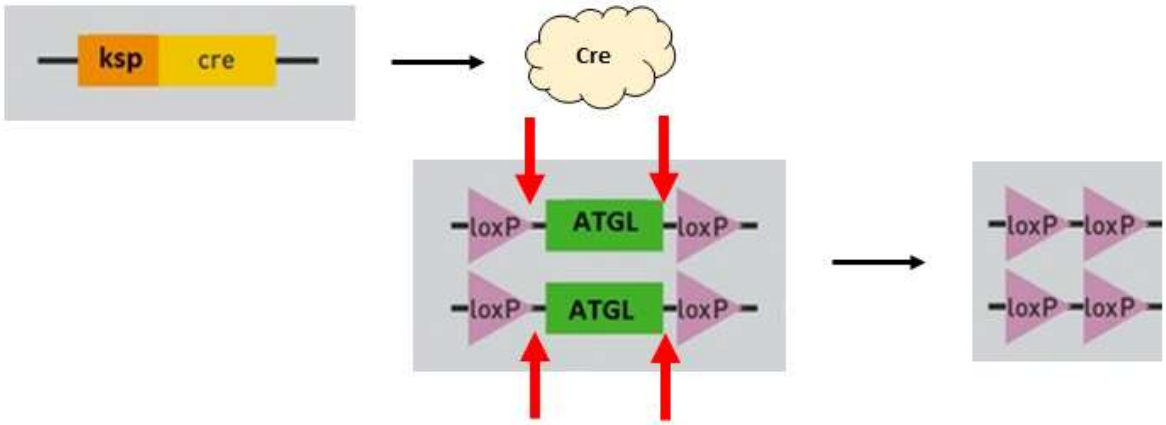

Figure 2: Cre-Recombinase Deletion of Kidney Atgl using the Cre-LoxP system.

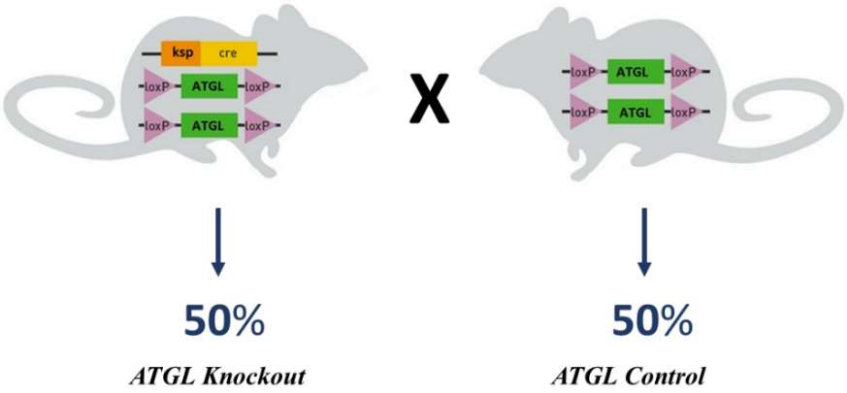

Figure 3: Breeding mice results in either RTSAKO mice or unaltered ATGL-control littermates.

2.3 Atgl Gene Ablation Results in Renal Steatosis in RTSAKO mice

Lipolysis begins at the lipid droplet, where TAG is broken down by ATGL in the first, and rate-limiting, step. ATGL preferentially cleaves the fatty acyl chain from the glycerol backbone of TAG at the *sn-2* position, producing 1,3-diacylglycerol (DAG)[42–45]. The next enzyme in the lipolytic pathway, HSL, localizes to the lipid droplet upon phosphorylation by protein kinases at three serine residues (S563, S565, and S660)[42–45]. Once activated, phospho-HSL (PHSL) sequentially cleaves the next fatty acyl chain at either the *sn-1* or *sn-3* position of DAG to make monoacylglycerol (MAG) (Figure 4) [42–45]. Monoglyceride lipase (MGL) follows to liberate the glycerol and last fatty acyl chain in the final step of lipolysis.

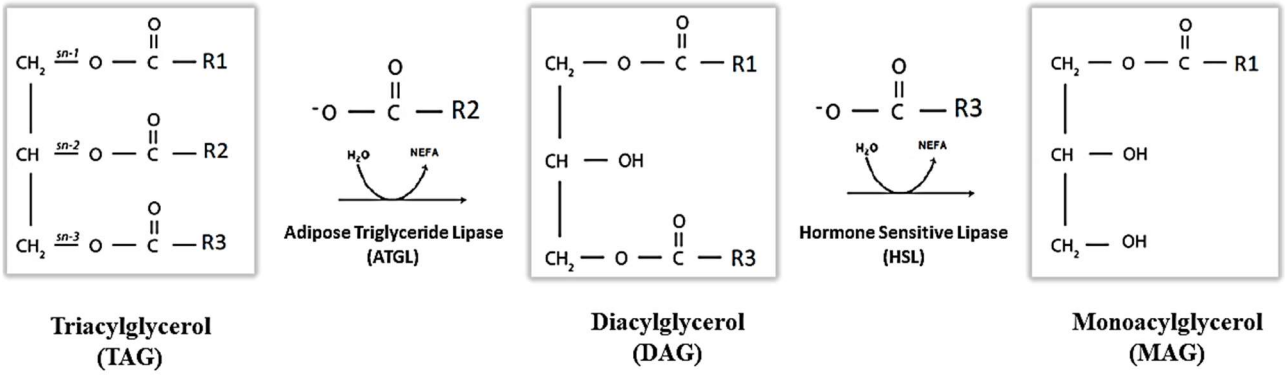

Figure 4: Triacylglycerol hydrolysis and release of NEFAs during lipolysis by ATGL and HSL

Atgl gene ablation in renal-tubules of the *RTSAKO* mice is a suitable model to study the broad effects of renal steatosis. Prior work in our laboratory has indicated that this approach successfully increased the triacylglycerol content of the kidney by ~2-fold, which is similar to

that seen in obese individuals[35,46]. This model therefore recapitulates a physiologically relevant level of kidney lipid overstorage. In contrast, *Atgl* total-*knockout* mice show a >15-fold increase in renal TAG, which is supraphysiologic[28].

2.4 The RTSAKO Phenotype – Prior Findings by the Duncan Lab

This mouse model was designed to test whether the ectopic accumulation of TAG in renal-tubule cells affects blood glucose *control*. Prior findings by the Duncan Lab have already established that *RTSAKO* males present with early-onset glucose intolerance by 16 weeks of age (the equivalent to late twenties in human years). At this time-point, the new-onset of dysglycemia in male *RTSAKO*s is coupled with significantly lower basal insulin and elevations in the bioactive lipid signaling molecule, Lysophosphatidic Acid (LPA).

Insulin is an important regulatory hormone that is responsible for the maintenance of carbohydrate, lipid, and protein energy homeostasis[47]. Insulin stimulates gluconeogenesis in the liver, increases the translocation of GLUT4 in the muscles and adipose tissue for glucose disposal, inhibits lipolysis in adipose tissue, and upregulates energy storage processes like glycogenesis and lipogenesis in the fed state to allow tissues to store incoming nutrients[11,47–49]. As a result, maintenance of insulin levels within a physiologic range is integral for health, and an offset can prove pathological. Furthermore, LPA is a small, ubiquitous, bioactive lysophospholipid known to regulate many physiological processes [50,51]. The action of LPA has gained substantial attention recently because of its role as a potent lipid signaling molecule and the complexity of its signaling and expression in all species and tissues[50–54]. Elevated blood and urine LPA have been found to be associated with obesity and obesity-related metabolic pathologies, and fibrosis [50,51,55–60]. LPA is predominantly produced by adipose tissue, and the mediator responsible for increased production in this model was unknown.

Chapter 3: Biochemical Foundations

3.1 Overview

Nutrient homeostasis is comprised of a complicated network of regulatory pathways that involve constant communication between various metabolic tissues (Figure 5). The organs most often considered in the discussion of glucose homeostasis regulation are the pancreas, liver, adipose tissue, and skeletal muscle. More recently, however, the significant regulatory role of the kidneys has been appreciated[61]. The disruption of renal nutrient metabolism by steatosis may affect the function of other metabolic tissues engaged in whole-body nutrient regulation through renal-organ crosstalk, since the kidney is both a source and a sink for glucose and fatty acids[16].

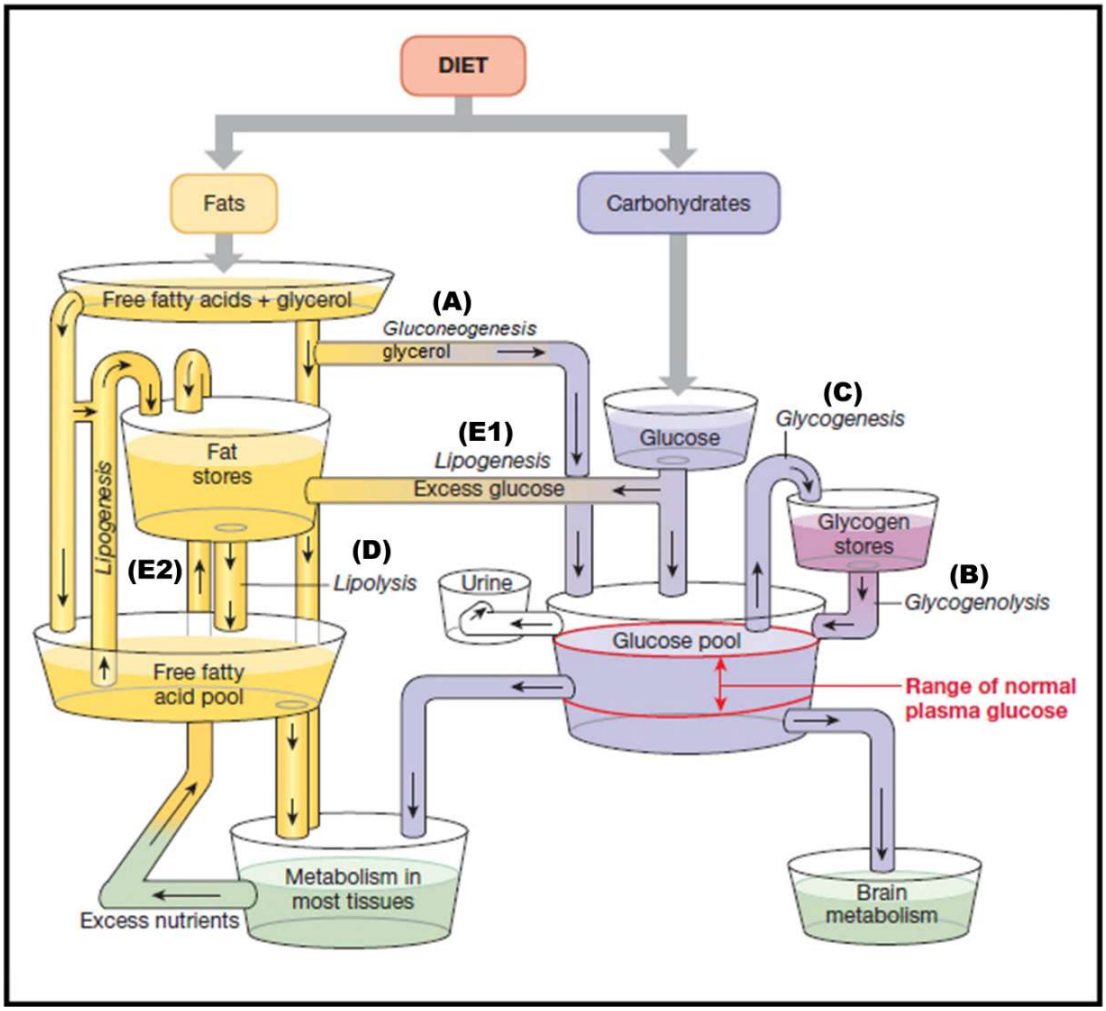

Figure 5: Nutrient Homeostasis Involves a Balance Between Various Processes. Carbohydrate metabolism is regulated by (A) Gluconeogenesis, (B) Glycogenolysis, (C) Glycogenesis, and Glycolysis. Lipid Metabolism is Regulated by (D) Lipolysis and (E1 and 2) Lipogenesis. (Adapted from Silverthorne 2014)[62]

3.2 Glucose Regulation in Kidney, Liver, Adipose Tissue, and Skeletal Muscle

During times of energy deprivation, the liver is the major source of glucose for the body, supplying ~75% of blood glucose from the breakdown of glycogen stores and from gluconeogenesis[62]. In addition, studies have shown that the kidneys contribute about 25% of total systemic glucose, and can produce glucose at a rate comparable to the liver (although the lower relative mass of the kidneys results in a lower overall contribution to blood glucose)[9,10]. Both organs carry a profile of gluconeogenic and glycolytic enzymes, which allow them to both synthesize and utilize glucose, contributing to net blood glucose appearance and disappearance[13]. In contrast, the adipose tissue and skeletal muscle are glucose utilizers and are unable to liberate glucose for systemic use once absorbed[62].

Glucose homeostasis is a delicate balance of glucose production (glycogenolysis and gluconeogenesis) and glucose utilization for energy or storage (glycolysis and glycogenesis respectively) (Figure 5-7). Glycogenolysis liberates glucose from glycogen stores, while gluconeogenesis (Figure 5A, 6) is the process through which non-carbohydrate substrates like glycerol and amino acids are used to synthesize glucose *de novo*[62]. Both processes contribute to systemic glucose during a state of hypoglycemia in an attempt to increase available circulating glucose, however, in a pathological state these processes may act contribute to overall hyperglycemia[13,61,63]. Both the kidney and liver can produce and liberate glucose to systemic circulation by different means, but the main enzyme that confers this ability is Glucose-6-Phosphatase (G6Pase or G6PC) which catalyzes the final step in glucose liberation, the dephosphorylation of G6P into free glucose[64]. Both the kidney and liver undergo gluconeogenesis, but only the liver can produce glucose through glycogenolysis[62,64]. This is because the liver has significant glycogen stores, whereas the kidney does not efficiently synthesize glycogen[65]. However, the kidney possesses an alternative secondary process that contributes to systemic glucose, through the complete reuptake of glucose from filtrate and return to circulation. This reuptake occurs through active transport using Sodium-Glucose Cotransporters (SGLT1 and SGLT2) on the apical surface of the proximal tubule cell. SGLTs mediate glucose removal from filtrate into the tubule cell, followed by reintroduction into circulation by simple diffusion through basolateral GLUT1 and GLUT2 transporters[63,65]. Therefore gluconeogenesis, alongside complete glucose reabsorption through SGLTs, are unique to the kidneys. In contrast, gluconeogenesis and glycogenolysis predominate in the liver.

Together these processes characterize the systemic contributions of renal and hepatic glucose production.

Renal and hepatic glucose production is chiefly dependent on the synthesis and liberation of free glucose by G6Pase. Studies have shown that G6Pase is consistently overactive in the kidneys of diabetic animals, contributing to the hyperglycemic state[10], and that increases in G6Pase activity in kidney are of a similar magnitude to liver[10,66]. Insulin inhibits renal and hepatic glucose production, in part, by suppressing the regulation and activity of G6Pase[10,64,66]. In insulin resistance, impaired downregulation of hepatic G6Pase contributes to hyperglycemia. Recent insulin infusion studies in patients with T2DM have revealed that renal glucose release also remains high, indicating that kidney G6Pase regulation is also attenuated in the presence of insulin resistance, and may contribute to associated hyperglycemia[10,13,67]. Therefore, *G6Pase* expression is directly associated with circulating insulin and is an important mediator in glucose homeostasis. In contrast, glucose reuptake by SGLTs is not insulin-dependent, but rather is regulated by hyperglycemia[63]. In the event of excess glucose in filtrate, as is the case in diabetic patients, SGLTs become completely saturated and high levels of glucose remain in the filtrate. To compensate, SGLT expression and translocation to the apical cell surface is upregulated in response to glucosuria, thereby increasing glucose reuptake, which further exacerbates the hyperglycemic state[63].

The converse of glucose release is glucose disposal, which is primarily carried out by glycogenesis and glycolysis (Figure 5C, 6, 7). Glycogenesis is the process through which glucose is stored for future use by linking glucose monomers into a long complex-carbohydrate chain called glycogen, which is predominantly stored in the liver and skeletal muscle[62]. Glycolysis, on the other hand, is the first step in the breakdown of glucose for the generation of energy and is utilized ubiquitously in all cells[68]. Glucose can only enter glycogenesis or glycolysis through phosphorylation into G6P, which is the primary intermediate in both processes. Glucose phosphorylation is catalyzed by a family of enzymes called hexokinases[62]. There are four hexokinase isoforms[68]. The first three have high affinity for glucose, and are allosterically inhibited by their major product, G6P[68–71]. Hexokinase I (HK1) is a ubiquitously expressed enzyme and is unaffected by hormone signaling or shifts in metabolism[68–71]. Hexokinase II (HK2) is chiefly expressed in metabolic tissues like the kidney, liver, heart, and muscle, but is also upregulated in some cancers and has been found to be sensitive to insulin

signaling[68–71]. Little is known about Hexokinase III (HK3). Hexokinase IV, otherwise known as Glucokinase (GCK), is a special isoform that exclusively phosphorylates glucose, and is not allosterically inhibited by G6P[68–72]. GCK is expressed predominantly in the liver, but is also found at much lower levels in the kidneys and pancreas[72]. GCK is active when glucose levels are high, and so it serves as a sensor, driving glucose trapping into hepatocytes from circulation to be used in glycogenesis and glycolysis[72] (Figure 6-7). Glycogenesis is the primary driving force for glucose disposal in the liver, however in the kidneys rates are much lower since renal cells have very limited glycogenic ability. Instead, the kidneys dispose of glucose through energy utilization. This is especially true in the renal medulla, which has high energy demand in comparison to the gluconeogenic renal cortex[12].

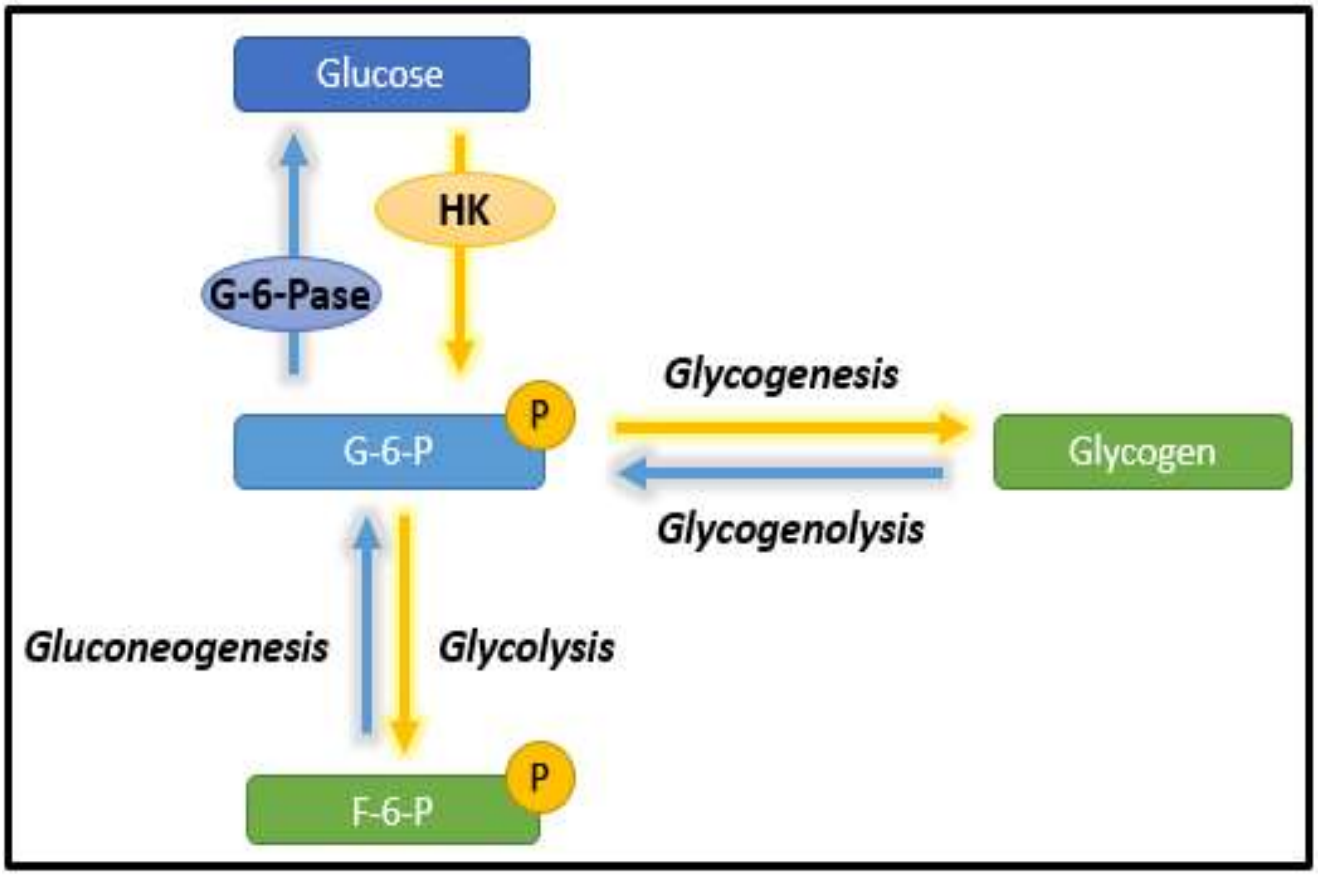

Figure 6: Glucose homeostasis is regulated by an equilibrium between glucose production and glucose disposal, contributing to net glucose movement.

Attenuated circulating insulin causes decreased glucose disposal at the level of the liver, kidney, adipose tissue, and skeletal muscle through direct and indirect action[62]. Insulin does not

directly stimulate glucose release and disposal in the liver, which utilizes facilitated diffusion of glucose through GLUT2 transporters[47]. Instead, insulin signaling regulates intracellular glucose stores in hepatocytes by upregulating enzymes used in glycogenesis (GCK) and downregulating those used in gluconeogenesis and glycogenolysis (G6Pase) [47,63,66,73]. As a result of low insulin, glucose releasing activity outweighs those mediating glucose disposal, increasing intracellular levels of liberated glucose in hepatocytes, and driving net movement of glucose into circulation through facilitated diffusion[47,63]. In a state of dysglycemia, as presented in *RTSAKOs*, such action would contribute to hyperglycemia (Figure 6-7). Similarly, insulin indirectly regulates glucose release in the kidneys by inhibiting the expression of gluconeogenic enzymes, like G6Pase[13,47]. However, in a low-insulin or insulin resistant diabetic state, gluconeogenic enzymes are not attenuated, glucose synthesis and release into circulation is continuous, and would advance the hyperglycemic state[61,67,73].

In contrast to the liver and kidney, insulin does directly regulate glucose disposal in adipose tissue and skeletal muscle[47]. Insulin binding to the adipocyte or myocyte cell surface triggers a signal cascade that results in the translocation of GLUT4 transporters from internal vesicles to the surface of the cell membrane, allowing glucose disposal into the cell through facilitated diffusion[47,74,75]. Decreased insulin causes mitigated GLUT4 translocation, inhibiting the ability of adipocytes or myocytes to internalize circulating glucose (Figure 7).

LPA can also have an effect on the regulation of glucose metabolism, although this likely occurs indirectly. A novel study by Rancoule and colleagues[76] observed that mice injected with LPA showed impaired glucose metabolism, primarily through attenuated glucose-stimulated insulin secretion at pancreatic beta-islets. In addition, a single study by Yea and colleagues suggests that LPA increases GLUT4 translocation in adipocytes in a dose dependent manner, but this finding is not conclusive[77].

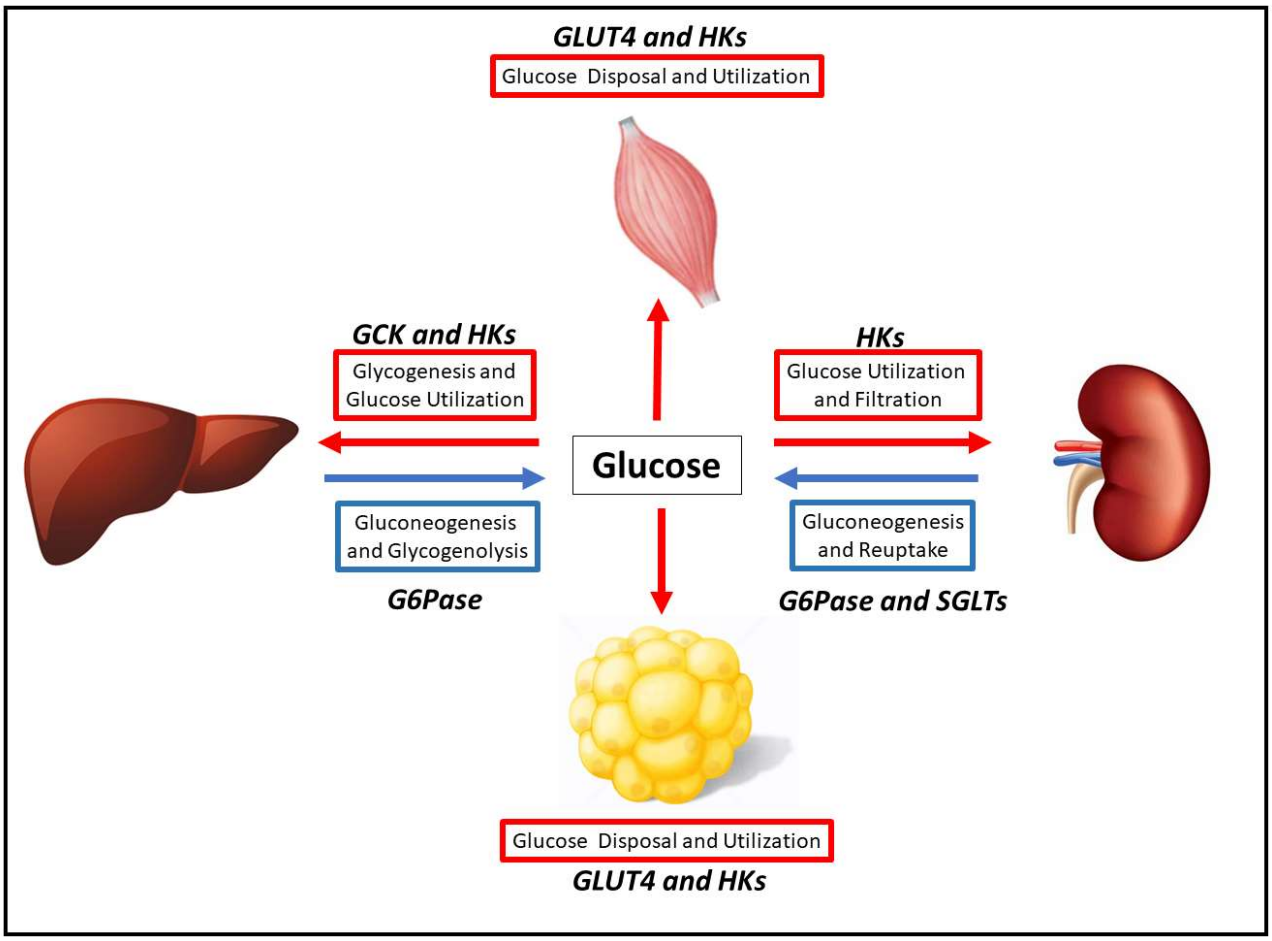

Figure 7: Glucose homeostasis consists of a balance between glucose production and glucose disposal mainly mediated through regulation at the level of the kidney, liver, adipose tissue, and skeletal muscle. Central glucose represents systemic circulating glucose levels.

3.3 Lipolysis and Lipogenesis in Kidney, Liver, and Adipose Tissue

Lipolysis and lipogenesis exist as a "see-saw" of regulatory homeostasis in a healthy state, where alterations in one usually leads to the opposite response in the other (Figure 5D/E). In the fed state, lipolysis is attenuated, and lipogenesis is upregulated to promote energy storage. In the fasted state, lipolysis is upregulated to liberate NEFAs for energy use and lipogenesis is attenuated[18]. Adipose tissue is the predominant site for lipid storage and release, however, the liver and kidneys also play a role in lipid homeostasis. The liver and adipose tissue are both key regulators of blood NEFAs and TAG levels, which involves the regulation of lipolysis and lipogenesis[78]. The general model of lipolysis, and the key enzymes involved (ATGL and HSL), were described prior (section 2.3) and apply to the kidneys, liver, and adipose tissue. The following section deals with lipid synthesis in these organs.

De novo lipogenesis is the process whereby fatty acids are produced from non-lipid substrates (*i.e.* excess glucose and amino acids like glutamine). The process of fatty acid synthesis begins with the generation of citrate in the mitochondria that is exported and converted into acetyl-CoA[79]. Acetyl-CoA is then carboxylated by Acetyl Co-A Carboxylase (ACC) to form malonyl-CoA in an irreversible reaction that commits the acetyl group to fatty acid synthesis (Figure 8). Fatty Acid Synthase (FAS) is a complex enzyme that elongates fatty acid chains by acyl (two carbon unit) additions[79]. The final product is a long chain fatty acyl-CoA that can be utilized in triglyceride synthesis[62]. Both endogenously synthesized fatty acyl-CoAs, and diet-derived fatty acyl-CoAs, can enter cells through integral membrane proteins called fatty acid translocases (CD36), and join complex lipid biosynthesis to acylate a glycerol backbone and produce a final TAG product[75]. This is done through the Kennedy pathway for glycerolipid synthesis, which was initially described in 1956 by Eugene Kennedy[80].

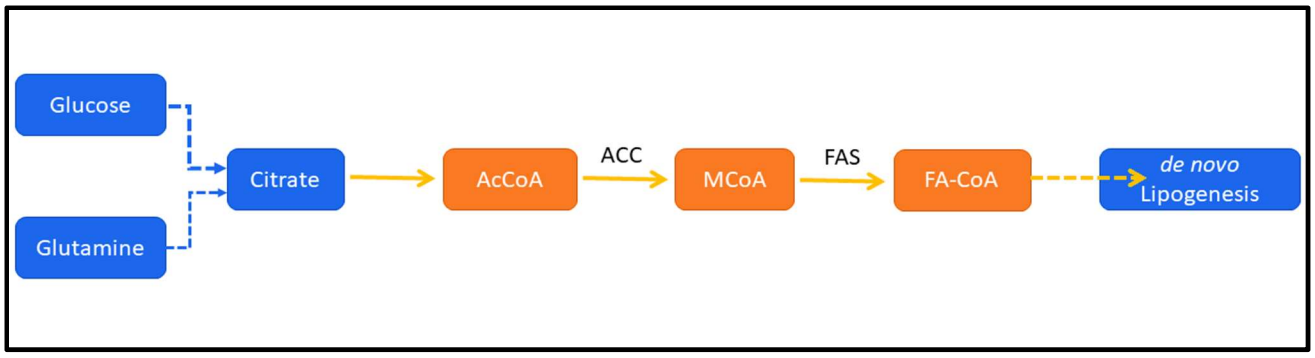

Figure 8: Simplified Fatty Acid Synthesis

The Kennedy pathway begins with the glycolysis intermediate, glycerol-3-phosphate (G3P). In the initial step, G3P is acylated using acyl-coenzyme A (CoA) at the *sn-1* position of the glycerol backbone. This acylation step is catalyzed by a family of glycerophosphate acyltransferase (GPATs), and results in the production of 1-acylglycerol-3-phosphate, which is also known as 1-acyl-lysophosphatidic acid (or 1-acyl-LPA)[80–83]. Next, LPA is further acylated at the *sn*-2 position forming phosphatidic acid (PA) by a group of enzymes belonging to the acylglycerol-3-phosphate-O-acyltrasnferase (AGPAT) family, also known as lysophosphatidic acid acyltransferases (LPAATs)[83]. Phosphatidic acid is a precursor for generating DAG by dephosphorylation at the *sn-3* position by a phosphatidic acid phosphatase (PAP/LIPIN), forming 1,2-diacylglycerol[81,82]. The enzyme phosphatidate cytidylyltransferase 1 (CDS1) also aids in lipid processing at this step. To complete the triglyceride synthesis pathway, a fatty acyl-CoA is

transferred to the *sn-3* position of DAG by a diacylglycerol acyltransferase (DGAT) enzyme to form the final TAG product for storage (Figure 9)[84].

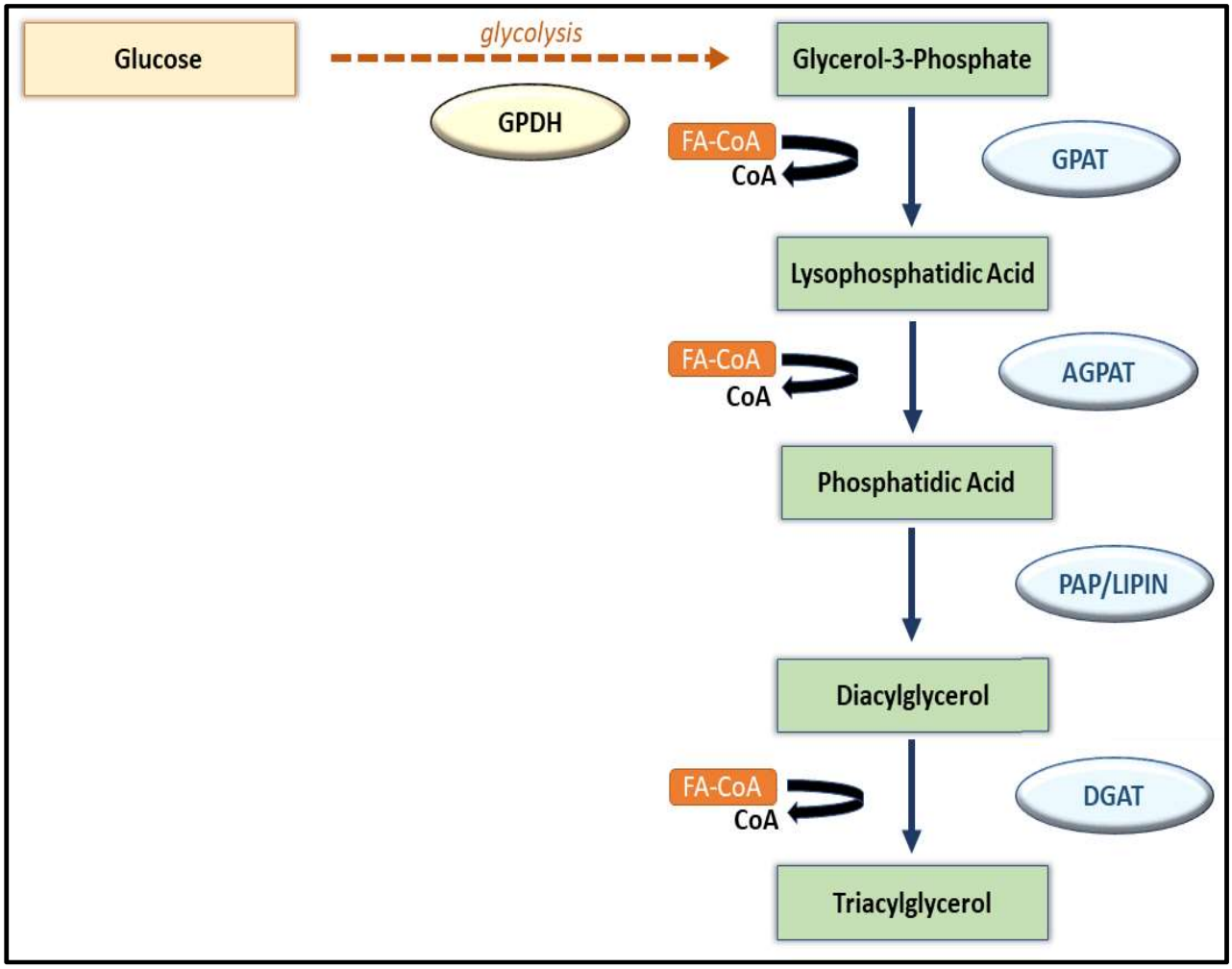

Figure 9: The Kennedy pathway for the de novo synthesis of triacylglycerol

Both the kidney and the liver are sites of *de novo* lipogenesis and complex glycerolipid synthesis. Accelerated lipogenesis is associated with obesity and renal damage[18,20,30]. TAG formed in the liver can be packaged into lipoproteins and secreted to the circulation for uptake by adipose and other tissues[85]. Although there is mounting evidence that the kidneys may play a role in the catabolism, reuptake, and recirculation of some serum-derived lipoproteins during urinary filtration (notably lipoprotein (a)), they do not synthesize ApoB, and therefore do not secrete TAG-rich lipoprotein[86]. Lipolysis of renal TAG can, however, generate NEFAs that will diffuse into the circulation. Serum NEFAs bound to albumin are readily reabsorbed from the urinary

filtrate and transferred back to the blood by renal-tubule cells during filtration[18]. NEFAs in high concentrations can have a disruptive 'detergent-like' effect on membranes that can kill cells, therefore most cells, including renal-tubule cells, actively esterify incoming fatty acids to form inert TAG, which is rapidly mobilized again as needed[19,32]. Both processes of lipolysis and TAG synthesis are therefore typically active at most times in cells, but the net effect (i.e. greater net release of NEFAs, or greater net storage of TAG) depends on the relative balance of activities.

Insulin plays an integral role in the regulation of lipid metabolism by mediating pro-lipogenic and anti-lipolytic effects. Insulin acts on the kidney, liver, and adipose tissue to promote lipid synthesis and fatty acid uptake. Insulin acts by upregulating lipid synthesis enzymes like sterol-regulatory-binding proteins (SREBPs), which are important in NEFA and cholesterol synthesis and regulate expression of ACC and FAS[87]. As a result, insulin promotes NEFA synthesis by stimulating ACC and FAS activity[47]. The abundance of available NEFAs drives forward TAG synthesis and storage. In an opposing manner, insulin acts to inhibit lipolysis by primarily inhibiting the activity of HSL. This occurs by regulating the active phosphorylated state (PHSL) by a combination of phosphatase action and kinase inhibition through cAMP reduction[47]. Insufficient insulin signaling, as observed in *RTSAKOs*, would therefore influence lipid metabolic regulation, due to the absence of adequate lipogenesis stimulation and lipolysis inhibition.

The effect of LPA on adiposity and lipid homeostasis remains unclear, so the impact of *RTSAKO* LPA elevations on lipid metabolism is not entirely understood. However, preliminary studies have shown that LPA may play a role in lipid metabolism and obesity either by modulation of insulin or directly[56–59,88–93]. LPA has been predominantly shown to effect lipogenesis by inhibition of preadipocyte differentiation into mature adipocytes capable of lipid storage, synthesis, and transport. A study by Simon and colleagues saw a reduction in the triglyceride synthesis of adipocytes in a LPA dose-dependent manner, as well as an adaptive downregulation in *Hsl* expression[92]. In addition, LPA exposure caused reduced expression of peroxisome proliferator-activated receptors gamma (PPARγ), which promotes adipocyte differentiation and lipid synthesis, as well as fatty acid binding protein 4 (FABP4), which enables fatty acid entry and transport[92]. Nobusue et al., showed that adipocyte exposure to LPA led to a reduction in glycerol-3-phosphate dehydrogenase (GPDH) expression, an enzyme

responsible for lipid biosynthesis[93] (Figure 9). Oil red staining showed significant reduction in lipid droplet accumulation in adipocytes paralleling reduced GPDH activity as a result of LPA exposure[93].

Investigations in LPA receptor *knockout*s has also shed light on the impact LPA may have on lipid metabolism[59,90]. LPA receptor nullification showed evidence of uninterrupted adipocyte differentiation and TAG accumulation when injected with LPA relative to *control* littermates[92]. Furthermore, studies on Autotaxin (ATX), the primary LPA synthesizing enzyme localized chiefly in adipose, have also aided in elucidating the role of LPA[91,94]. Adipose tissue specific *Atx knockouts* are obesity prone and have larger fat pads when placed on a HFD in comparison to *control* littermates[59]. Assessment of adipose depots in this LPA deficient model revealed that the number of available adipocytes did not increase, rather adipocytes were larger and more lipid laden, confirming a relationship between LPA and inhibited lipogenesis[59,90,93]. This same effect was observed in obese mice treated with an LPA inhibitor, suggesting that LPA attenuates lipogenesis and that blocking its action upregulates lipid accretion[59]. The impact of LPA on lipid synthesis in non-adipose tissue, however, is unknown.

3.4 Adipocyte Differentiation

Adipogenesis is the term used to describe the differentiation process of fibroblast-like preadipocytes into mature adipocytes capable of lipid storage and insulin responsiveness[48]. These progenitor cells undergo a morphological and transcriptional change so that they can become functional adipocytes. Adipogenesis is a finely tuned process involving the balance and activation of numerous transcription factors[88]. Adipogenesis involves the activation of many differentiation-specific genes such as the CCAAT/enhancer-binding proteins (CEBPs α, β, γ), PPARγ, SREBP1, signal transducers and activators of transcription (STATs), and insulin-like growth factor 1 (IGF-1), as well as the down-regulation of the antiadipogenic preadipocyte factor (PREF1)[95]. Adipogenesis is often assessed by examination of the nuclear factors CEBPα and PPARγ, since these are directly involved in pro-adipogenic transcriptional changes. These nuclear transfactors increase the synthesis of proteins required for lipid storage and release, such as FABP4, FAS, and perilipin (PLIN)[88,96]. Fluctuations in adiposity (adipose depots mass) can be attributed to changes in the number and type of adipose cells, or in the size of lipid-laden mature adipocytes, or both[88].

Insulin is a potent hormone with pro-adipogenic properties, although the mechanism by which insulin modulates adipocyte differentiation is incompletely understood[95,97]. Generally, insulin binds to its receptor on the surface of preadipocytes which results in an intrinsic cascade of upregulated pro-adipogenic transcription factors that steer cellular development toward maturation[95,97]. Studies in insulin receptor *knockouts* have shown that preadipocytes are unable to differentiate in the absence of an insulin receptor[95,97]. Therefore, it can be rationalized that diminished levels of insulin hormone can negatively impact the progression of adipogenesis in *RTSAKO* mice.

In contrast, chronic exposure to LPA has been shown to cause anti-adipogenic effects through the inhibition of lipid accumulation and differentiation-specific gene expression[48,92,93,98]. PPARγ is a pro-adipogenic nuclear receptor that tightly regulates gene expression for fat cell differentiation and recruitment[48,92,93,98]. LPA acts to prevent adipogenesis by reducing PPARγ-induced differentiation, and downregulating both the transcription and phosphorylation of the receptor[92,93]. LPA transcriptionally downregulates PPARγ-dependent gene expression via the Rho-Kinase pathway[88,92,93,96,99]. LPA also prevents adipogenesis by inhibiting downstream PPARγ phosphorylation through the MAPKinase pathway [88,92,93,96,99]. Interestingly, the PPARγ2 nuclear receptor has been defined as a putative intracellular LPA receptor, although the relevance of this in the context of adipogenesis remains elusive[92,100,101]. Since preadipocytes do not have significant lipolytic and lipogenic function, inhibition of adipogenesis by LPA causes indirect mitigation of these processes. Finally, LPA has additionally been shown to enhance preadipocyte proliferation, so that depots have higher preadipocyte number and less maturation into mature adipocytes[93]. Overall, LPA acts to inhibit adipogenesis through downstream downregulation of various pro-differentiation transfactors and causes the proliferation of progenitor preadipocytes. In conclusion, the cooccurrence of high LPA and low insulin in *RTSAKOs* may potentially have an additive effect on the inhibition of preadipocyte differentiation.

3.5 LPA Synthesis in the Kidneys

Disrupting lipid metabolism in the renal-tubules of *RTSAKO* mice led to elevated plasma LPA, reductions in glucose stimulated insulin secretion, and consequently impaired glucose disposal. However, the identity of the enzyme responsible for renal LPA production remains unknown. The likely contender for LPA synthesis, as suggested by the literature, is ATX. LPA

production by ATX occurs in a two-step process. The primary step involves phospholipase A (PLA1 or PLA2) deacylation of a fatty acid from the glycerol backbone of a phospholipid at either the *sn*-1 (PLA1) or *sn*-2 (PLA2) position to produce a lysophospholipid[102,103]. The predominant species converted in this process is the abundantly available phosphatidylcholine (PC) into lysophosphatidylcholine (LPC)[103]. In the second step, the now bioavailable lysophospholipids are hydrolyzed by ATX into LPA (Figure 10). Plasma LPA is predominantly produced by ATX secreted by adipose tissue and platelets, however the role of ATX in the kidney has yet to be elucidated[88,103]. Preliminary work on the renal expression of *Atx* shows upregulation in renal carcinomas and diabetic nephropathy, but its activity and impact on LPA production, and the repercussions of upregulation in the kidneys, remains unclear[104,105].

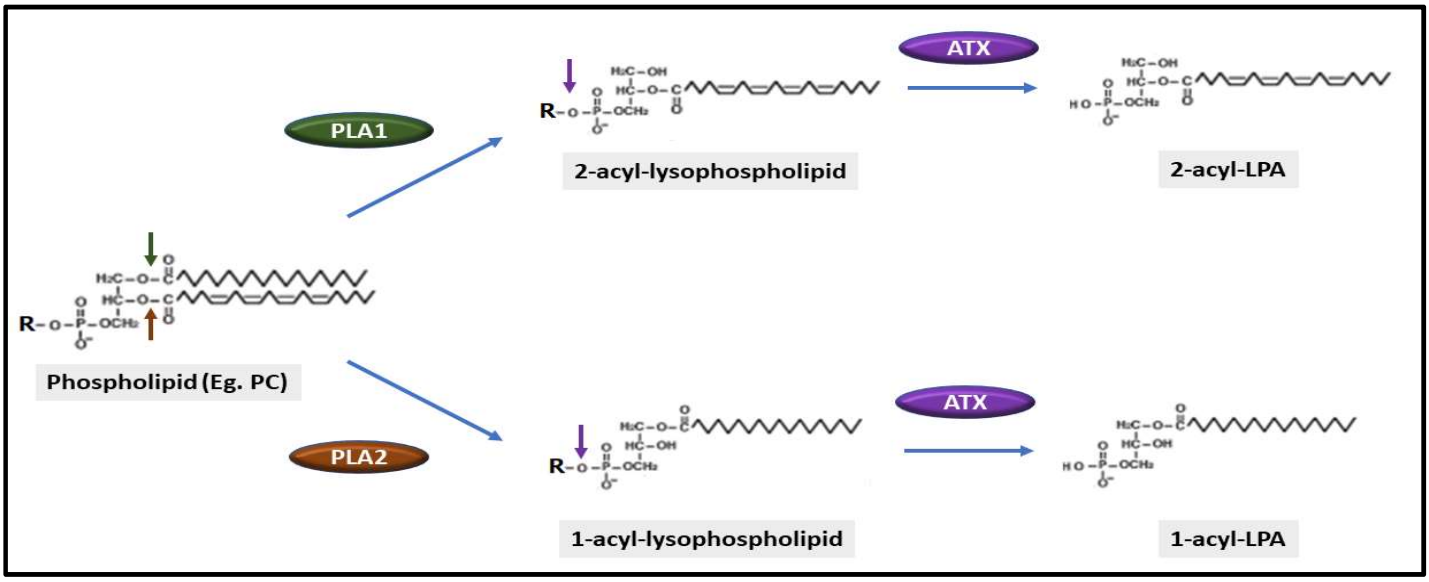

Figure 10: Autotaxin synthesizes LPA from lysophospholipid precursor

In addition to ATX, another likely process that can be the driving force for renal LPA production is the phosphorylation of DAGs and MAGs by an acylglycerol kinase (AGK)[94,106]. A recent study proposed that ATX alongside AGKs produce proinflammatory LPA and should be used as biomarkers for diabetic nephropathy[107]. However, of the two, an AGK is the more probable culprit in the *RTSAKO* model, where attenuated ATGL causes TAG accumulation and compensatory HSL activity[106] (Figure 11). HSL has broad substrate specificity, and because of excess TAG substrate, it can take on the role of preliminary TAG deacylation[42,108]. However, HSL has ten-fold greater substrate specificity toward DAG than TAG, and thus can rapidly

convert DAG to MAG [42,43,78,108]. As a result, an AGK will likely act on readily available MAG to produce bioactive LPA. There are numerous AGKs that may phosphorylate MAG to LPA, however the literature suggests a diacylglycerol kinase (DGK) is likely responsible[106,109]. DGKs phosphorylate DAG into phosphatidic acid, however in the presence of elevated MAG they adapt monoacylglycerol kinase (MGK) activity[106,109]. Seven isoforms of DGKs have MGK functionality, but DGKβ, DGKγ, DGKε, and DGKθ exhibit 7.9-19.2% affinity to 2-MGK in comparison to their DGK activity[106,109]. Since ATGL has *sn*-2 activity and is attenuated, and HSL has *sn*-1 and *sn*-3 deacylation properties, the MAG produced is most likely a 2-MAG[106].

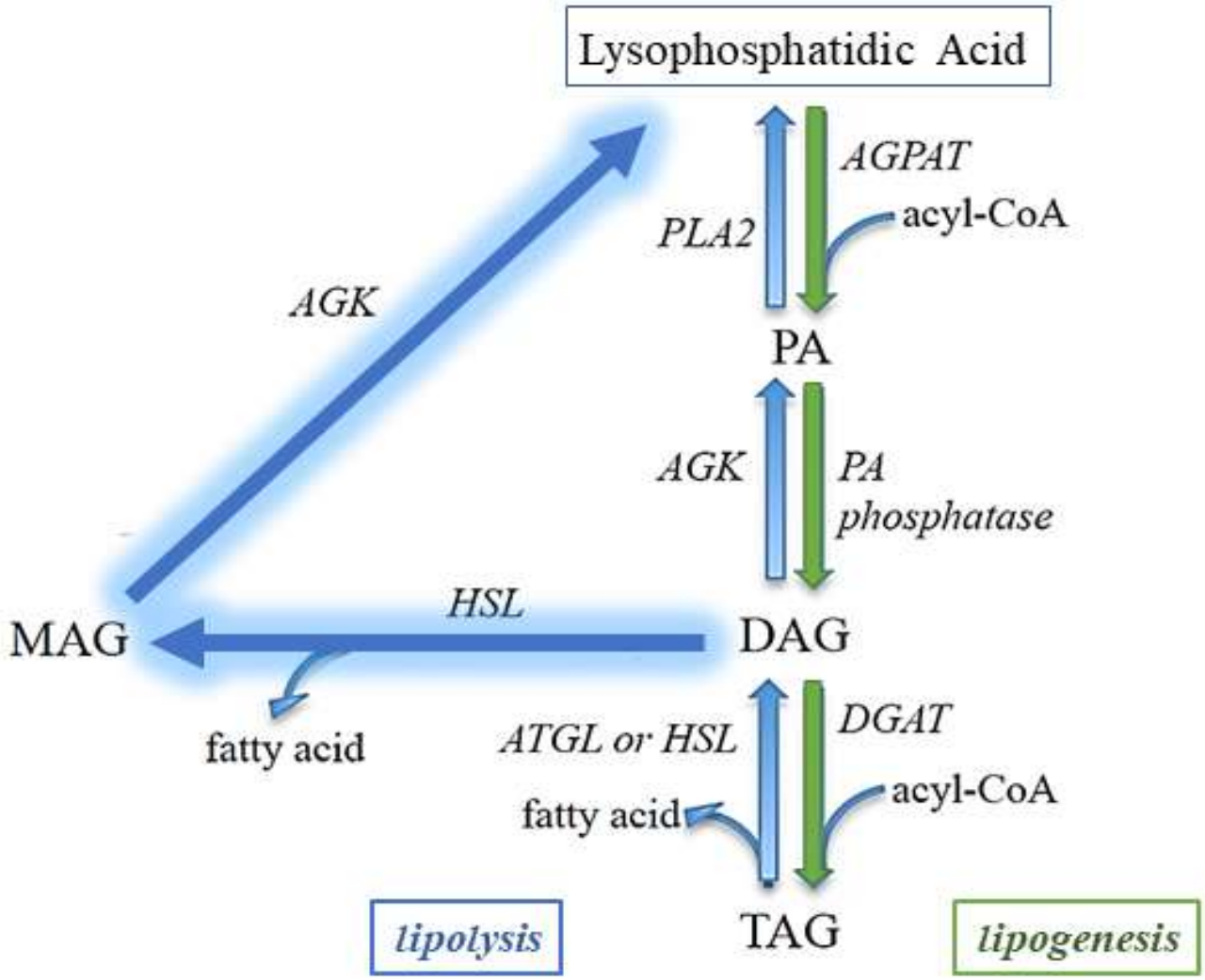

Figure 11: An AGK is the likely culprit for LPA synthesis from a MAG precursor

Chapter 4: Overall Rationale, Objectives, and Hypothesis

4.1 Rationale

Prior findings by the Duncan Lab have already determined that male *RTSAKO* mice develop glucose intolerance by 16 weeks of age, alongside decreased insulin and elevated LPA levels. As presented in the previous chapter, both LPA and insulin can regulate catabolic and anabolic processes in glucose and lipid metabolism. Therefore, systemic changes in these humoral factors have the potential to affect multiple tissues. A possible role in mediating the phenotype will be discussed through the assessment of gene and protein expression over the course of early development. The differences in expression observed in *RTSAKOs* relative to normoglycemic *controls* could thus be interpreted as adaptive (normalizing) or maladaptive (pathogenic) contributions to the progression of dysglycemia.

Therefore, I have designed experiments to examine differences in gene and protein expression at timepoints prior to the development of dysglycemia (i.e. 9-12 wks of age), coincidental with the onset of dysglycemia (i.e. 16-18wks of age), and after chronic exposure to dysglycemia (23-25wks cohort). Assessments focused on three main tissues, namely the kidneys, liver, and adipose tissue. Analysis of skeletal muscle and pancreas, although important in a model with impaired glucose metabolism, will be completed by others in our lab and will not be examined in this thesis. However, findings in the kidneys, liver, and adipose, may have implications for the pancreas and skeletal muscle and could inform future studies.

This thesis focuses on characterizing differences in the expression of genes and proteins in the kidneys, liver, and adipose tissue of male *RTSAKO* mice by comparison with expression patterns in *control* littermates. The identity of the enzyme responsible for increased renal LPA production is of interest. Assessments of the gene expression of various known enzymes involved in LPA synthesis in the kidneys will be conducted to investigate a potential mediator responsible for inducing the dysglycemic phenotype in *knockouts*. Furthermore, expression differences in glucose-regulating genes will be assessed in the kidneys and livers, since these two organs are major producers of systemic glucose. In addition, the impact of dysregulated renal lipid metabolism, coupled with low insulin and elevations in LPA, on the expression profiles of lipid metabolism regulators will be determined by gene expression and protein abundance

measures of various lipolytic and lipogenic enzymes in the three tissues assessed. Adipogenesis gene expression will be assessed in four different adipose depots since low insulin and elevated LPA have both been shown to transcriptionally inhibit preadipocyte differentiation into mature adipocytes capable of lipid storage. Differences apparent in the expression of genes and regulation of proteins over the course of early aging and dysglycemia development will help inform how renal-organ cross-talk may impact and mediate adaptive and maladaptive responses in metabolism.

All analyses in *RTSAKO* mice were made relative to healthy, normoglycemic, age-matched *control* littermates. Only male mice were studied, as female *RTSAKO* mice do not manifest glucose intolerance at 16 weeks of age. The cause of this sexually dimorphic phenotype is of interest and will be the subject of future studies by the Duncan Lab, but is outside the scope of this thesis.

4.2 Objectives

The overall aim of my thesis was to characterize differences in the genetic and protein expression profiles of *RTSAKO* kidney, liver, and adipose tissue, in comparison to age-matched *control* littermates, with the intent to inform the possible role these organs play in the cross-communication that results in the development of dysglycemia.

This goal was met through completion of the following objectives:

1. To identify a potential enzyme mediator involved in the production of renal LPA.
2. To identify differences in the expression of glucose production and disposal genes in the kidneys and livers of male *RTSAKO* mice.
3. To identify differences in the expression of lipolytic and lipogenic genes and proteins in the kidneys, livers, and adipose of male mice, as well as to identify differences in adipocyte differentiation gene expression in four different adipose depots.

4.3 Hypothesis

1. Renal LPA Production:

Autotaxin is likely not the enzyme responsible for renal LPA production, and so I predict that expression will not be higher in *RTSAKO*s relative to *control*s at 9-12, 16-18, or 23-25 weeks of age. Rather I predict that an acylglycerol kinase is likely involved.

2. Glucose Regulator Gene Expression:

Kidneys: *RTSAKO G6Pase*, *Hks*, and *Sglt* expression will not be significantly different from healthy *control*s at 9-12weeks of age, as dysglycemia has yet to manifest. However, with the onset of dysglycemia and low circulating insulin at 16-18 weeks of age, *RTSAKO* mice will present with higher transcription of the glucose producing and conserving genes *G6Pase* and *Sglts* in comparison to normoglycemic *controls*. This expression will be maintained at 23-25weeks of age, although differences will become more pronounced and reach significance because of chronic hyperglycemia and hypoinsulinemia. *Hk1* and *Hk3* expression is expected to show no difference at any of the time-points, however *Hk2* and *Gck* expression is expected to be lower at 16-18 and 23-25 weeks of age since they are the only hexokinase variants negatively regulated by insulin.

Livers: At 9-12 weeks of age, no significant difference will be observed in the expression of any of the glucose regulators, but by 16-18 weeks of age *G6Pase* expression will be higher and *Gck* expression will be lower in *knockout*s relative to *control*s. Chronic exposure (23-25 weeks) to high glucose and LPA, and low insulin, would only exacerbate these differences in expression. Similar to the kidneys, no differences in *Hk1* and *Hk3* expression are expected, however *Hk2* expression will likely be lower in *RTSAKO*s relative to *control*s as a result of attenuated insulin levels at 16-18 and 23-25 weeks of age.

3. Lipolysis, Lipogenesis, and Adipogenesis Expression:

Kidneys: *RTSAKO* mice are expected to have lower *Atgl* gene expression and protein abundance. Expression of other lipolysis sand lipogenesis regulators, like *Hsl* and those listed in Figure 12, are not expected to be different from *control*s at 9-12 weeks of age in *RTSAKO* mice. However, I predict that by 16-18 and 23-25 weeks of age, the conjunction of *Atgl* ablation alongside attenuated circulating insulin, will cause an increase in the expression and phosphorylation of HSL. In addition, lipogenesis gene expression and protein abundance will be lower in *RTSAKO*s relative to *controls* at 16-18 and 23-25 weeks of age since lipogenic gene expression could be attenuated by renal steatosis and low insulin.

Livers: At 9-12 weeks of age, *RTSAKO*s will show no significant difference in the expression of lipolysis and lipogenesis mediators relative to *control*s. However, by 16-18 weeks of age, low circulating insulin will cause a significantly higher expression, abundance, and activation of lipolysis genes and proteins, and lower lipogenic expression and protein abundance. At 23-25 weeks of age, chronic exposure to low circulating insulin would heighten these differences in expression, and reach significance.

Adipose: Adipose tissue lipolysis and lipogenesis can be regulated by both low insulin and elevated LPA. At 9-12 weeks of age, the lack of dysglycemia suggests LPA and insulin levels are not significantly different in *RTSAKOs* relative to *control*s, and as a result no differences in lipolysis, lipogenesis, or adipogenesis gene expression are expected. However, by 16-18 weeks of age, elevations in LPA in conjunction with low circulating insulin would enhance inhibition of preadipocyte differentiation, causing significantly lower expression of lipogenesis and adipogenesis gene expression in *knockouts* relative to *controls*. However, differences in lipolytic gene expression could be mitigated since insulin and LPA act antagonistically on one another to regulate lipolysis and may cancel out. By 23-25 weeks of age, gene expression differences will reach significance, and depots mass would appear lower in *knockouts* relative to *controls*.

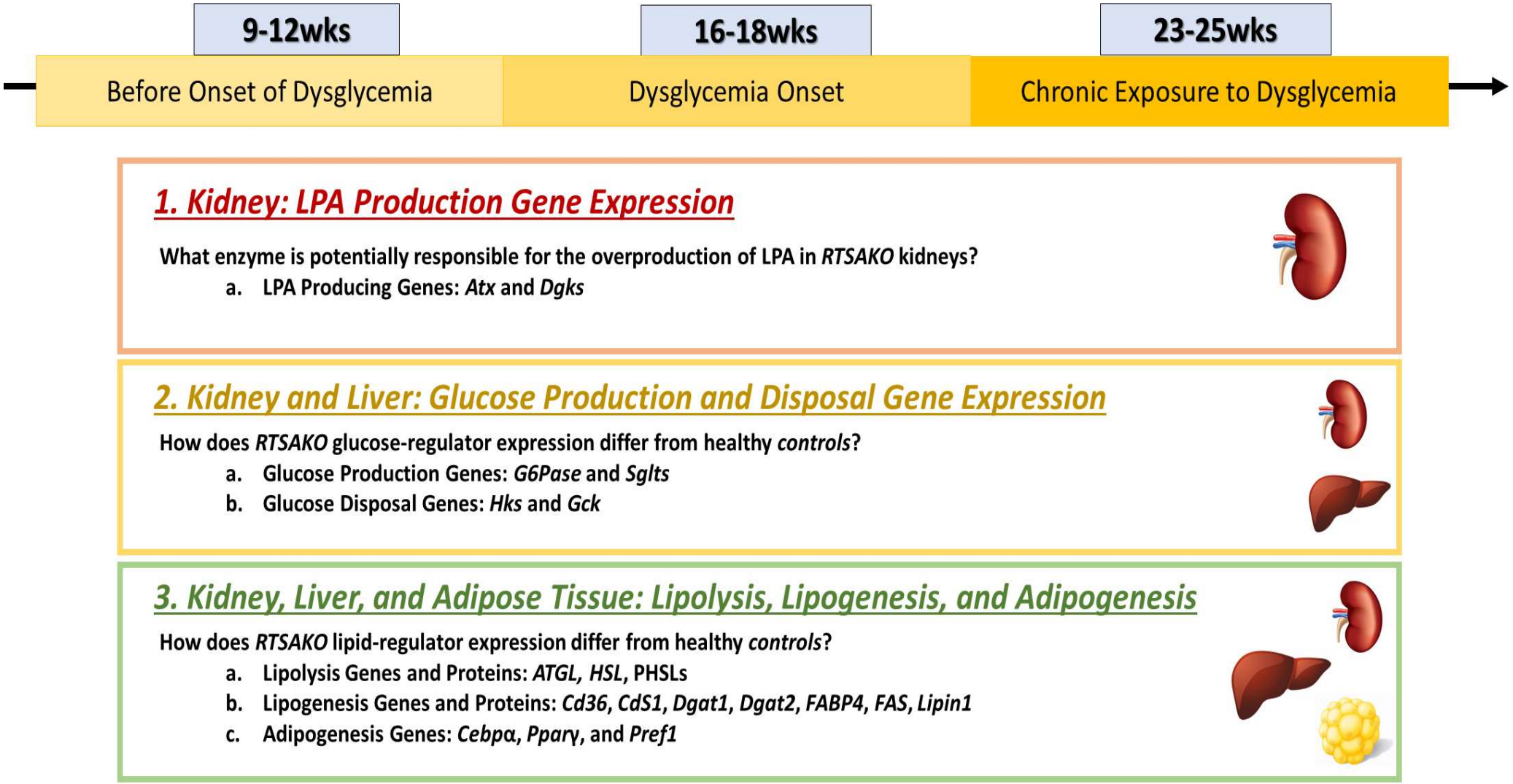

Figure 12: A graphic outline of objectives and experiments intended to answer key questions that will aid in the characterization of the kidneys, livers, and adipose tissue of RTSAKO mice.

Chapter 5: Methods

5.1 Animals and Knockout Model

RTSAKO mice, aged 9-12 weeks, 16-18 weeks, and 23-25 weeks old were used in experiments alongside age-matched *control* littermates. *RTSAKO* mice were generated using the *Cre*-LoxP transgenic system to excise the catalytic region of *Atgl* in the renal-tubules of the kidneys. Mice homozygous for *Atgl* with the entire first exon flanked by LoxP sites were a generous gift from Dr. Hei Sook Sul at the University of California, at Berkley. The floxed mice were bred with commercially available transgenic mice that have a kidney-specific promoter controlling the expression of *Cre*-recombinase (B6. Cg-Tg(Cdh16-cre)$^{91Igr/J}$ from Jackson Laboratories). Both strains of mice had been backcrossed >10 generations onto a C57Bl/6J background prior to mating. Expression of *Cre*-recombinase in the presence of LoxP sites results in the cleavage and deletion of the floxed exon, with the rejoining of the LoxP sites. In the *RTSAKO* model, *Cre* expression results in the deletion of *Atgl* in the tubule epithelium of the kidneys, producing the *knockouts* (Figure 13)[27]. In the absence of *Cre*, the *Atgl* gene remains intact, producing littermate *controls* that retain the LoxP sites, but otherwise have an unaltered gene. Prior work on other tissue-specific *knockout* models generated with this same strain of *Atgl*-deficient mice has demonstrated that in the absence of *Cre*, they are essentially indistinguishable from *wildtype* C57Bl/6J mice, and therefore are an excellent *control* for *RTSAKO* mice[39,110].

To establish a colony with litters that are all homozygous *Atgl* floxed and either Cre-positive (*knockouts*) or negative (*controls*), Ksp-*Cre* transgenic mice (hemizygous) (Figure 13A) were mated with homozygous *flox/flox-Atgl* transgenic mice. This would produce mice that were all heterozygous for the floxed *Atgl* allele, but where 50% were hemizygous and 50% were *wildtype* for *Cre*. Mice hemizygous for *Cre* and heterozygous for *Atgl* were intercrossed with the mice homozygous for the floxed-*Atgl* allele, but lacking *Cre* (Figure 13B). These mice were then genotyped to find progeny both transgenic for *Cre*, and homozygous for the *Atgl* flox/flox allele. Mice for experiments were generated by crossing homozygous floxed *Atgl* mice (Figure 13C) hemizygous for *Cre* to homozygous floxed *Atgl* mice without *Cre*, to produce a progeny that is completely homozygous for floxed *Atgl*, but that either have Cre (*knockouts*) or no Cre

(*controls*). These mice (Colony 8 *RTSAKO*) are the strain used in these experiments and are continually bred at the University of Waterloo's Central Animal Facility.

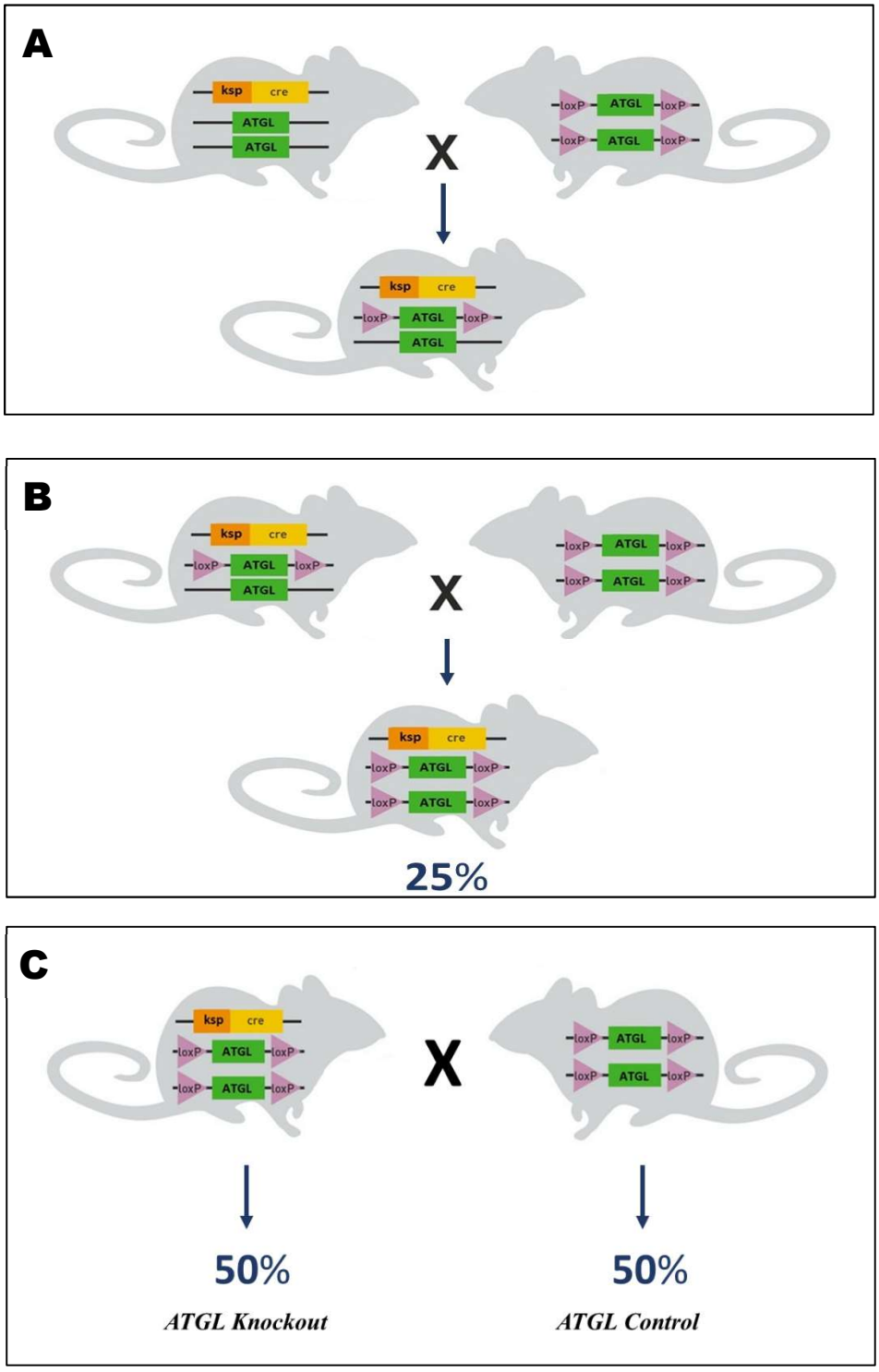

Figure 13: Colony 8 breeding strategy. (A) Floxed Atgl mice mated with Cre-transgenic mice. (B) Cre positive offspring backcrossed with Floxed Atgl mice. (C) Colony 8 RTSAKO mice used in experiments.

5.2 DNA Isolation and Genotyping

DNA was extracted from ear notches collected from mice. Ear punches were placed in thin-walled PCR tubes using sterilized tweezers, and digested in 20 µL of 25 mM NaOH/0.2 mM EDTA in a T100 Thermal Cycler (Bio-Rad, Hercules CA) using the following protocol: 95ºC for 1 hour, followed by cooling to 4ºC, and neutralization with 20 µL of 40 mM Tris-HCl. DNA was stored at -20ºC.

The genotype of animals was determined by amplicon visualization in a 1.5% agarose EtBr gel. Gels were prepared using agarose dissolved in Tris-acetate-EDTA (TAE) Buffer. Before cooling, EtBr was added at 5µL/100mL for visualization of DNA. To differentiate between the *knockout* and *control* mice, primers screened for the presence of *Cre*. Mice that had the *Cre*-recombinase gene were *knockouts*, and those lacking were *control* littermates. Homozygosity of the floxed allele was periodically confirmed. Using primers specific for the first and second introns of *Atgl,* mice homozygous for flox/flox produce an amplicon of 315 bp, whereas the absence of floxing results in a 180 bp amplicon. Heterozygotes show both amplicon sizes. To confirm floxing genotype, the *Atgl* floxing primers used were forward: 5'-CTCACCGCCACAGCGCTGGTCAC-3' and reverse: 5'-GTCCCTCTCTACCGCTTCTAC-3'. Mice used for study were homozygous for the floxed allele, and solely generate the 315 bp amplicon (Figure 14A).

Genotyping for *Cre* was performed using 1 µL of extracted DNA added to a PCR tube with 19µL of reaction mix containing a 5U/µL FastStart Taq polymerase (0.1µL), 10X PCR Buffer containing $MgCl_2$ (2 µL), PCR Grade10mM each dNTPs Mix (0.4 µL), ddH_20 (15.86 µL), and forward and reverse primers (0.32 µL of a 20µM working stock) (SIGMA®). The *Cre* forward: 5'-AGGTTCGTTCACTCATGGA-3'; reverse: 5'-TCGACCAGTTTAGTTACCC-3', primers produce a 270 bp amplicon in the presence of *Cre*-recombinase (*knockout*) but show no amplification in the absence of the gene (*control*) (Figure 14B). Samples were run in the thermocycler under the following conditions: 95ºC for 4 min, followed by 40 cycles of denaturation at 95ºC for 30s, annealing at 60ºC for 30s, and extension at 72ºC for 1 min, and finally 72ºC for 7 min. Once samples have cooled, 4 µL of 6X DNA dye was added to each tube, vortexed, centrifuged, and loaded into the wells of the 1.5% agarose gel alongside a 100 bp DNA ladder (Quick-Load®). The gel was run in 1X TAE Buffer at 100V for 32 min, then imaged in the ChemiDoc™ Touch Imaging System (Bio-Rad) under UV light.

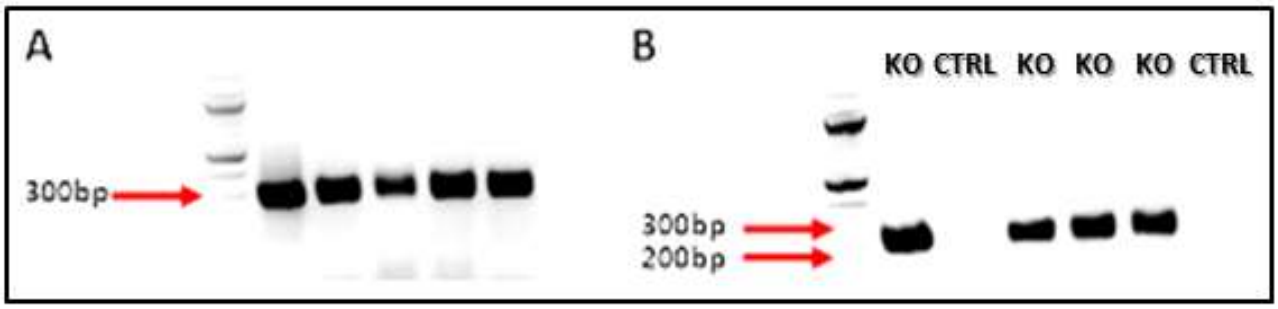

Figure 14: Flox and Cre genotype confirmation. (A) Genotyping to prove homozygous floxing, homozygous animals show one strong band at 315bp. (B) Genotyping for the presence of Cre, knockouts show a 270bp band for Cre and controls show no band due to gene absence.

5.3 Tissue Collection

Genotyped mice were weighed, then euthanized by cervical dislocation, sprayed with ethanol, and pinned in a supine position on a dissection mat. An incision was made from the thorax to the tail, and the skin and fascia pulled back to expose the chest and abdominal cavity. A needle was used to quickly collect blood from the heart before coagulation. Epididymal white adipose tissue (ewat) was removed from the area around the testes, reproductive tissue within the depot was dissected away, and the white adipose tissue (WAT) was flash frozen in liquid nitrogen. Next, the liver was removed to expose the kidneys and frozen. Adipose tissue surrounding the kidneys, termed perirenal WAT (pwat), was carefully removed and collected, followed by the kidneys. The adipose depots at the back of peritoneal cavity, behind the kidneys, called retroperitoneal WAT (rwat) were also collected. The mouse was then flipped so that the dorsal plane faced upwards, and an incision was made from the cervical spine to the tail. Brown adipose tissue (BAT) which is localized to the cervical-supraclavicular region, was collected and flash frozen, taking care to remove any surrounding WAT. The skin was pulled back from the gluteofemoral region to reveal thigh subcutaneous fat pads (subc), which were excised and flash frozen. Finally, gluteal inguinal WAT (iwat) was collected by stripping back the skin and collecting adipose tissue flanking the tail (Figure 15). All tissue weights were recorded prior to flash freezing in liquid nitrogen. Tissue was used immediately or stored at -80ºC. Tissues collected from males at the three-time points were utilized in experiments outlined in this thesis. Tissues collected from females at these time points have been archived for future investigations. In females, gonadal WAT (gwat) surrounding the ovaries and uterus was collected in the place of male ewat.

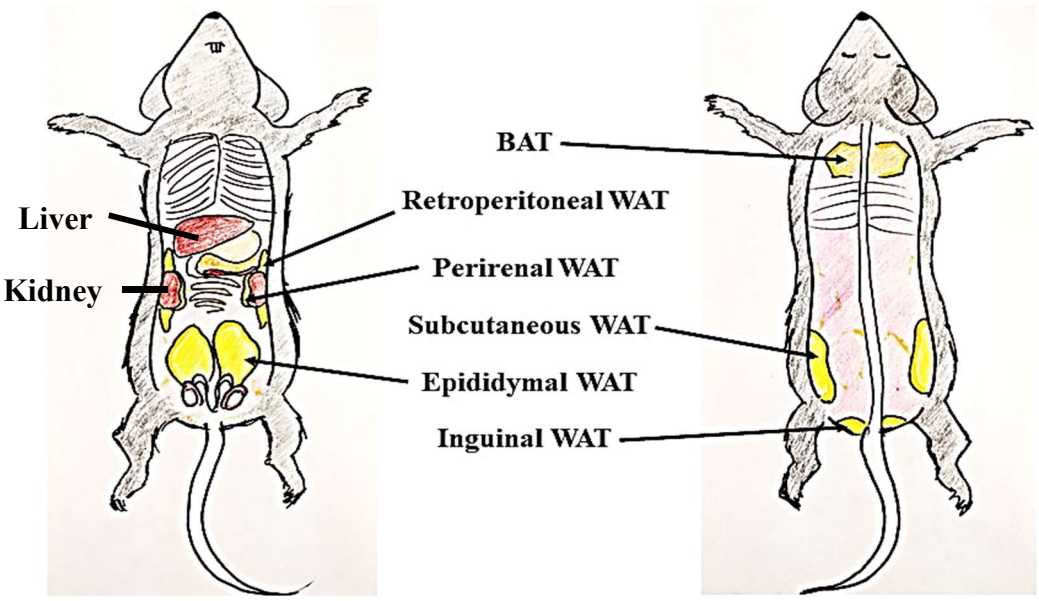

Figure 15: Excised tissues and adipose depots of interest location shown ventrally (right) and dorsally (left)

WAT depots can be characterized as either visceral or subcutaneous. Visceral WAT are adipose depots that surround the inner organs in the thoracic or abdominal cavity[111]. Epididymal, perirenal, and retroperitoneal adipose are all visceral depots[111]. Epididymal WAT is the gonadal adipose tissue specific to males because of proximity to the testes and epididymis. In females, this depot surrounds the ovaries and fallopian tubes, and is called gonadal fat. In rodents, BAT is specifically located dorsally in the cervical-supraclavicular region. Subcutaneous WAT is adipose tissue that lies directly beneath the skin. The subcutaneous regions of interest are the gluteofemoral WAT surrounding the upper hindlimbs (thigh subc), and inguinal WAT, found flanking the tail region of the mouse[111]. It is important to note that in mice each depot is contained and can be discerned from adjacent adipose and tissues.

5.4 Gene Expression Analysis: RNA Isolation and Reverse Transcription (RT-PCR)

The fume hood and tools were sanitized using RNAse Zap, and aseptic technique was used to maintain integrity and stability of RNA. RNA was isolated from the tissues using 1mL of chilled TRIzol® reagent (Ambion®). Tissues were homogenized at maximal velocity using a Polytron® homogenizer (VWR) and incubated for 5 min on ice. Two hundred microliters of chloroform were added to each tube and inverted vigorously, followed by an additional 2-3 min incubation period on ice. Samples were then centrifuged for 15 min at 12,000 × *g* and 4ºC in a

5424R Eppendorf centrifuge. The top clear layer containing the RNA was carefully pipetted and transferred into a new RNAse-free 1.5 mL tube (Figure 16). Isopropanol (0.5 ml) was added to the supernatant, inverted to precipitate the RNA, and incubated on ice for 10 min. Once precipitated, samples were centrifuged for 10 min at 12,000 × *g* at 4ºC to pellet RNA. The aqueous layer was removed, and the pellet resuspended and washed using 1 mL of 75% ethanol. Samples then underwent a final centrifugation for 5 min at 7,500 × *g* at 4ºC. The aqueous layer was removed, and the pellet allowed to air dry for 10 min. The RNA pellet was then resuspended in 35 µL ultra-pure water and incubated at 60ºC for 10 min at 300 rpm to facilitate dissolution of RNA. Concentration and purity (260/280 ≥ 1.8) of isolated RNA was determined using the Nanodrop-2000 spectrophotometer (Thermo Scientific).

Once RNA concentrations were determined, the volume containing 2 µg of RNA was calculated and loaded into PCR tubes with ddH_2O (bringing the total volume to 10 µL). To convert RNA to cDNA, a high capacity DNA kit (Applied Biosystems) was used. Two microliters of 10X RT-Buffer, 0.8 µL of 25X dNTPs, 2 µL10X RT-Random Primers, 1 µL of Reverse Transcriptase Enzyme, and 4.2 µL of ddH_2O were added per sample for a total volume of 20 µL. RT-PCR was completed by subjecting samples to 25˚C for 10 min, 37˚C for 2 h, and 85 ˚C for 5s in the thermocycler. The cDNA stock was used to prepare a 1/5 working dilution for gene analysis by qPCR. Both stock and dilution were stored at -20˚C.

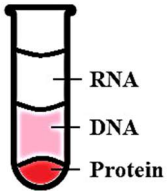

Figure 16: Top aqueous supernatant containing RNA was removed carefully

5.5 Primer Design for Quantitative PCR

To study the expression of genes, primers that are specific to the gene transcript must be designed. All primers used in this study were ordered from SIGMA®. The mRNA sequence was obtained from the National Center for Biotechnology Information (NCBI). Primers were designed to fall within the coding region (CDS) of the gene, excluding the 5'- and 3'-untranslated regions. Each gene transcript has a unique accession number that can be used to identify the gene of interest in the NCBI "primer blast" tool that provides various primer combinations for the production of an amplicon. Primers were selected for use if they fell within

the CDS, formed an amplicon that is an ideal length (in quantitative PCR analysis, the ideal amplicon length is below 80 bp for efficient replication, and although constructs as large as 300 bp can still amplify, amplicon size below 150 bp is considered ideal[112]), and had low self-complementarity. At times, primers for certain genes suggested in the literature were selected and confirmed by matching primer sequences to their position in the CDS.

Primers used in these quantifications arrived in a desalted form. Therefore, they were reconstituted in deionized water to a stock concentration of 100 µM. Once dissolved in solution, a working concentration is made up for use in gene analysis. Stock primers are diluted 1:4 in deionized water for a final working concentration of 25 µM.

5.6 Gene Expression Analysis: Quantitative PCR

Quantitative PCR (qPCR) was performed using a Bio-Rad CFX96 Touch™ Real-Time PCR Detection System in order to provide a relative quantification of gene expression based on the amplification of template cDNA using SYBR-Green Fastmix®. SYBR Green (Thermo Fischer) requires the separate analysis of a housekeeping gene and the gene of interest. Therefore, a single well was allocated for analysis of expression of a housekeeping gene, and another well was allocated for the gene of interest, for each analysis. The quantity of the gene of interest (ΔC_t) was calculated as a value relative to the housekeeping control, where $\Delta C_t = [C_t$ (gene of interest) - C_t (housekeeping gene)] and C_t represents the number of cycles required to achieve luminescence that breaks through a certain threshold. To compare the gene expression in *knockouts* relative to *controls*, the $\Delta\Delta C_t$ was determined by $\Delta\Delta C_t = \frac{2^{\Delta CT\ Gene-Knockout}}{2^{\Delta CT\ Gene-Control}}$. The fold difference between the two groups is expressed as $2^{-\Delta\Delta Ct}$.

The master mix for a qPCR reaction using SYBR-Green contains 5µL of SYBR-Green, 3µL of ddH_2O, 0.5µL each of the forward and reverse primer, and 1µL of diluted cDNA per well. Target genes and control genes are run alongside in separate wells on the same plate. Cycling conditions used were as follows: 95ºC for 2 min, followed by 40 cycles of 95ºC for 10 s and 60ºC for 20 s. A melt curve was used following reaction completion to verify a single amplicon.

The housekeeping control gene used as a reference point for all gene expression assessments was the abundantly expressed ribosomal 18S (Table 1). Genes involved in LPA synthesis, glucose regulation, lipid metabolism and differentiation, were examined to determine if *knockouts* show differences in expression relative to *control* littermates (Table 2-6).

Table 1: Control Primers for House-Keeping Genes

Gene	Direction	Primer Sequence	Amplicon size
18S	Forward	5'-GATCCATTGGAGGGCAAGTCT-3'	113 bp
	Reverse	5'-AACTGCAGCAACTTTAATATACGCTATT-3'	

Table 2: LPA-Synthesis Genes

Gene	Direction	Primer Sequence	Amplicon-size
Atx	Forward	5'-GACCCTAAAGCCATTATTGCTAA-3'	81 bp
	Reverse	5'-GGGAAGGTGCTGTTTCATGT-3'	
Dgkβ	Forward	5'-GTGGGAAGCAAGGAGAACGA-3'	100 bp
	Reverse	5'-TGTAACCCTGGCATTGGTCC-3'	
Dgkε	Forward	5'ACTGGAAATCGTTGGCGTCT-3'	111 bp
	Reverse	5'-CACTTCAAAGTCAGCCGCAC-3'	
Dgkγ	Forward	5'-AGCTTCAGACCTATACTGAAGGAG -3'	98 bp
	Reverse	5'-GTGGTCATTCCCCCGTTGAT-3'	
Dgkθ	Forward	5'-GCTGTGAAGTGTGTGTGAGCTG-3'	109 bp
	Reverse	5'-CCTCCAGTGGTGGTGATACG-3'	

Table 3: Glucose Regulatory Gene Primers

Gene	Direction	Primer Sequence	Amplicon size
G6Pase	Forward	5'-CAGTGGTCGGAGACTGGTTC-3'	110 bp
	Reverse	5'-TATAGGCACGGAGCTGTTGC-3'	
Hk1	Forward	5'-GTGGGATGGAAAGTCGACCA-3'	179 bp
	Reverse	5'-CATAACACATTCCACCACCAGC-3'	
Hk2	Forward	5'-ACTGTGGCTAAATGAGACTGGG-3'	112 bp
	Reverse	5'-ACCATGCCAAGGAGCTTGAT-3'	
Hk3	Forward	5'-CACTTAACCAATCTCGGAGT-3'	79 bp
	Reverse	5'-AGGCTATCACTTTCGATCTC-3'	
Gck	Forward	5'-CAACTGGACCAAGGGCTTCAA-3'	133 bp
	Reverse	5'-TGTGGCCACCGTGTCATTC-3'	
Sglt1	Forward	5'-CTGCCCATGTTCCTCATGGT-3'	108 bp
	Reverse	5'-TGGTGTGCCGCAGTATTTCT-3'	
Sglt2	Forward	5'-TTGTGTTGGCTTGTGGTCT-3'	117 bp
	Reverse	5'-ATGTTGCTGGCGAACAGAGA-3'	

Table 4: Lipolysis Regulatory Gene Primers

Gene	Direction	Primer Sequence	Amplicon size
***Atgl*-Exon1**	Forward	5'-AACGCCACTCACATCTACGG-3'	113 bp
	Reverse	5'-GCCTCCTTGGACACCTCAATA-3'	
Hsl	Forward	5'-GGAGTCTATGCGCAGGAGTG-3'	80 bp
	Reverse	5'-GCTTCTTCAAGGTATCTGTGCC-3'	

Table 5: Lipogenesis Regulatory Gene Primers

Gene	Direction	Primer Sequence	Amplicon size
Cds1	Forward	5'-TGGACATGGCGGGATAATGG-3'	111 bp
	Reverse	5'-TGGAGCACTTTGCTGGGATT-3'	
Dgat1	Forward	5'-CTGGATTGTGGGCCGATTCT-3'	94 bp
	Reverse	5'-ATACATGAGCACAGCCACCG-3'	
Dgat2	Forward	5'-AAGACATCGACCTGTACCATGC-3'	92 bp
	Reverse	5'-CTCAGTCTCTGGAAGGCCAAA-3'	
Lipin1	Forward	5'-CCTTAGGGAGCCGGAAGACT-3'	91 bp
	Reverse	5'-ATTGTTGGCGACTGGTCACT-3'	
Fabp4	Forward	5'-GTGGGATGGAAAGTCGACCA-3'	70 bp
	Reverse	5'-CATAACACATTCCACCACCAGC-3'	
Fas	Forward	5'- TTGCTGGCACTACAGAATGC -3'	180 bp
	Reverse	5'- AACAGCCTCAGAGCGACAAT -3'	
Cd36	Forward	5'-ACTGTGGCTAAATGAGACTGGG-3'	93 bp
	Reverse	5'-ACCATGCCAAGGAGCTTGAT-3'	

Table 6: Adipogenesis Regulatory Gene Primers

Gene	Direction	Primer Sequence	Amplicon size
Cebpα	Forward	5'-GCAAAGCCAAGAAGTCGGTG-3'	114 bp
	Reverse	5'-TCTCCACGTTGCGTTGTTTG-3'	
Pparγ	Forward	5'-CACAATGCCATCAGGTTTGG-3'	82 bp
	Reverse	5'-GCTGGTCGATATCACTGGAGATC-3'	
Pref1	Forward	5'-GACAGGCCATCTGCTTCACC-3'	116 bp
	Reverse	5'-GTTGTAGCGCAGGTTGGACA-3'	

5.7 Protein Extraction and Immunoblotting

Tissues excised from *RTSAKO* mice were homogenized in lysis buffer (50 mM Tris, pH 7.4, 1 mM EDTA, 0.1 M sucrose, 5mM sodium fluoride, 10 mM sodium orthovanadate, with protease inhibitor cocktail (1:100)) using a Polytron® homogenizer (max VWR). The samples were then sonicated on ice at 65 amp for 6s, 3 times. Samples were centrifuged at 10,000 × *g* for 10 min at 4˚C, and the aqueous protein was collected, taking care to avoid the pellet of cellular debris, and transferred to a clean 1.5 mL tube.

Protein concentrations were determined using a Bradford Assay (Bio-Rad). One microliter of protein lysate was placed in the well of a 96-well plate (Falcon®) along with 20 µL of Bradford Reagent and 79 µL of ddH_2O. Each well was mixed and incubated for 5 min before absorbance readings were taken at 595 nm. Absorbance values collected for each protein sample were compared to the premeasured absorbance curve of known bovine serum albumin (BSA) standards. Absorbance was measured by a SPECTRAmax PLUS-384 spectrophotometer.

Once protein concentrations for each sample were determined, equivalent amounts of protein were diluted into lysis buffer to maintain a constant volume, and equal amounts of 6X loading dye (375 nM Tris HSL, 9% SDS, 50% glycerol, 0.03% bromophenol blue) was added to each tube. Samples were vortexed and heated for 5 min at 95ºC in an Eppendorf thermomixer. Samples were then loaded into the wells of an SDS-PAGE acrylamide gel composed of a 12% resolving and 4% stacking layer, or Bio-Rad 10% TGX Stain-Free FastCast Acrylamide gels with 4% stacking layer. Gels were run alongside a Bio-Rad Precision Plus Protein™ standard with a 10-200 kDa wide range at 120V for approximately 2hrs. If the fast-cast gel system was used, equal protein loading was confirmed using the stain free imaging feature of the ChemiDoc™ for quantification of total relative protein content per well. Once proteins are completely separated by size, the gel was transferred onto a nitrocellulose membrane at 350 mA for 90 min. To confirm successful transfer, membranes were stained with Ponceau to visualize protein bands on membrane then destained, or imaged using the ChemiDoc™ stain free blot feature. Next, the membrane was blocked with 5% BSA (w/v) in TBST (50 mM Tris-HCl, pH 7.4, 150 mM NaCl, 0.1% Tween-20) for 1 h at room temperature. The membrane was then incubated with the primary antibody for the protein of interest at 4˚C overnight on a shaker at a concentration of 1:1000 in 3% BSA. The next morning, membranes were washed in TBST for 5 min, 3 times, to remove unbound primary antibody. The membranes were then treated for 1 h at

room temperature with a secondary antibody (1:5000 to 3% BSA) that is horseradish peroxidase (HRP)-conjugated and raised against IgG in the same animal as the primary. The secondary antibody was then poured off, and the blot was washed 3 times for 5 min per wash, once again using TBST. The membrane was coated in 1 mL of Luminata™ Crescendo HRP substrate chemiluminescence reagent that is hydrolyzed by horseradish peroxidase on the secondary antibody to generate luminescence. Protein luminescence was measured using the ChemiDoc™ Touch Imaging System, and protein identity was determined by comparison of band location to a molecular weight ladder. All primary antibodies were purchased from Cell Signaling (Beverly, MA). It is important to note that BSA was substituted for Skim Milk for some westerns as dictated by the Cell Signaling protocol sheet that accompanies the antibodies. Protein abundance was determined by measuring band intensity using either Image Lab™ Software or Photoshop.

5.8 Quantitative PCR versus Western Blotting

Quantitative PCR assesses gene expression and is a measure of the transcriptional activity of a specific gene of interest. In contrast, western blotting is a post-transcriptional measure, as it assesses the total abundance of a specific protein in a sample. Quantitative PCR is a much more systematic assessment tool. Various genes and/or a larger sample size can be measured on a single plate during a 1.5hr run, with expression values available immediately after completion. In contrast, western blotting is a much more complex, sensitive, and time-consuming procedure. A single western blot typically holds a sample size of 4 for each group and takes two days to complete. In addition, the sensitivity of the blot leaves various opportunities for errors that impede acquiring results, and often requires troubleshooting. As a result, qPCR is utilized as a systematic preliminary assessment of differences between *RTSAKOs* and *controls*, and western blotting aims to act as a supplementary analysis of tissues of interest at time points that are expected to show significant differences (mainly 16-18wks and 23-25wks of age).

5.9 Statistical Analysis

All evaluations of *knockout* mice were made relative to *control* littermates. Results are presented as means ± SEM. Significance between groups was determined by Student's unpaired, two-tailed t-test. Significance between multiple groups was calculated by one-way analysis of variance (ANOVA) with Bonferroni's post hoc test. Values of $P < 0.05$ were accepted as significantly different.

Chapter 6: The Kidneys

6.1 Introduction and Rationale

The kidneys were studied to survey differences in the expression of important glucose and lipid regulators at three important metabolic time points, that is before dysglycemia is apparent (9-12 weeks of age), at the time of initial dysglycemic onset (16-18 weeks of age), and after chronic exposure to dysregulated metabolism (23-25 weeks of age). This time-course analysis of gene and protein expression will aid in the characterization of this novel mouse model with the aim of elucidating the potential contributions of disrupted renal metabolism on the onset and progression of glucose intolerance.

RTSAKO mice do not differ genetically from *control* littermates except for the renal-tubule ablation of the *Atgl* gene. *Knockout*s presented with significant early-onset dysglycemia (at 16-18 weeks of age which is equivalent to a human in their late-twenties). Assessment of metabolic gene expression in the kidneys is therefore integral to understanding the phenotype of these mice.

The analyses chosen, including differences in gene and protein expression, and post-translational protein regulation, are based on predicted differences stemming from observed age-dependent changes in exposure to elevated blood glucose (i.e. hyperglycemia) and decreased circulating insulin[10]. Exposure to chronic post-prandial hyperglycemia and low circulating insulin (observed at 16-18 weeks of age), are predicted to alter kidney expression of genes involved in renal glucose metabolism. *Sglt2* is induced by hyperglycemia, and thus is expected to be elevated, while *G6Pase* is negatively regulated, and some hexokinases are positively regulated, by insulin, and therefore are also expected to be altered in *RTSAKO* mice. These analyses are important for understanding the dysglycemic phenotype of *RTSAKO* mice, especially maladaptive gene-expression for glucose handling, since the kidney is not just a consumer of glucose but also a significant producer[73].

These analyses were also chosen based on the prediction that attenuated renal-tubule ATGL is likely to cause changes in kidney lipid metabolism, and eventual lipotoxicity with chronic TAG accumulation. In the absence of ATGL, HSL is the predominant TAG lipase in most tissues, including the kidney[113]. HSL may be induced as a cellular response to loss of ATGL, and this induction may also be enhanced due to the reduced circulating insulin (observed

at 16-18 weeks of age), which is a regulator of HSL activation. Identification of time-dependent differences in these measures will help elucidate the overall phenotype of *RTSAKO* mice, and the impact of induced renal steatosis on systemic metabolism.

Also important in the assessments of the kidneys, is the identification of a potential mediator responsible for the synthesis of elevated LPA. LPA is predominantly synthesized in the adipose tissue by the enzyme ATX, however the role of ATX in the kidneys is unknown. Another potential synthesizer of LPA is an acylglycerol kinase, and is a more probable contender in *RTSAKO* mice, as some DGKs have MAG kinase activity and can phosphorylate a monoacylglycerol precursor into LPA. Since *RTSAKO* mice show accumulation of TAG and attenuated ATGL, HSL can act in a compensatory manner by taking on TAG hydrolysis. Since HSL preferentially breaks down DAG, TAG substrate would rapidly be hydrolyzed into DAG, then MAG. With increased MAG, DGKs have more substrate availability for phosphorylation into LPA, and could explain elevations. Therefore, assessment of various DGKs could pinpoint the isoform responsible for LPA synthesis in *knockout* kidneys.

6.2 Kidney-Specific Objectives

The following section (6.3) presents my findings in the kidneys of male mice prior to (9-12wks old), during (16-18wks old), and after (23-25wks old) onset of glucose intolerance. All results are comparative, and show differences in gene and protein expression of *RTSAKO*s relative to their age-matched *control* littermates. Quantitative PCR findings were used as a preliminary assessment of differences in gene expression, and western blotting for protein abundance and phosphorylation were used to supplement differences observed in lipolysis and lipogenesis regulators.

Characterization of kidneys from male mice included investigation of:

i. *Cre* mRNA expression in kidney and other tissues to confirm specificity.
ii. Alterations in kidney weight as a potential consequence of disrupted lipid metabolism (i.e. renal steatosis).
iii. Alteration in the expression of major enzymes involved in LPA synthesis, to identify a possible mediator.
iv. Alterations in the expression and regulation of enzymes and transporters involved in renal glucose metabolism.
v. Alterations in the expression, regulation, and phosphorylation of lipolysis and lipogenesis enzymes in response to the metabolic imbalance caused by attenuated renal *Atgl*.

6.3 Results and Discussion

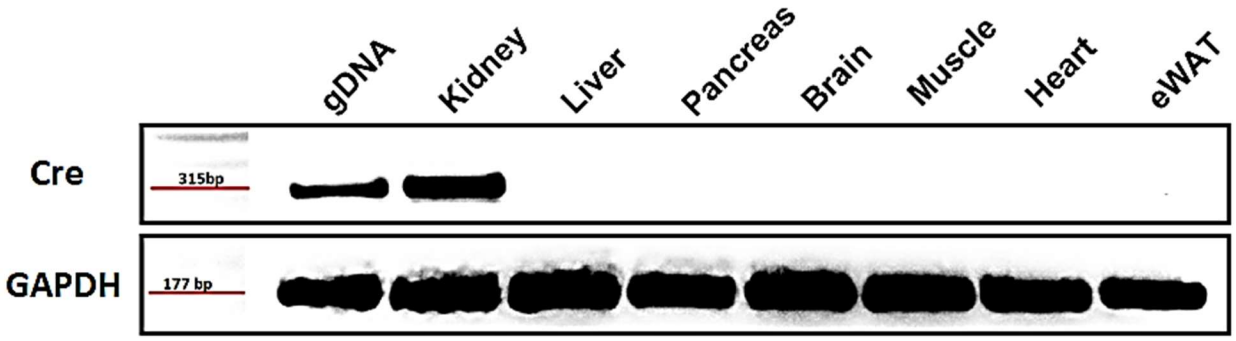

Figure 17: *Cre*-Recombinase mRNA was detected only in *RTSAKO* kidneys.
Cre-Recombinase expression only occurs in the kidneys of knockout mice, confirming that the kidneys were the only site of Atgl gene ablation. Cre gene expression was assessed using RNA extraction, cDNA synthesis, and PCR amplification of the Cre gene. GAPDH was used as a comparative control housekeeping gene.

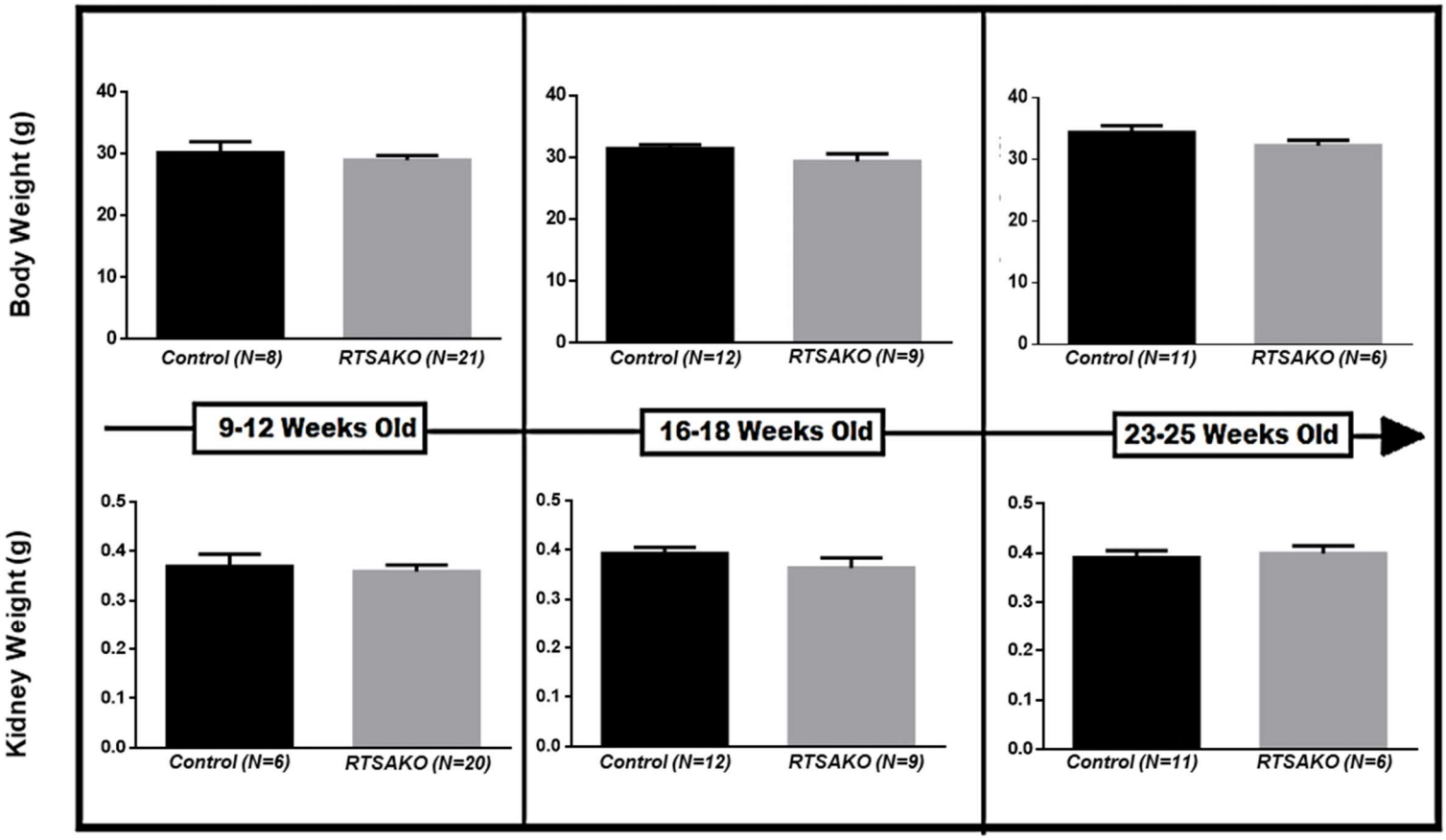

Figure 18: Body and Kidney Weights of Male Mice.
No significant differences were detected between control and knockout body weights (above) or kidney weights (below) at the time points evaluated over the development of dysglycemia (right to left).

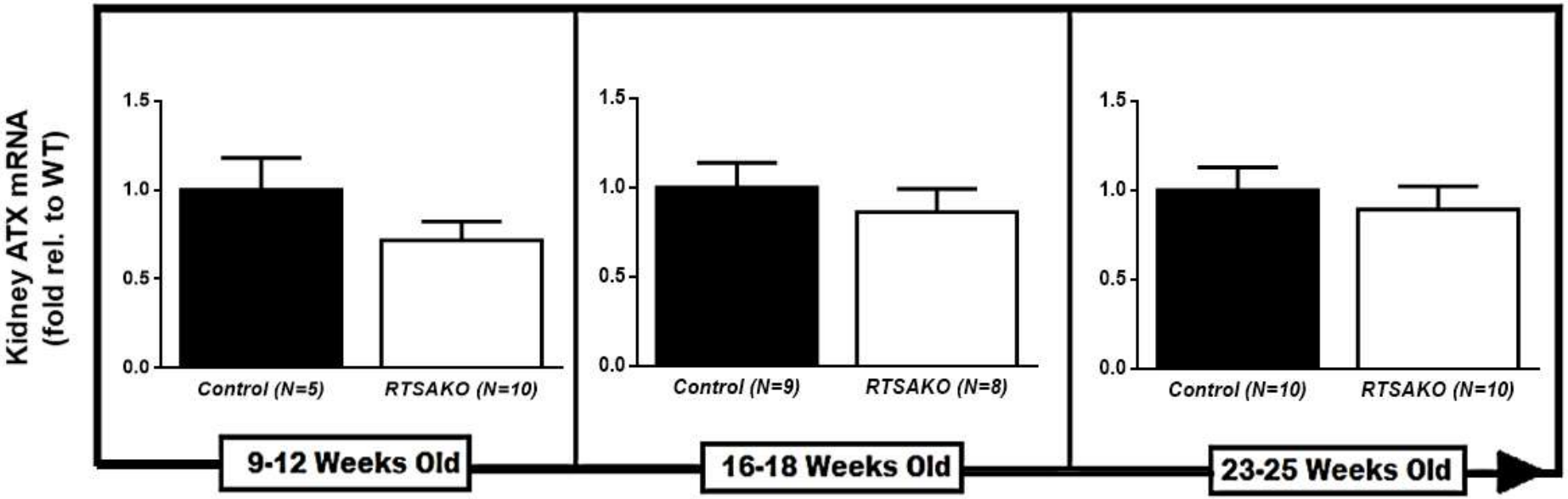

Figure 19: Gene Expression of Autotaxin in the Kidneys of Male Mice.
There was no significant difference in the expression of this LPA synthesizing enzyme in the kidneys of male mice at any timepoint tested. (N=5-10).

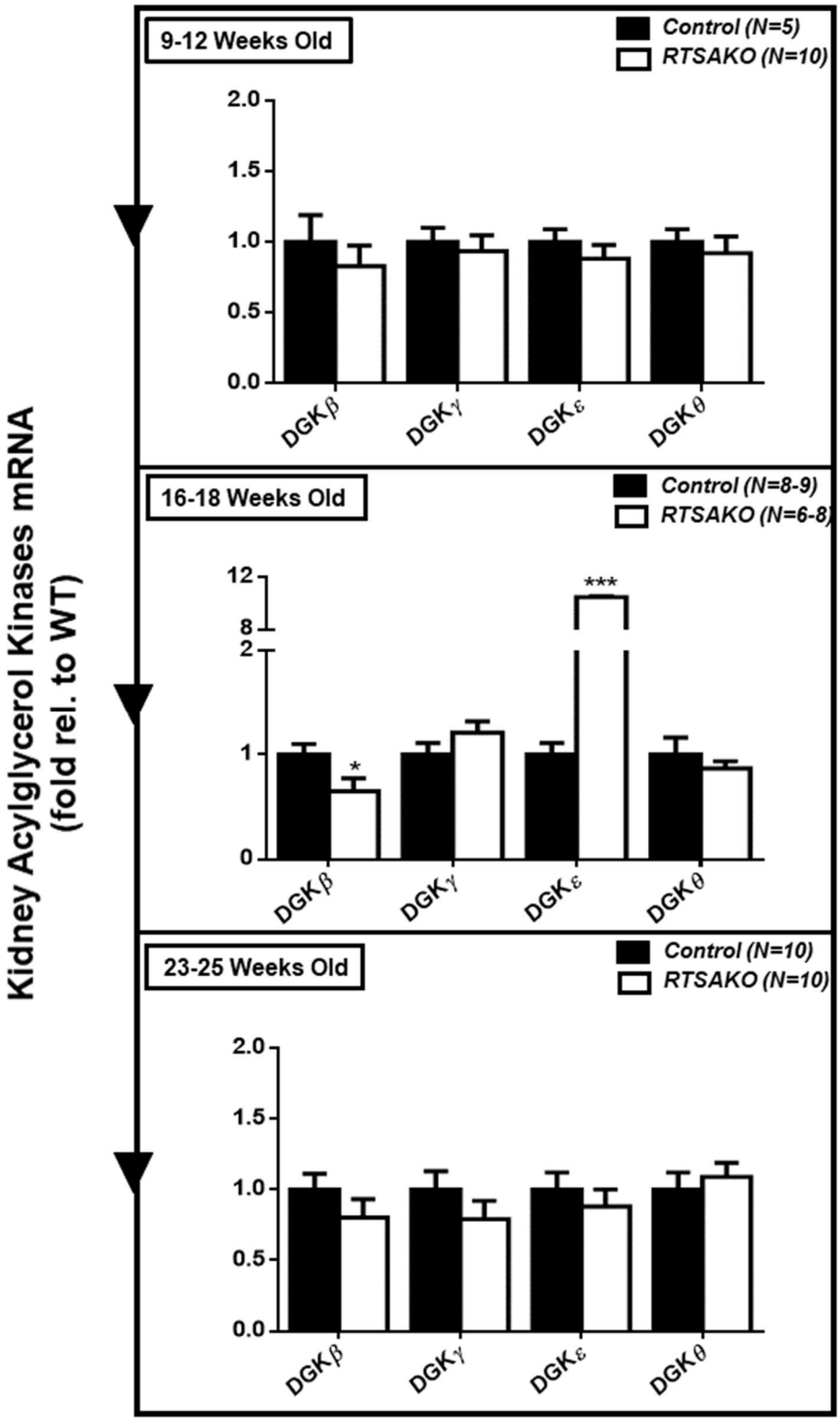

Figure 20: Expression of Diacylglycerol Kinase Variants in the Kidneys of Male Mice.
*No significant differences were observed in the expression of any of the DGK variants between RTSAKO and control littermate mice before or after chronic dysglycemia (top and bottom). However, at initial onset (16-18 wks), Dgkβ expression is significantly lower and Dgkε expression is significantly higher in RTSAKOs relative to controls (middle). *P<0.05, ***<0.0001; (N=5-10).*

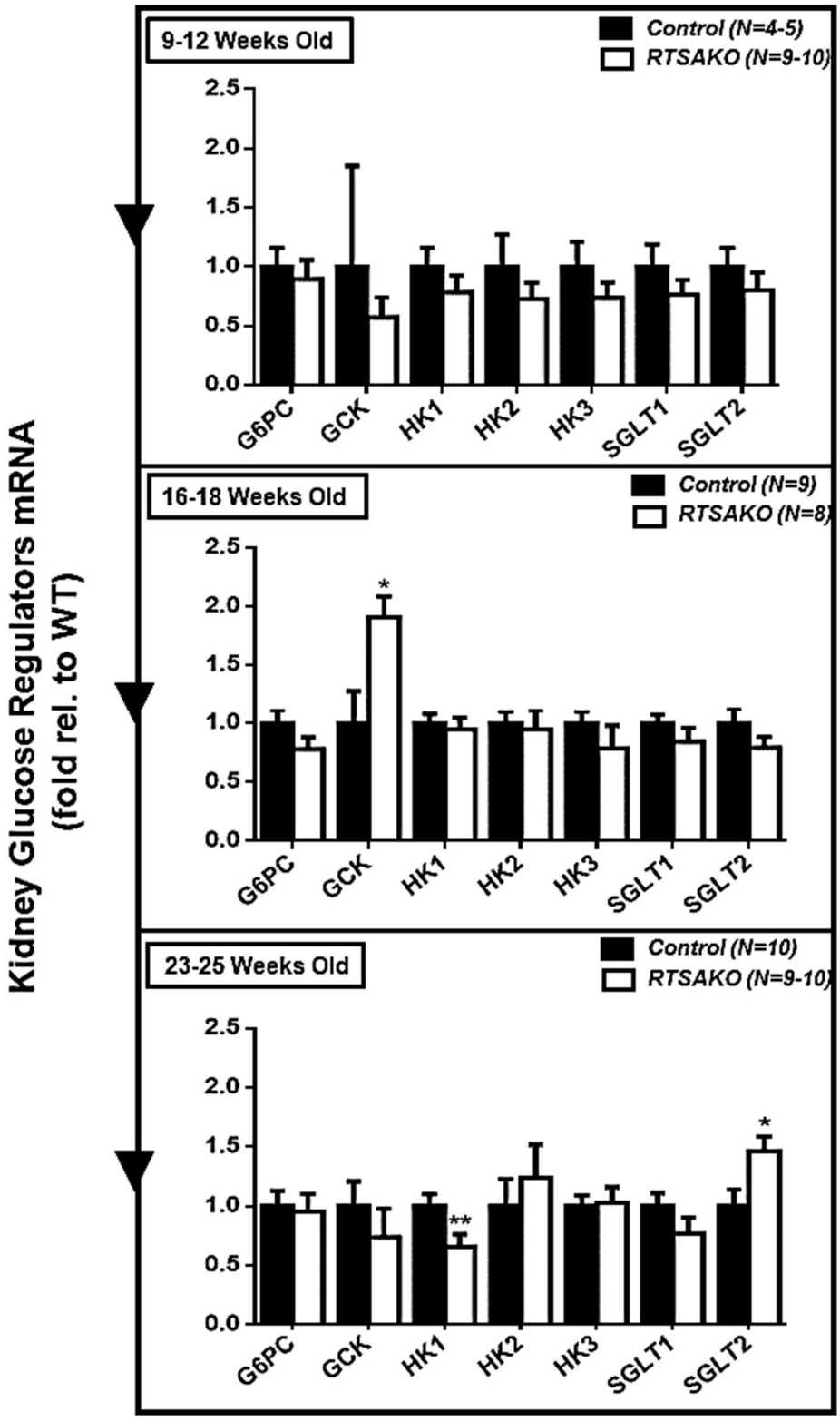

Figure 21: Expression of Glucose-Regulating Genes in the Kidneys of Male Mice.
*No significant differences were seen prior to onset of dysglycemia (top). Gck expression was significantly higher in knockouts relative to controls at the time of onset (middle). By 23-25 weeks of age, Hk1 expression was significantly lower and Sglt2 expression was significantly higher in RTSAKO mice relative to control littermates (bottom). *P<0.05, **P<0.01; (N=4-10).*

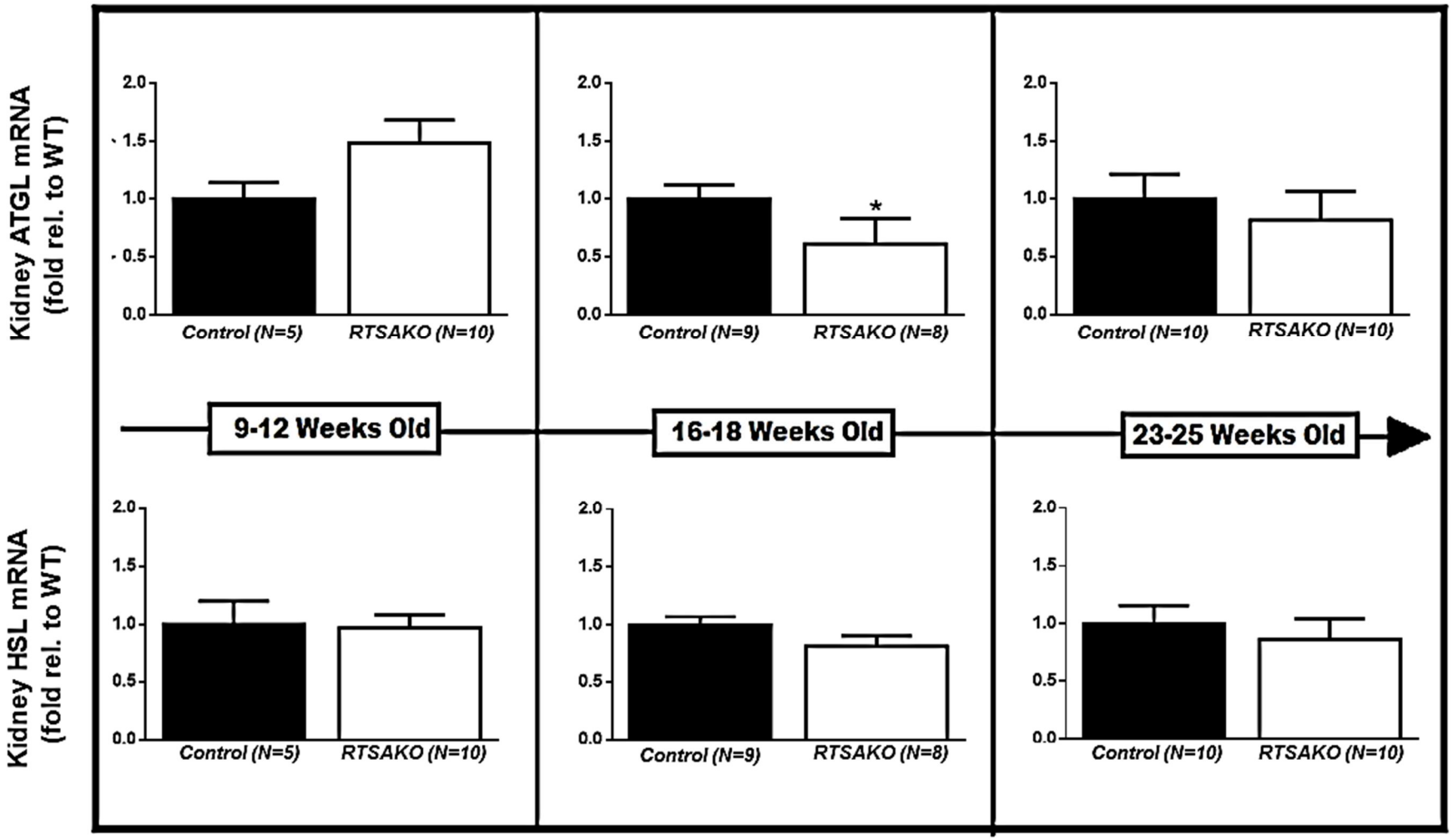

Figure 22: Expression of Lipolysis Regulating Genes in the Kidneys of Male Mice.
*No significant differences were observed in kidney Atgl expression in RTSAKO versus control littermate mice at 9-12 weeks and 23-25 weeks. At 16-18 weeks (middle) Atgl expression is significantly lower in knockouts relative to controls. Total Hsl gene expression did not appear to be significantly different between the two groups at any of the time points. *P<0.05; (N=5-10).*

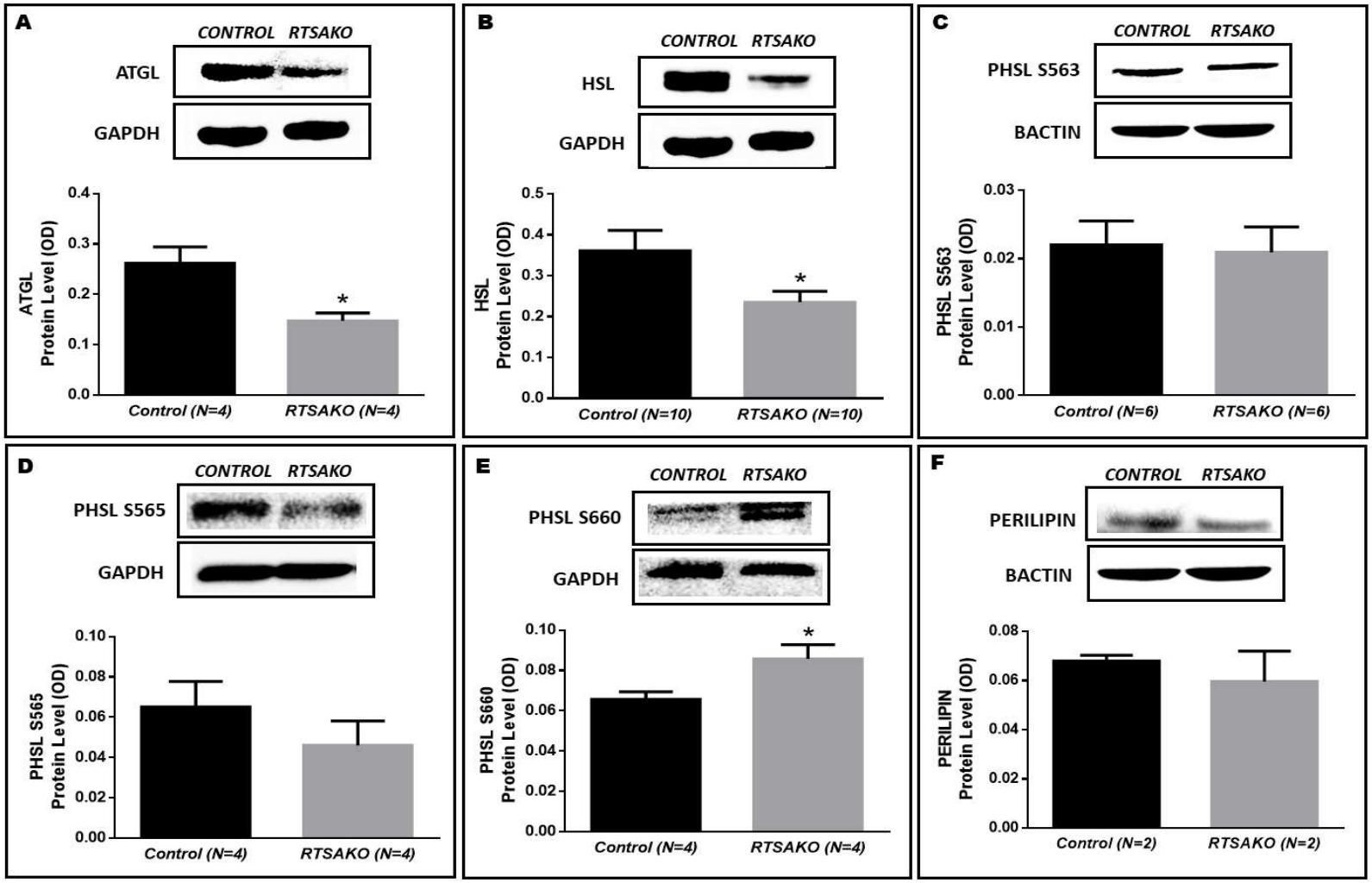

Figure 23: Quantification of Lipolysis Regulating Proteins in the Kidneys of Male Mice at 16 wks-of-age.
*(A) Total ATGL and (B) HSL protein were significantly lower in the kidneys of knockouts in comparison to controls. Activated HSL (phosphorylation at S563, 565, and S660) showed that (C) PHSL S563 abundance was not different between RTSAKOs and controls, (D) PHSL S565 abundance was lower in RTSAKOs but did not reach significance, and (E) pro-lipolytic PHSL S660s was significantly more abundant in the kidneys of RTSAKOs relative to controls. (F) No difference was observed in preliminary measures of renal perilipin. Immunoblot protein quantification is relative to total protein per lane. BACTIN and GAPDH were used as house-keeping loading controls. *P<0.05; (N=2-10).*

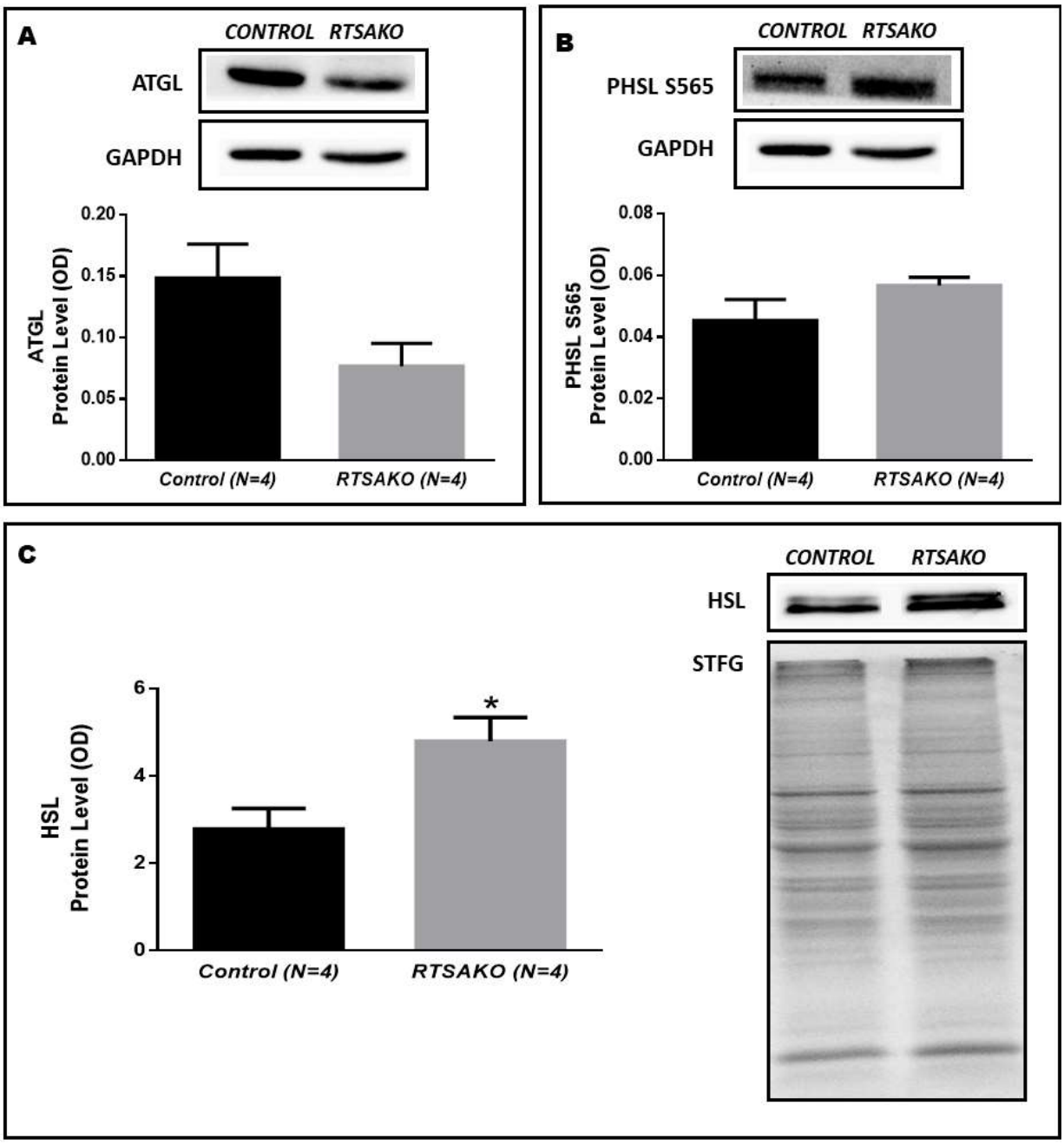

Figure 24: Quantification of Lipolysis Regulating Proteins in the Kidneys of Male Mice at 23-25 weeks of age.

*(A) Total ATGL is lower in RTSAKOs in comparison to control littermates but does not reach significance. (C) Total HSL protein is significantly more abundant in knockouts in comparison to control littermates. (D) PHSL S565 abundance was slightly higher in RTSAKOs relative to controls but did not reach significance. Immunoblot protein quantification is relative to total protein per lane. GAPDH was used as a house-keeping loading control, otherwise, a stain free gel (STFG) was used to show equal loading. *P<0.05; (N=4).*

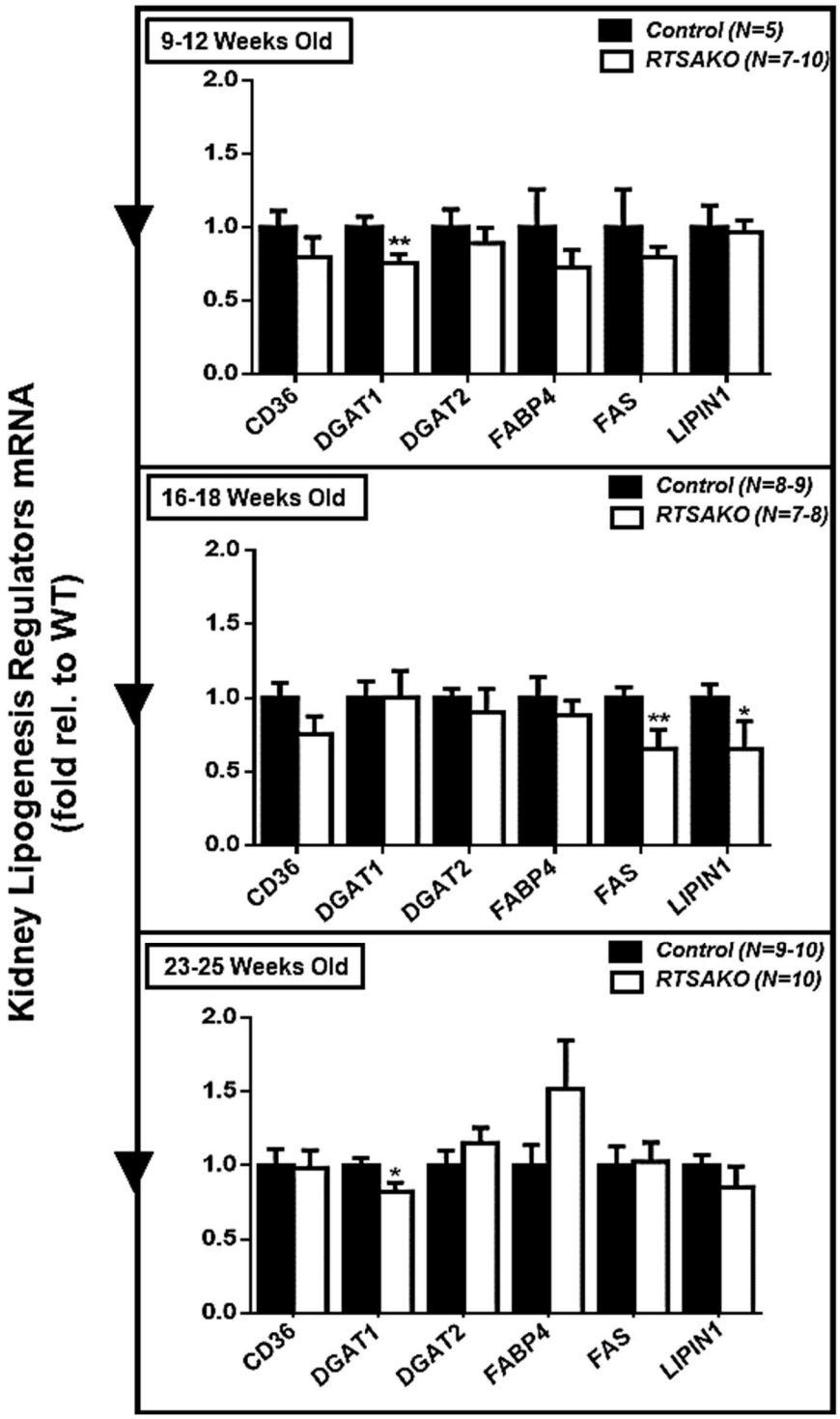

Figure 25: Expression of Lipogenesis Regulating Genes in the Kidneys of Male Mice.
*Before glucose intolerance onset (top), knockouts appear to have less Dgat1 expression relative to controls. At onset (middle) knockouts present with a significantly lower expression of Fas and Lipin1 relative to controls. After onset (bottom) Dgat1 appears to, once again, be significantly lower in knockouts. All other genes show no significant difference in expression between knockouts and controls at the different time points. *P<0.05, **P<0.01; (N=5-1).*

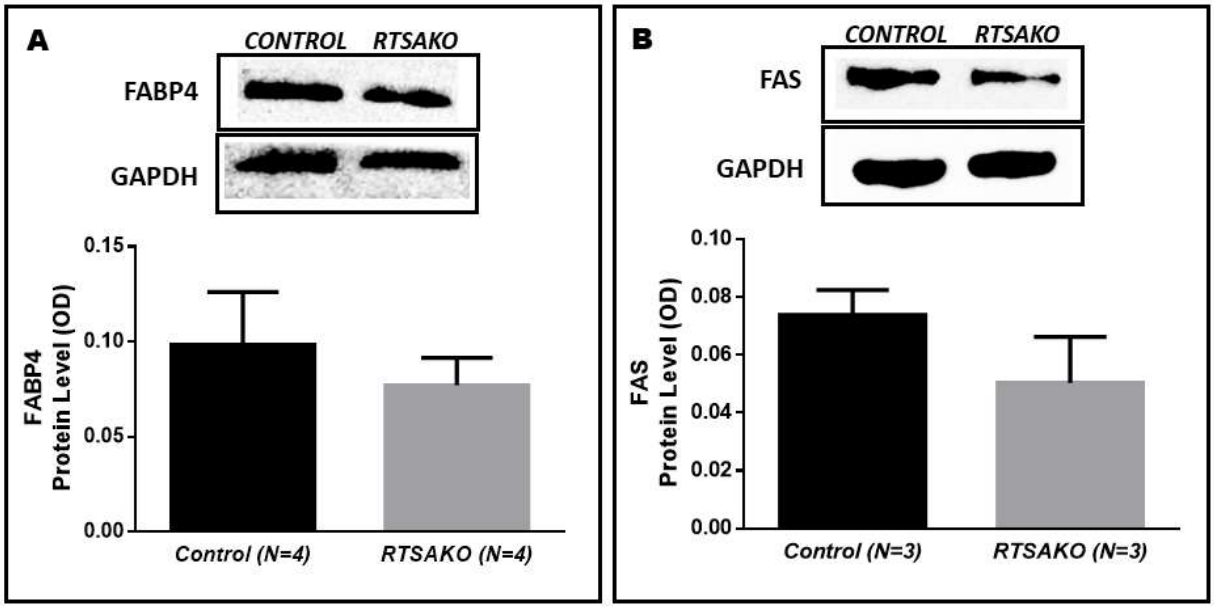

Figure 26: Quantification of Lipogenesis-Regulating Proteins in the Kidneys of Male Mice at 16 weeks of age.

(A and B) No significant differences were detected by immunoblot analysis for the abundance of FABP4 and FAS proteins in the kidneys of 16wk-old male mice, although both appeared to be lower in knockouts relative to controls at this time point. Protein quantification is relative to total protein per lane. GAPDH was used as a house-keeping protein loading control. (N=3-4)

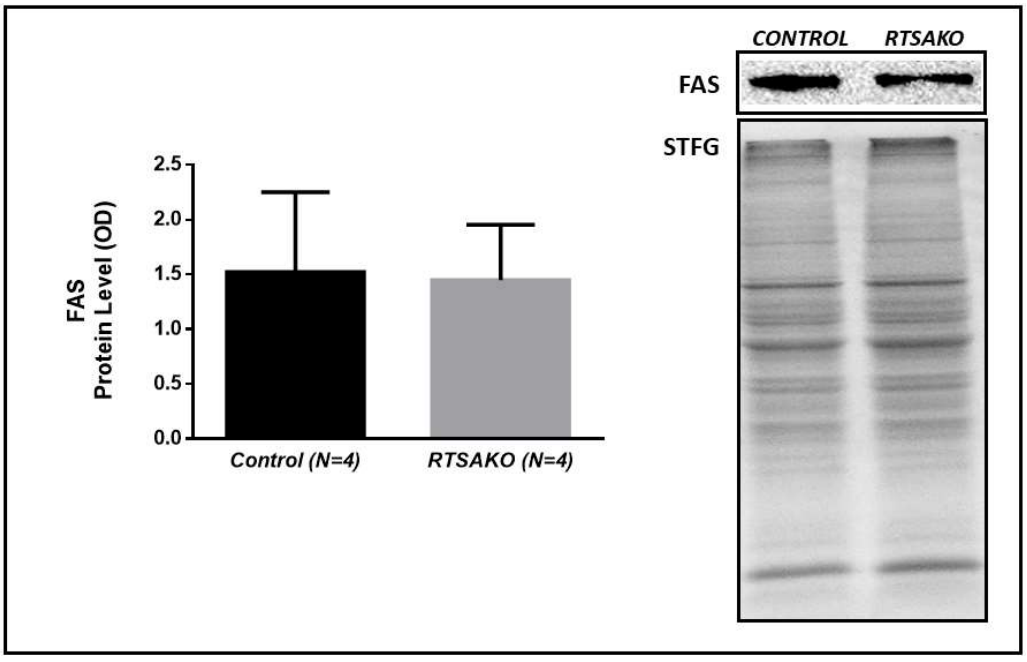

Figure 27: Quantification of Lipogenic FAS protein in the Kidneys of Male Mice at 23-25 weeks of age.

Immunoblot quantification of FAS protein levels in the kidneys of 23-25 wk old male mice showed no difference in abundance between the knockouts and controls. Protein quantification is relative to total protein per lane. A stain free gel (STFG) was used to show equal protein loading. (N=4).

Cre-expression is Restricted to the Kidney

To confirm the specificity of *Atgl* ablation, analysis of *Cre*-recombinase mRNA expression was conducted in various tissues from a *knockout* mouse (Figure 17). The *Cre*-recombinase gene exists downstream of a kidney-specific promoter, Ksp-cadherin, and is predicted, and has been shown by others, to only be expressed in regions where this promoter would be active (i.e. exclusively in basolateral tubule epithelial cells)[114]. In contrast, *Cre* is present throughout the genome, but is not expected to be expressed in any other tissue. This was confirmed after RNA was collected from various organs from a *knockout* mouse and converted to cDNA for gene expression analysis by PCR using primers specific for *Cre* and primers for the housekeeping gene, *Gapdh* (Figure 17). The first lane shows an amplification of genomic DNA prepared from tail snips that demonstrates the genomic presence of the *Cre* transgene. This is not a measure of the expression of this gene, but merely demonstrates its presence in the genetic code. The next lane shows that kidneys express *Cre*-recombinase, since RNA collected and converted to cDNA contains *Cre* transcripts that encode for the Cre protein, which will excise floxed *Atgl*. All other tissues tested do not show any trace of *Cre* transcript, but abundant expression of the *control* gene *Gapdh*. Therefore, *Cre*-recombinase is solely expressed in the kidneys of *knockout* mice, confirming renal specificity of *Atgl* ablation, and the validity of this model for the study of isolated renal steatosis in glucose regulation.

Kidney Mass is Not Increased Despite Induced Steatosis

Changes in the weight of an organ may indicate the presence of pathologies and organ irregularities, such as lipid accumulation (steatosis)[115]. As presented in Figure 18, there were no significant difference in body weight or kidney weight between the *knockouts* and *control* mice. This was somewhat unexpected. With attenuated lipolysis, occurring as a result of *Atgl* ablation, I expected to see a slight increase in *RTSAKO* kidney weight as a result of lipid accumulation. However, ablation was restricted to the renal-tubules and the contribution of lipid accumulation may not be discernable in the overall kidney weight. To distinguish the lipid accumulation occurring in the kidneys of *knockout* mice, more sensitive measures should be employed, such as thin layer chromatography (TLC) lipid extraction to confirm TAG accumulation or through the localization of lipid accumulation in renal-tubules by Oil-Red-O staining.

DGKε is the potential mediator for LPA synthesis in *RTSAKO*s

Autotaxin is the predominant enzyme responsible for the synthesis of LPA in blood. Mice totally deficient in this enzyme are not viable, but heterozygous total *knockouts* have been studied and present with a 50% reduction in plasma LPA. The expression of *Atx* has been assessed in the kidneys, and upregulation has been associated with the development of renal

disease and diabetic nephropathy[105]. Despite elevations in LPA production, the expression of *Atx* in the kidneys of *RTSAKO*s show no significant difference in comparison to *controls* at any of the time points assessed (Figure 19).

Another potential mediator responsible for the production of renal LPA is a DGK, which can produce LPA by phosphorylating MAG[60,94]. There are various DGKs that could complete this synthesis reaction, and may be responsible for LPA elevations observed at 16-18 weeks. DGKs have been implicated in a wide variety of pathophysiological events[106] and have demonstrated significant MAG kinase activity[106]. At 9-12 weeks of age, as expected, all DGK variants assessed showed no difference in expression between the *RTSAKO*s and *control*s (Figure 20). Similarly, at 23-25 weeks no differences were observed. However, at 16-18 weeks, the time of dysglycemia onset and significantly elevated LPA, a ten-fold higher *Dgkε* expression was observed in *RTSAKO* kidneys relative to *controls* and suggests it may be the potential mediator responsible for increased LPA synthesis. Of interest, *Dgkε* is constitutively expressed in murine kidneys, and is implicated in the development of membranoproliferative glomerulonephritis (MPGN), a condition characterized by fibrotic kidneys[109]. It also is heavily expressed in podocytes, and appears to play a key role in lipid mediated intracellular-signaling[109]. Furthermore, it is believed that perturbations caused by this variant in the kidneys extend to endothelium signaling[109], but this requires verification, although it may explain the elevation of LPA in serum. The lack of higher *Dgkε* expression in *knockout*s at 23-25 weeks of age could potentially be a result of the constitutive activity of the enzyme. It will be important to run immunoblotting analyses and lipid kinase assays to determine if protein levels are increased, even if mRNA levels are no longer significantly higher in the older animals.

Chronic exposure to dysglycemia results in differences in glucose-regulator gene expression that could exacerbate hyperglycemia

The indirect contributions of the kidneys in dysglycemic onset (through lowered insulin) have already been established since a causative relationship between renal-LPA signaling and dysglycemia has been confirmed. However, the direct contributions of the kidneys in aggravating glucose levels were unknown. Since the kidney play an important role in systemic glucose production and utilization, and these processes are regulated by insulin, I hypothesized that a reduction in insulin signaling could contribute to hyperglycemia during a glucose challenge in *RTSAKO* mice, at least in part, by allowing for the continuous over activity of glucose producing enzymes (G6Pase, SGLTs) in kidney, coupled with a lack of renal induction of hexokinases responsible for glucose trapping and utilization (HK1-3).

As expected, at 9-12wks of age prior to the onset of dysglycemia, *RTSAKOs* show no significant difference in the expression of any glucose regulating enzymes relative to *controls*. At

the time of onset of glucose intolerance (i.e. 16-18wks), however, there appears to be a significantly higher expression of *Gck* in *knockout* kidneys in comparison to *controls,* but no significant differences in the expression of other glucose regulating genes (Figure 21). GCK is a unique hexokinase in that, unlike HK1-3, it is not inhibited by its product G6P and has low affinity to glucose. As a result, it is predominantly active during periods of elevated glucose availability and is positively regulated by insulin. I expected lower expression in *knockouts* because of attenuated insulin, but high expression could be a result of increased glucose availability in renal cells through reuptake, although *Sglt* expression was not significantly different. However, *Gck* expression is especially abundant in the pancreas and liver, and little is known about its expression in the kidneys[72]. Upon further assessment of the data, it appears that expression of *Gck* is very low in the kidneys of both *knockouts* and *controls*, and that qPCR threshold is reached at a very high Ct level (~32) relative to most other genes that reach Ct below 20 cycles. Thus, the relative abundance of GCK is likely quite low, and the importance of this gene in regulation of kidney glucose trapping is likely also to be minimal.

At 23-25wks, *knockouts* present with significantly lower expression of *Hk1*, alongside significantly higher *Sglt2* expression relative to *control*s (Figure 21). There are three *Hks* that are expressed in the kidney, however, HK1 is the principle isoform accounting for 70% of total glucose phosphorylating enzymes in the functional kidney[69,116]. HK2 and HK3 make up the remaining 30%, and *Hk2* has been shown to be regulated by insulin and was expected to be lower, but little is known about *Hk3*[69,116]. Little is also known about the transcriptional regulation of *Hk1*, however it is mitochondria bound and allosterically inhibited by its product, G6P[69,116]. HK1 acts to promote glycolysis by mediating the commitment of glucose to glucose-6-phosphate for energy use[70]. At this time point, the kidneys of *RTSAKO* mice have had consistent exposure to elevated glycemia. Constant high levels of glucose in the filtrate leads to increased substrate for HK1, and also increased G6P synthesis. This increase in G6P production could potentially explain a downregulation in HK1 protein, although this was not measured, but allosteric negative feedback, which is a post-translational effect, does not *per se* explain the lower gene expression.

This raises the question of glucose transport into renal cells. *Sglt1* is expressed in the kidneys at low levels, however *Sglt2* is predominantly expressed in the proximal tubules of the kidney. *Sglt2* expression is often upregulated in diabetics in response to increased glucose in renal filtrate, which supports the significantly higher expression observed in 23-25wk old *knockouts* in comparison to normoglycemic *control*s (Figure 26)[12]. SGLT2 receptors exist on the apical (filtrate) surface of the proximal tubule epithelia and act through active co-transport of sodium to move glucose from the filtrate to the cytoplasm of the tubule cells[12]. Under normal conditions, all glucose in the filtrate is reabsorbed[62]. With chronic hyperglycemia, glucose in the

filtrate is increased, and SGLT2s are saturated. As a result, expression of these receptors are upregulated to meet with the demands brought on by increased filtered glucose. On the basolateral side of the cell exist GLUT2 transporters, that allow for the diffusion of glucose to the vasculature and other surrounding renal cells. High *Sglt2* expression would lead to increased glucose reuptake and potentially exacerbate hyperglycemia.

Higher expression of the gluconeogenic enzyme G6Pase in *knockouts* was hypothesized but not observed transcriptionally in any of the age cohorts. The literature suggests that G6Pase activity is upregulated in diabetes and negatively regulated by insulin[13]. Therefore, a decrease in insulin and a hyperglycemic state strongly suggests that *RTSAKO* mice should show higher expression of *G6Pase* in comparison to *control*s. However, it is possible that *RTSAKO* mice adaptively inhibit G6Pase activity through allosteric regulation to prevent furthering hyperglycemia, and it is recommended that an enzyme assay be employed to test for activity of this enzyme despite no differences in transcription.

Attenuated renal ATGL, alongside pro-lipolytic low insulin, likely causes an adaptive compensation by *knockout*s with regards to HSL-mediated lipolysis

*RTSAKO*s have decreased renal-tubule lipolysis as a result of *Atgl* ablation. However, diminished circulating insulin results in HSL phosphorylation, and may elevate HSL-mediated lipolysis. I hypothesized that *RTSAKO*s would have lower *Atgl* expression at 9-12 wks in comparison to *controls*, but no significant differences in lipid regulating enzymes otherwise. However, these mice showed no significant difference in *Atgl* or *Hsl* expression at this earliest timepoint (Figure 22). The reason for this is not clear, although it is likely attributable to a slight, adaptive induction of ATGL in surrounding cells with intact *Atgl*. In 16-18 and 23-25 week old mice, I expected that *Atgl* expression would be attenuated due to gene ablation, and that *Hsl* would be higher in *knockout*s in response to lower circulating insulin. In agreement, *Atgl* expression was significantly lower in 16-18wk old *knockouts* relative to *controls*. Additionally, western blot analysis of *RTSAKO* kidneys at 16-18wks showed significantly lower abundance of ATGL protein in *knockouts* versus *controls* (Figure 23A). Notably, the magnitude of this effect was larger than the effect that was evident for mRNA regulation, suggesting translational or posttranslational mechanisms of ATGL regulation in *RTSAKO* mice. Gene expression of *Atgl* was not significantly lower in 23-25wk old *RTSAKO* mice, and once again could suggest an adaptive increase in expression within surrounding renal cells, masking any differences expected (Figure 22). Immunoblotting at this time point revealed, as expected, lower ATGL abundance in *knockout*s relative to *control*s although not reaching statistical significance (Figure 24A)

With a reduction in available ATGL, I suspected that HSL would compensate in the mediation of TAG breakdown because of its broad substrate specificity, in the 16-18 and 23-25

week old *knockout* mice. Although no differences in *Hsl* were observed transcriptionally at either of these time points (Figure 22), western blot analysis showed significantly lower HSL protein abundance in *knockouts* at 16-18wks (Figure 23B) but significantly more abundant levels of activated PHSL S660 protein in *knockouts* (Figure 23E). HSL action is regulated by phosphorylation at its serine residues, mediating different activities, and phosphorylation can be regulated by different enzymes in response to various stimuli[29,42]. PHSL S660 phosphorylation is driven by protein kinase A (PKA) activity which is inhibited by insulin stimulation[29]. Therefore, impaired insulin secretion likely prevents the inhibition of PKA, increasing HSL phosphorylation at S660, which stimulates lipolysis. Assessment of activated HSL at serine 563 (Figure 23C) showed no difference in abundance between the two groups. The exact role PHSL S563 plays in lipolysis remains unknown and its activation is often delayed in response to stimulation in comparison to phosphorylation at other serine residues. PHSL S565 is a target of adenosine monophosphate-activated protein kinase (AMPK) phosphorylation, and although not reaching significance, appears lower in *knockout* kidneys relative to *controls* (Figure 23D). Studies are conflicting on whether AMPK activity promotes[117] or inhibits[118] lipolysis activity, although Daval and colleagues[118] found that AMPK phosphorylation at the S565 residue prevents HSL translocation to the lipid droplet. Therefore, higher pro-lipolytic PHSL S660, coupled with a lower in anti-lipolytic PHSL S565, is expected to favour HSL-mediated lipolysis in *RTSAKO* mouse kidneys. Perilipin, the enzyme responsible for the translocation of HSL to the lipid droplet, does not appear to show a difference in abundance between *knockouts* and *controls* although more mice are needed for statistical analysis (Figure 23D). I did not assess perilipin phosphorylation, but it would be interesting to determine if patterns are altered, since this protein is regulated by some of the same enzymes that mediate HSL phosphorylation.

Finally, total HSL is significantly more abundant in *knockouts* after chronic exposure to dysglycemia and impaired insulin secretion (23-25wks) (Figure 24C). Assessment of PHSL S565 showed slightly more abundance in *knockout*s relative to *control*s, but was not significant. Analysis of HSL phosphorylation at other serine residues would be required to better understand the activity of HSL at this time point (Figure 24B). These findings corroborate the hypothesis that chronic exposure to low insulin secretion alongside attenuated *Atgl* results in an adaptive shift towards expression patterns that promote HSL-mediated lipolysis.

Low circulating insulin and elevated TAG may mediate lower lipogenic expression

Insulin acts to promote lipogenesis. Thus, with diminished circulating insulin, expression of enzymes promoting lipogenesis should become attenuated. I hypothesized that prior to glucose intolerance (9-12wks) no significant differences would be observed in the expression of these enzymes, but that with impaired insulin secretion during (16-18wks) and after prolonged

glucose intolerance (23-25wks), lipogenesis would be decreased. As shown by Figure 25, no significant difference was observed in the expression of the regulatory genes assessed at 9-12wks, except for *Dgat1* which showed significantly lower expression in *knockouts* in comparison to *controls*. DGAT1 is responsible for the acylation of DAG to form TAG. Reduced *Dgat* expression can be a result of TAG accumulation, causing negative feedback, although little is known about transfactors regulating *Dgat* expression[119].

At 16-18wks of age, *Fas* and *Lipin* both show significantly lower expression in *knockout* mice relative to *controls*, but no notable differences were observed in other lipogenesis genes (Figure 25). FAS expression was supplemented by western blotting. FAS abundance at this time point also appeared lower in *knockouts*, but did not reach statistical significance (Figure 26B). FAS is responsible for the synthesis of fatty acids, and is tightly regulated by insulin [120] and so a reduction in insulin stimulation causes a downregulation in FAS levels and activity. LIPIN dephosphorylates phosphatidic acid to produce DAG, and its regulation remains poorly understood. The literature presents contradictory findings, suggesting that *Lipin* is downregulated in response to insulin[121], or that insulin does not alter transcription but induces LIPIN activity[122,123], and also that insulin shows no LIPIN inducing effects[124]. Finally, assessment of FABP4 showed no differences in both gene and protein expression (Figure 25 and 26A).

After chronic exposure to glucose intolerance (23-25wks), *knockouts* show no significant difference in the expression of various lipogenesis promoting enzymes, but *Dgat1* is significantly lower in *knockout*s relative to *controls* (Figure 25). Once again, little is known about *Dgat1* regulation, so whether this significantly lower expression can be a result of low insulin or accumulating TAG remains unclear. Western blotting at this time point also showed no significant difference in FAS abundance between *knockouts* and *controls* despite lower expression and abundance at the time point prior (Figure 27). Overall, *RTSAKO* kidneys show lower lipogenesis expression in comparison to their unaltered *control* littermates, which is an expected outcome in response to attenuated circulating insulin.

Chapter 7: The Liver

7.1 Introduction and Rationale

The liver is the main organ capable of glucose production in the body, and so plays an integral role in the maintenance of glucose homeostasis. After feeding, and elevated insulin signaling, the liver shifts enzymatic activity in favor of glucose disposal and glycogen synthesis, thereby lowering glycemia. However, in the fasted state, when the body is deprived of energy and circulating insulin is low, the liver acts to liberate glucose from glycogen stores (glycogenolysis) and through gluconeogenesis, for systematic use. These changes in liver glucose regulation are adaptive to systemic energy requirements. In the case of *RTSAKO*s, which present with low fasted insulin, glucose disposal is attenuated and dysglycemia manifests. Furthermore, chronically low circulating insulin can cause a maladaptive response in hepatic gene expression that favours glucose production over disposal and could potentially exacerbate hyperglycemia. However, the impact of indirect renal-LPA signaling (mediated through low insulin) on the expression of hepatic glucose-regulators is not known. In order to elucidate the effect of renal-hepatic communication in this model, and the contribution of the liver in mediating the dysglycemic phenotype observed, the expression of important mediators of glucose metabolism must be assessed. Therefore, the expression of genes involved in hepatic glucose production and storage regulators were measured in *RTSAKO* mice prior to (9-12 weeks), during (16-18 weeks), and after chronic exposure (23-25 weeks) to dysglycemia and compared to normoglycemic, healthy, age-matched *control*s.

In addition, the liver is a major regulator of blood lipids. Excess circulating glucose can be converted to fatty acids for storage in TAG[62]. While stored TAG must be liberated for incorporation into lipoproteins and exported from the liver, it also used as a metabolic fuel by hepatocytes. As a result, *RTSAKO* mice may respond to low insulin to enhance lipolysis expression, or, hyperglycemia may cause the liver to adapt towards storing TAG for metabolic use as a result of impaired hepatic glucose disposal. Thus, the expression of enzymes involved in lipolysis and lipogenesis must be tested over the course of dysglycemia progression and compared to values presented in *control* littermates to determine potential effects on hepatic lipid storage.

7.2 Liver-Specific Objectives

The overarching objective of this chapter is to study the expression of gene and protein regulators of glucose and lipid metabolism in liver prior to (*i.e.* 9-12 wks old), during (*i.e.* 16-18wks old), and after (*i.e.* 23-25wks old) onset of glucose intolerance in *knockouts* and normoglycemic *controls*.

Characterization of livers will include investigation of:

i. Alterations in liver weight.
ii. Alterations in the expression of enzymes involved in hepatic glucose release and disposal.
iii. Alterations in the expression and phosphorylation of lipolytic and lipogenic enzymes.

7.3 Results and Discussion

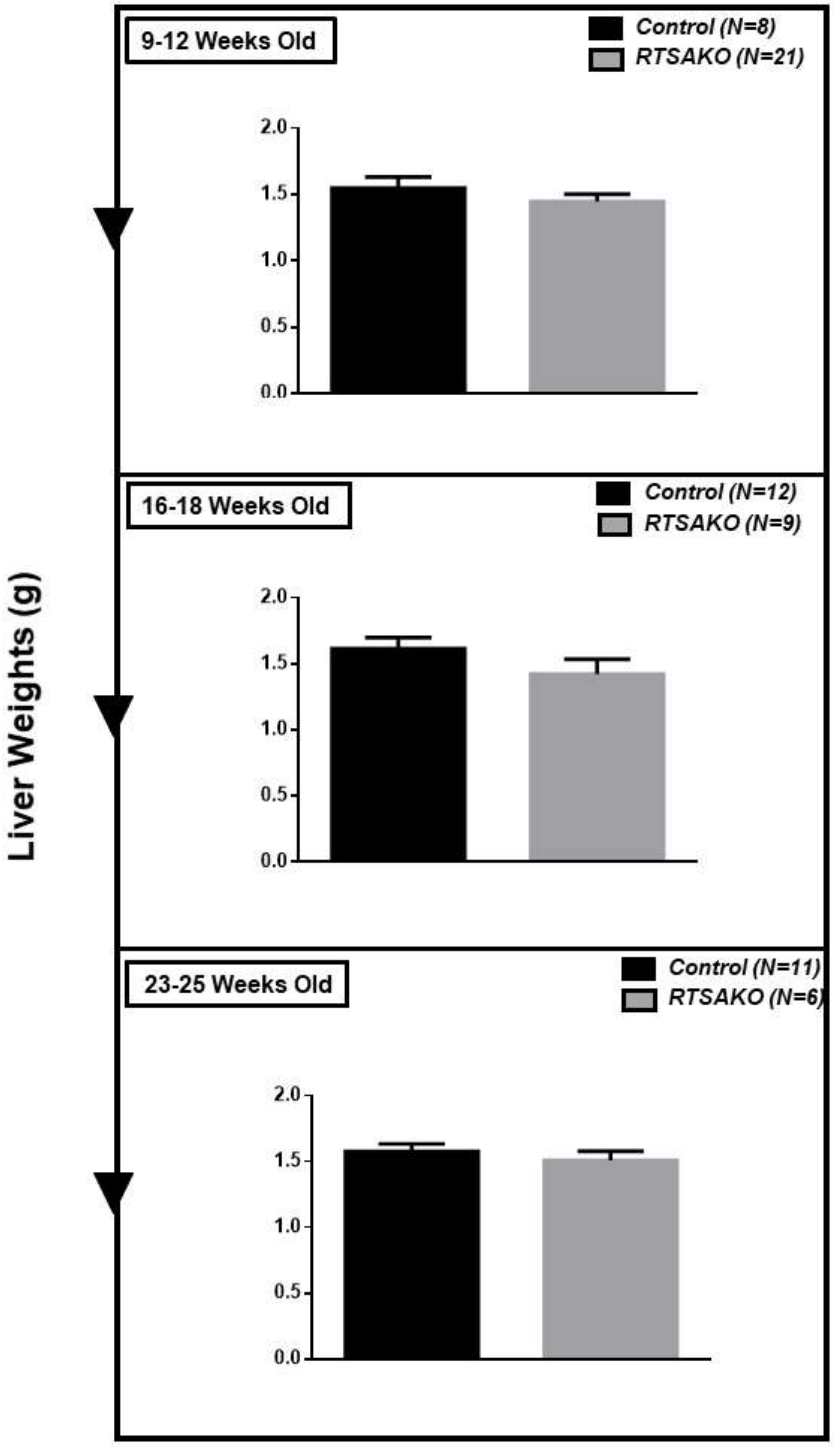

Figure 28: Liver Weights of Male Mice.
No significant differences in liver weight were observed between knockouts and controls over the course of aging (top to bottom). Knockout liver weights appeared slightly lower at 9-12 and 16-18 weeks of age, but were closer to controls by 23-25 weeks. (N=6-21)

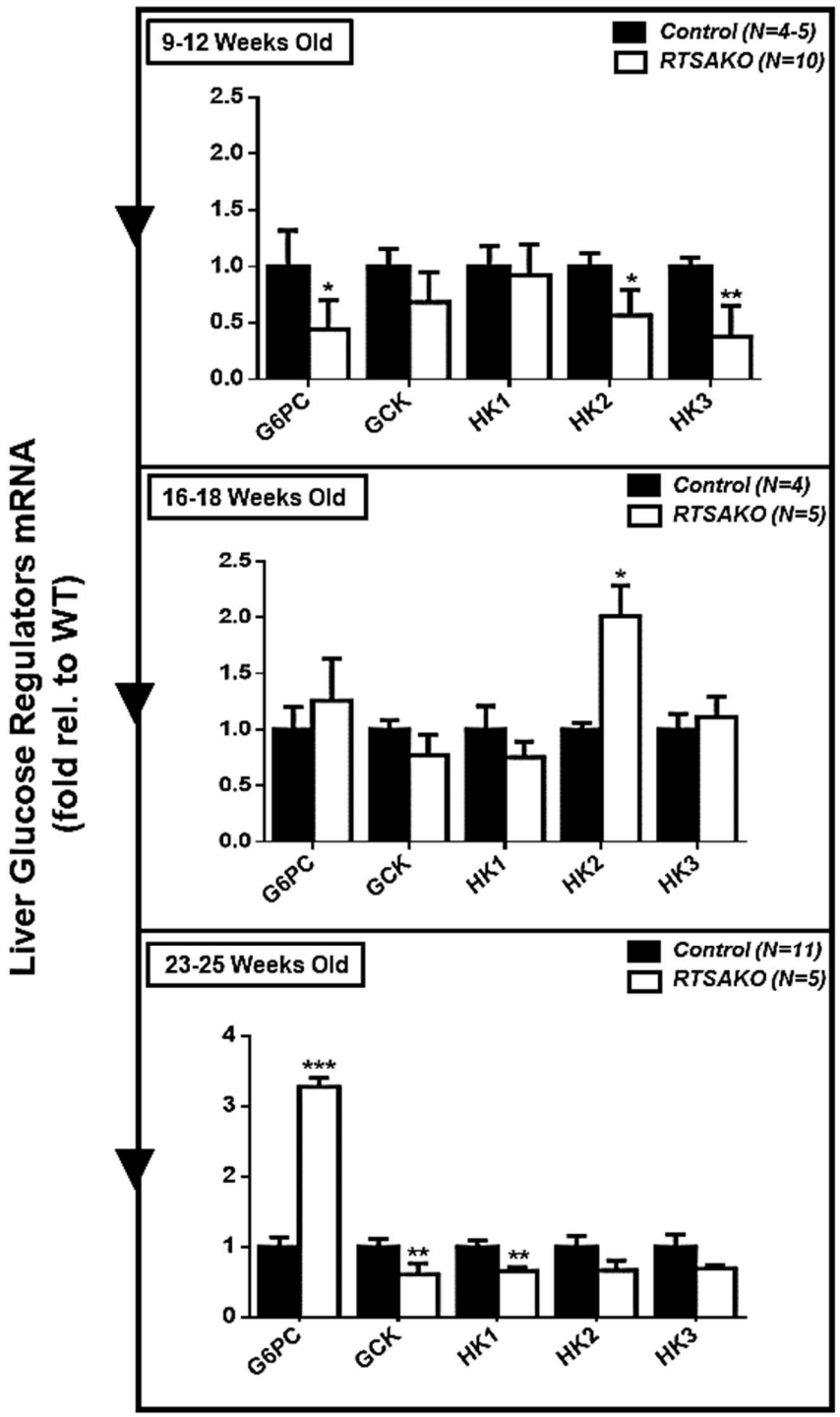

Figure 29: Expression of Glucose Regulating Genes in the Livers of Male Mice.
*Before the onset of glucose intolerance (top) RTSAKO mice showed significantly lower expression of G6pase, Hk2, and Hk3 in comparison to control littermates. During onset (middle) there was significantly higher expression of Hk2 in RTSAKO livers. After onset and chronic exposure to dysglycemia (bottom) RTSAKO males show significantly higher expression of G6pase and significantly lower expression of Gck and Hk1. All other genes at the various time points do not show a significant difference in expression in RTSAKO livers relative to controls. *P<0.05, **P<0.01, ***P<0.0001; (N=4-11).*

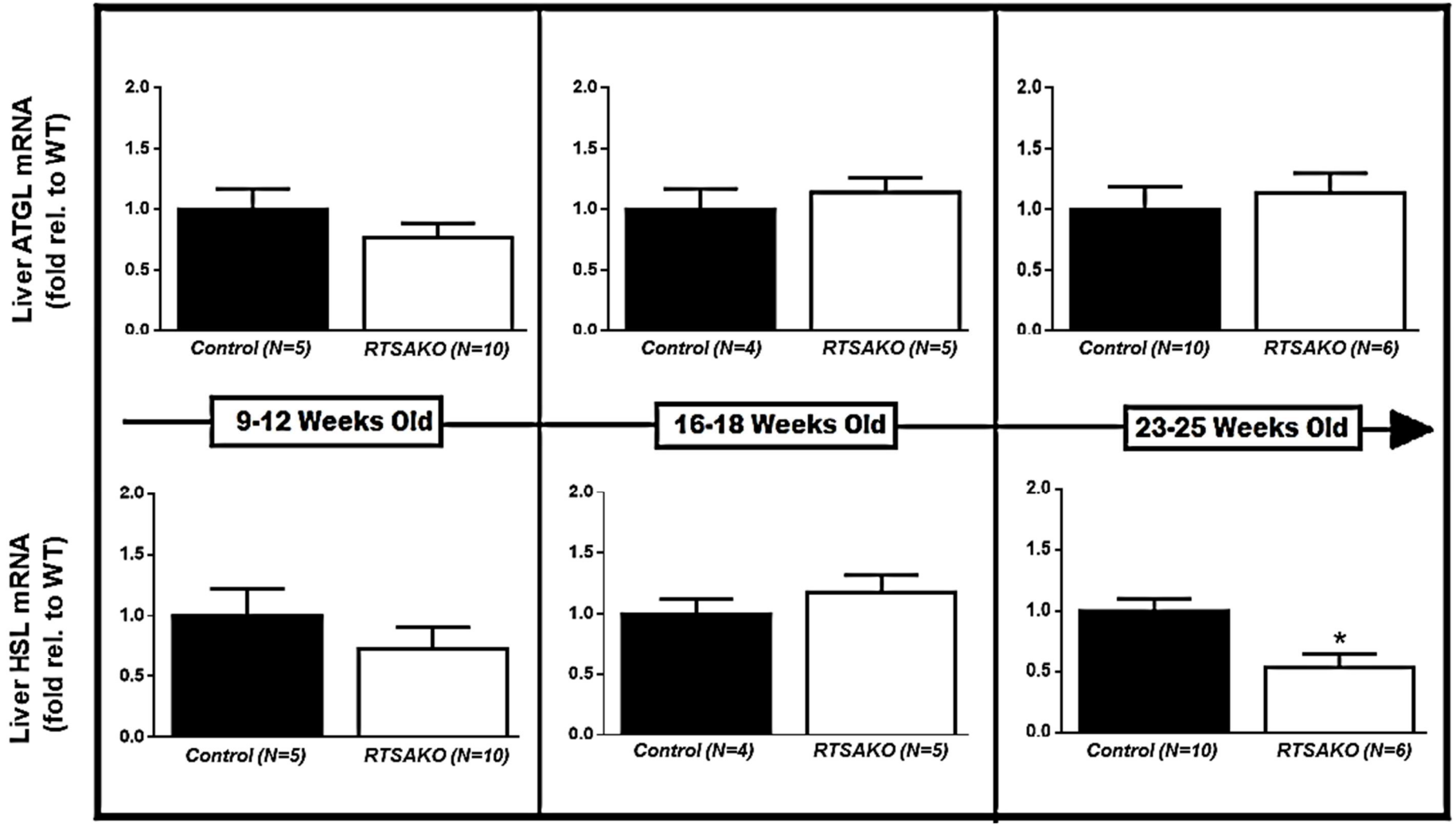

Figure 30: Expression of Lipolysis Regulating Genes in the Livers of Male Mice.

*No significant differences were observed in Atgl expression at any of the time points. Hsl expression was also not significantly different before or during onset, but after chronic dysglycemia (bottom right) Hsl expression was significantly lower in RTSAKOs in comparison to controls. *P<0.05; (N=4-10).*

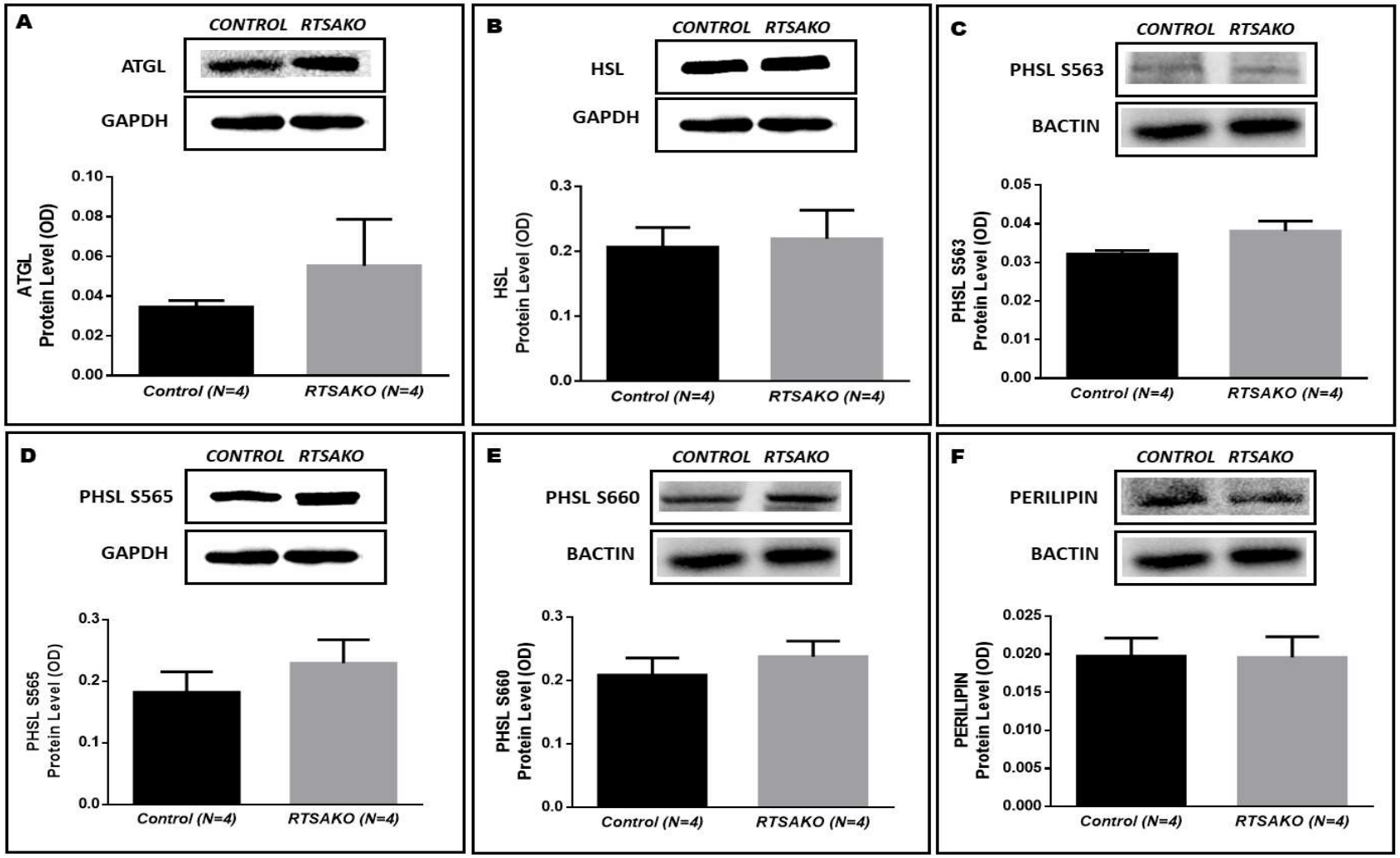

Figure 31: Quantification of Lipolysis Regulating Proteins in the Livers of Male Mice during dysglycemic onset (16-18wks).
No significant differences in protein abundance were observed in any of the proteins assessed at this time point. However, (A) ATGL and (C-E) PHSL S563, S565, and S660 all appear to have higher abundance in knockouts relative to controls, although (B) total HSL does not appear to be different. (F) Perilipin abundance also appears to be similar between the two groups. Immunoblot protein quantification is relative to total protein per lane. BACTIN and GAPDH were used as protein loading controls (N=4).

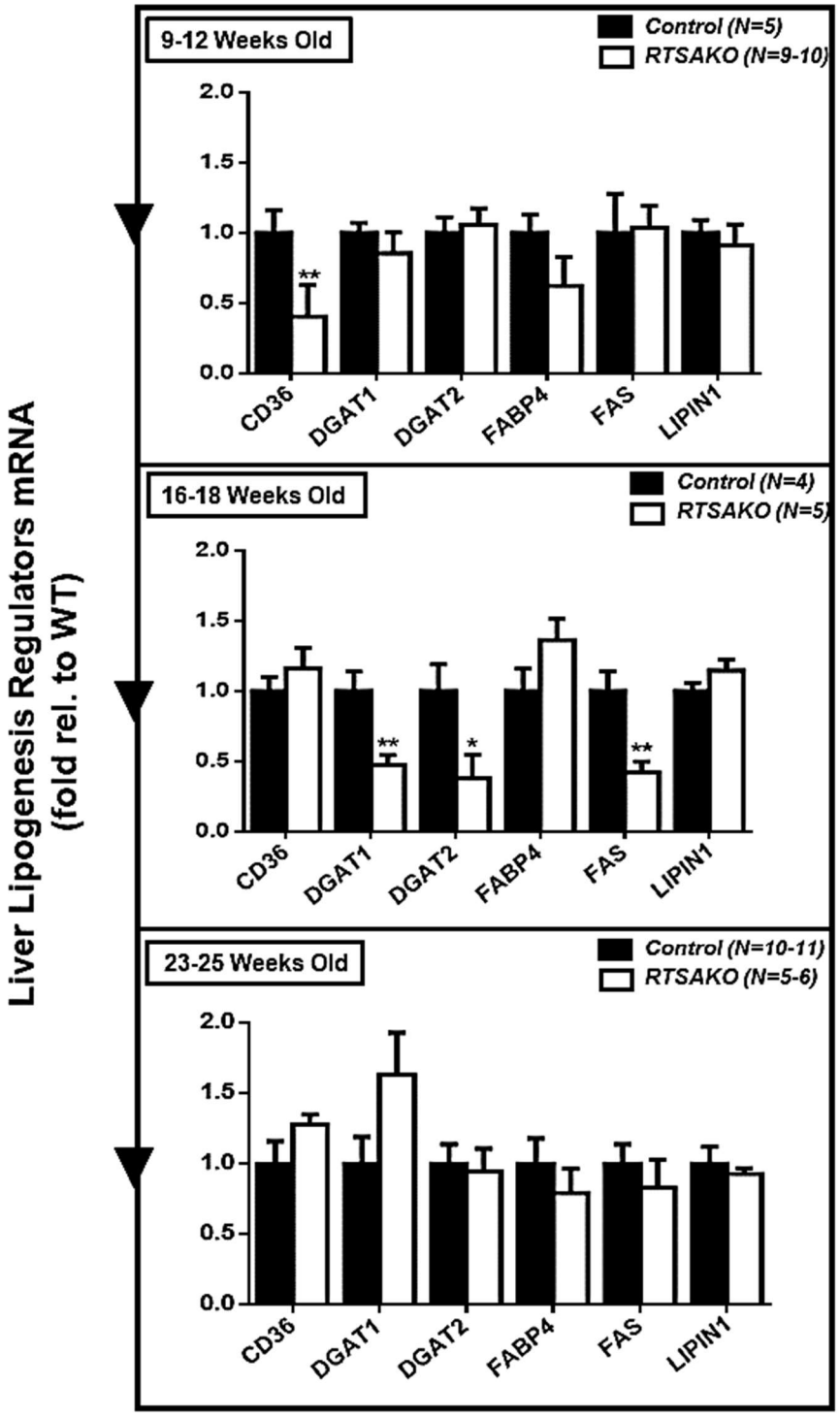

Figure 32: Expression of Lipogenesis Regulating Genes in the Livers of Male Mice.
*Before glucose intolerance onset (top), knockouts appear to have significantly lower Cd36 expression. At the point of onset (middle) knockouts present with significantly lower expression of Dgat1, Dgat2, and Fas. After onset (bottom), no significant differences were apparent in the expression of lipogenesis genes between the two groups. All other genes show no significant difference in expression between knockouts and controls at the different time points assessed. *P<0.05, **P<0.01; (N=5-10).*

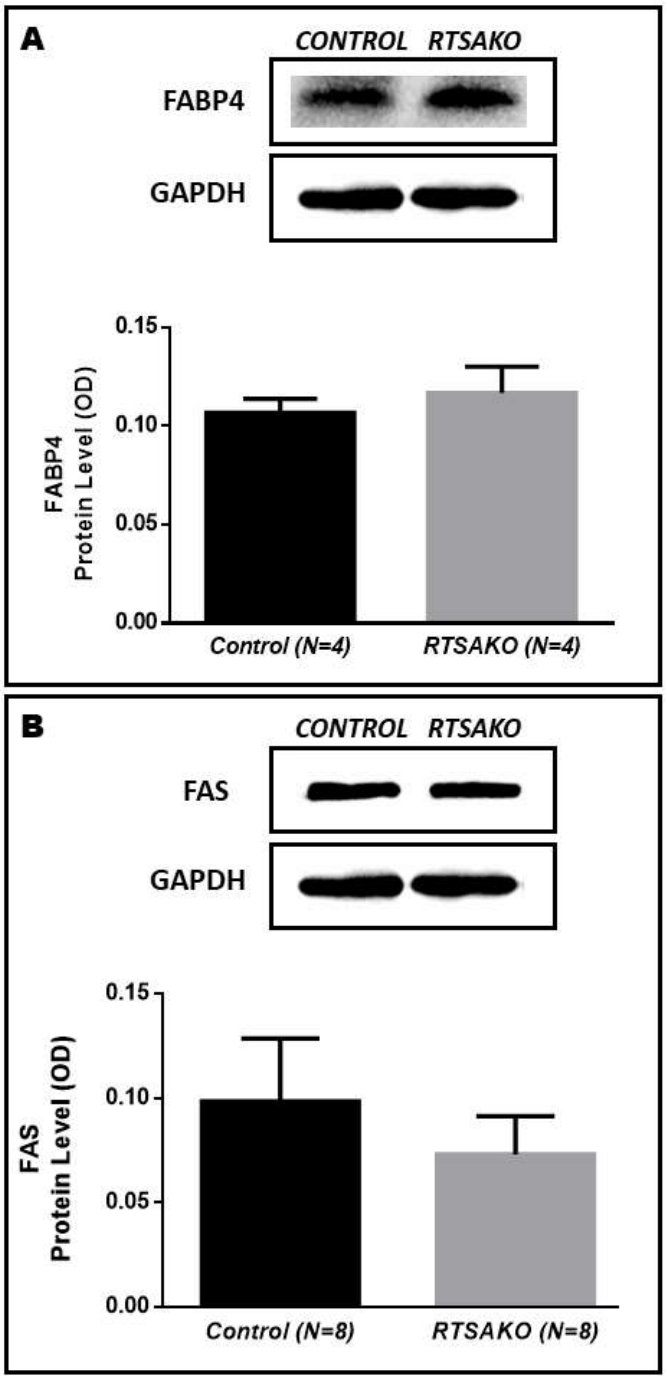

Figure 33: Quantification of Lipogenic Protein Abundance in the Livers of Male Mice during dysglycemic onset (16-18 wks).

FABP4 and FAS protein levels show no significant difference in abundance between the knockouts and controls, although FABP4 abundance appeared to be slightly higher while FAS was slightly lower in knockouts relative to controls which corroborates gene expression findings. Immunoblot protein quantification is relative to total protein per lane. GAPDH was used as a protein loading control (N=4-8).

RTSAKO liver mass is not different from normoglycemic *control*s, even after 5-7 weeks of chronic low insulin and dysglycemia

Similar to the kidneys, the livers showed no significant increase in weight in *knockouts* relative to *controls* (Figure 28). However, *knockout* liver weights appear lower at 9-12 and 16-18 weeks, but reach weights similar to *controls* by 23-25 weeks. Liver mass is used as a preliminary indicator of pathology, and as a marker of hepatosteatosis (lipid accumulation in the liver) which is a common risk factor association with chronic hyperglycemia[125]. In addition, the livers can be impacted by lipid accumulation in the kidneys, as they are a major site of lipid turnover. However, previous findings by the Duncan lab already established that despite accumulation of TAG in the kidneys, circulating NEFAs were no elevated in this model (data not shown). This suggests that *Atgl* ablation does not lead to hepatosteatosis as a result of the liver acting as a fatty acid sink. Despite this, chronic exposure to hyperglycemia, low insulin, and LPA can have proinflammatory and steatotic ramifications, and so this preliminary measurement is important.

Chronic exposure to low insulin and dysglycemia may induce maladaptive differences in gene expression that could further exacerbate hyperglycemia

The liver is an important organ in the regulation of glucose homeostasis; glucose disposal and release by hepatocytes significantly contribute to the regulation of circulating glycemia. As a result, the regulation of intracellular hepatic enzymes responsible for net glucose movement were assessed, since their activity is finetuned by insulin signaling[62]. At 9-12wks of age, *knockout*s show significantly lower expression of hepatic *G6pase*, *Hk2*, and *Hk3* relative to *controls*, but no difference in the expression of *Gck* (Figure 29). Moderately elevated insulin could explain lower *G6pase* expression in *RTSAKO* mice, but this is unlikely. Another explanation for this expression difference is if *knockout*s are more insulin sensitive in comparison to *control*s at this time point. *G6pase* is negatively regulated by insulin stimulation, and increased insulin sensitivity can cause enhanced downregulation of *G6pase* in hepatocytes[64]. However, this could not explain reduced expression of enzymes involved in glucose phosphorylation and trapping. In the liver, *Gck* is the primary hexokinase utilized for the disposal of glucose and the synthesis of glycogen, is induced by insulin, and is active with high glucose availability. The roles of *Hk2* and *Hk3* in the liver are unknown, but they are negatively regulated by their product G6P. If *knockouts* present with enhanced insulin sensitivity at this time point, low *Gck* could be explained by rapid disposal of available glucose by high-affinity hexokinases (HKs). This would also explain low *Hk2* and *Hk3* expression, since rapid disposal would mean high G6P levels that would inhibit hexokinase expression.

Dysglycemic onset at 16-18 weeks is likely a result of impaired insulin circulation. As a result, I hypothesized that low insulin would cause *knockout*s to present with higher expression

of hepatic glucose releasing genes (*G6Pase*), but lower expression of glucose disposal genes sensitive to insulin (*Hk2* and *Gck*). However, no significant differences in *G6Pase* or *Gck* expression were observed at this time point between the two groups (Figure 29). Interestingly, contrary to my original hypothesis, *knockouts* presented with significantly higher expression of *Hk2* relative to *controls*. *Hk2* is a cytosolic hexokinase that commits phosphorylated glucose to glycogen synthesis. It has been predominantly found in muscle, heart, and hepatic cancers. Furthermore, this specific isozyme has high affinity for glucose, is active at low glucose concentrations, and is positively regulated by insulin[68]. John *et al.*, suggest that *Hk2* converts glucose to G6P at low levels of intracellular glucose for glycogen synthesis, although this generation of G6P negatively regulates its activity[70]. The high expression of this hexokinase isozyme could be an adaptive response to reductions in glucose disposal, in an effort to utilize glucose as an energy source.

Interestingly, by 23-25wks of age, the observed patterns of gene expression in *RTSAKO* livers appear be maladaptive, and could potentially increase glycemia. This was an expected result considering chronic exposure to low insulin is considered maladaptive, and the resulting high G6Pase in combination with low GCK would favour a net movement of glucose extracellularly, furthering the development of hyperglycemia. At this time point, there was a significant, 3-fold elevation in *G6pase* (Figure 29 G6PC) expression in the livers of *knockouts* relative to *controls*. High *G6pase* expression in *knockout*s can prove detrimental, since this enzyme can contribute to hyperglycemia by constitutively liberating glucose from hepatocytes. Studies in diabetic animals have shown that dysglycemia is often coupled with upregulation in hepatic G6Pase activity[13]. In combination with higher glucose production gene expression, *knockout*s also showed lower glucose disposal gene expression in comparison to *control*s. Both *Gck* and *Hk1* expression were significantly lower in *knockout* livers and could potentially cause sustained and progressively worsening glucose intolerance (Figure 29). These differences in expression relative to *control*s is likely a consequence of reduced insulin stimulation[68]. As a result, chronic exposure to low insulin and dysglycemia in *knockout*s may have maladaptive consequences that would promote glucose release and further inhibit disposal, causing a potentially additive effect to dysglycemia.

RTSAKO hepatic lipid-regulation expression followed expected patterns at 9-12 and 16-18 weeks, however expression at 23-25 weeks was indicative of hepatosteatosis onset.

Transcriptionally, no differences were observed in the expression of *Atgl* or *Hsl* in the livers of *RTSAKOs* relative to *controls* at 9-12 wks or 16-18wks of age (Figure 30). The lack of significant difference at 9-12 wks was expected, because mice do not yet demonstrate metabolic impairments. *Knockouts* also showed significantly lower *Cd36* expression, which is a protein that

facilitates fatty acid transport from circulation into cells (Figure 32). Upregulated expression of this gene is implicated in the development of non-alcoholic fatty liver disease (NAFLD), so a significantly lower expression in *knockout*s may have protective effects on the liver by reducing fatty acid entry and lipid synthesis[126]. The reason for the reduced expression of this single gene prior to the onset of impaired glucose disposal is unclear.

The comparable transcription of *Atgl* and *Hsl* between *knockouts* and *controls* at onset (16-18wks), was also not surprising, since insulin is not typically regarded as a major transcriptional regulator of either of these enzymes, although it is a potent post-translational regulator of HSL (Figure 30). Western blot analysis at onset indicated that total protein levels of ATGL, PHSL S563, PHSL S565, and PHSL S660 were all higher in *knockout*s in comparison to *control*s, but none reach significance (Figure 31A, C-E). There is some evidence that ATGL protein levels may be negatively regulated by insulin in cultured adipocytes[127] and thus insulin-deficiency may increase hepatic ATGL levels, although analysis of additional samples, providing a greater *N*-value, will be needed to determine if a statistically significant effect is present. In accordance with the lack of difference in the transcriptional regulation of *Hsl*, total HSL protein abundance was not different at 16-18wks between *knockouts* and *controls* (Figure 31B). However, the slight elevations in the activated form (PHSLs) at all three residues could indicate a pro-lipolytic response to insulin, although increasing the *N*-value can shed light on whether any of these differences are significant. No differences in perilipin abundance were observed between the two groups.

In addition, low circulating insulin at 16-18 weeks is likely responsible for the significantly lower expression of lipogenic genes in *knockout*s relative to *control*s (Figure 32). *Dgat1*, *Dgat2*, and *Fas* were all significantly lower in *knockout* livers relative to *controls* as expected. The mechanism through which *Dgat1* is transcriptionally regulated is poorly understood[119]. The literature suggests that glucose starvation can increase *Dgat1* expression, but that insulin shows no effect on expression[119]. In contrast, *Dgat2* is positively regulated by insulin, and low levels could explain the lower *knockout* expression observed at this time point[119]. Notably, both of these genes are inversely regulated by activation of mitogen-activated kinase (MAPK). Inhibition of the MAPK pathway causes a 2-fold and 4-fold increase in the expression of *Dgat1* and *Dgat2*, respectively[119]. Since Holmström et al. found that LPA induces stimulation of the MAPK pathway[128], it is possible that renal-LPA is responsible for the decreases in *Dgat1* and *Dgat2*. *Fas* transcription was also significantly lower in *knockouts* at this time point (Figure 32), but FAS protein was not significantly less abundant (Figure 33B). *Fas* is primarily regulated by tight transcriptional *control* mediated primarily through changes in insulin level, so decreased expression can be attributed to reductions in circulating insulin[120]. FABP4 abundance and gene expression were not different between the two groups (Figure 32, 33A).

Therefore, findings at 16-18 weeks of age show expression patterns that could be explained by expected responses to circulating humoral factors (high LPA and low insulin).

However contrary to the original hypothesis, by 23-25wks of age, there appears to be significantly lower expression of hepatic *Hsl* in *knockouts* relative to *controls* and no differences in the expression of lipogenesis regulating enzymes (Figure 30 and 32). The reason for the lower *Hsl* expression is unclear, since lipolysis is induced in the presence of low insulin. To get a better understanding of HSL activity at this time point, the abundance of phosphorylated HSLs, especially at the S660 residue should be determined through immunoblotting. The lack of lowered lipogenesis gene expression was also unexpected, since insulin promotes lipid synthesis, and thus insulin-deficiency, which is presumed to be present at this time-point, should lower synthesis. It is important to note that patients with pre-diabetes often present with hyperglycemia, glucose intolerance, and a high prevalence of fatty liver disease. NAFLD is the progressive occurrence of hepatosteatosis in the absence of alcohol consumption and is comorbid with T2DM and other metabolic syndromes[129]. Thus, a reduction in hepatic lipolysis alongside the lack of lipogenic attenuation in 23-25 week old *knockouts* may suggest the first stages of lipid accumulation as a result of chronic hyperglycemia (i.e. hepatosteatosis onset) [129]. An assessment of lipid content in livers could clarify the presence of lipid accumulation in *knockouts*, while assessments of hepatic lipolysis and lipogenesis through the direct assay of a radiolabelled substrate could also help to answer the question of whether hepatic lipid metabolism is altered, since the regulatory mechanisms influencing this difference remain unclear.

Chapter 8: The Adipose Tissue

8.1 Introduction and Rationale

The adipose organ is composed of distinct WAT and BAT depots[111]. All depots share the ability to store and release fatty acids, however, their function and physiology is depot-dependent[130]. Adipocytes from different anatomical depots vary phenotypically because of variable genetic and developmental foundations[83,111,130,131]. This results in functional heterogeneities between the discrete depots, manifesting as differences in adipocyte size, protein content, and metabolic activity[83]. Furthermore, the variation in triglyceride storage capacity and adipokine secretion render the different depots metabolically distinct, and so each depot contributes to metabolic impairments differently[83,111,130], and there is evidence that indicates that the pattern of adiposity distribution confers different risk factors for metabolic disease[83,130,132]. Collectively, the visceral adipose tissue depots (*i.e.* pwat, rwat, ewat) contain more mitochondria and have a higher lipolytic activity, making this group the lead contributor to plasma free fatty acids and insulin resistance[133]. In contrast, subcutaneous tissues (*i.e.* subc, iwat) are more effective at TAG storage, and so tend to be metabolically beneficial, even when they increase in size[130]. Hypertrophic visceral adiposity has been associated with increased risk for metabolic diseases whereas subcutaneous adiposity has been shown to be protective[130]. In particular, the mass of visceral adipose depots is often positively correlated with insulin resistance and obesity-related pathologies, potentially due to the higher metabolic activity of the tissue[78,83,130,132]. The variation in triglyceride storage capacity and adipokine secretion render the different depots metabolically distinct, and so each depot contributes to metabolic impairments differently and should be studied in isolation[111,130]. However, in most studies, discoveries in one white adipose depot are often extrapolated to all other depots.

Assessment of adipose depots size is often a preliminary measure of changes in adiposity. Depot mass is contingent on two main factors, the first is the size of adipose cells (which is largely determined by TAG content) and the second is the number of cells contained in the depot. The adipose organ is comprised of two main adipose cell types. Preadipocytes are smaller, immature progenitor adipose cells that can differentiate into much larger, mature adipocytes capable of lipid storage through lipolysis and lipogenesis. Preadipocyte differentiation

(adipogenesis) has been shown to be negatively regulated by low circulating insulin and high LPA[59,95,134], both of which co-occur in *RTSAKO*s at the time of dysglycemic onset (16-18 weeks of age). As a result, these factors can act additively to significantly suppress differentiation of preadipocytes (Figure 34). *RTSAKO* adipose depots should thus be significantly smaller in comparison to *control*s, since their depots would have fewer large, mature, adipocytes. Adipocytes that are present could further be affected by LPA and insulin exposure since high LPA and low insulin have been found to cause attenuated lipogenesis, producing smaller adipocytes with impaired lipid retention[59,95,134]. However, LPA has also been shown to induce preadipocyte proliferation[93]. As a result, chronic exposure to LPA could increase the number of small preadipocyte cells within a depot, masking any reductive effects on total adipose depot mass. Therefore, adipose mass may be used as a preliminary measure of the effect of elevated LPA and low insulin on *RTSAKO* adipose depots. Assessment of lipolysis, lipogenesis, and adipogenesis gene expression would better elucidate adipose tissue adaptation over the course of dysglycemic progression and LPA exposure.

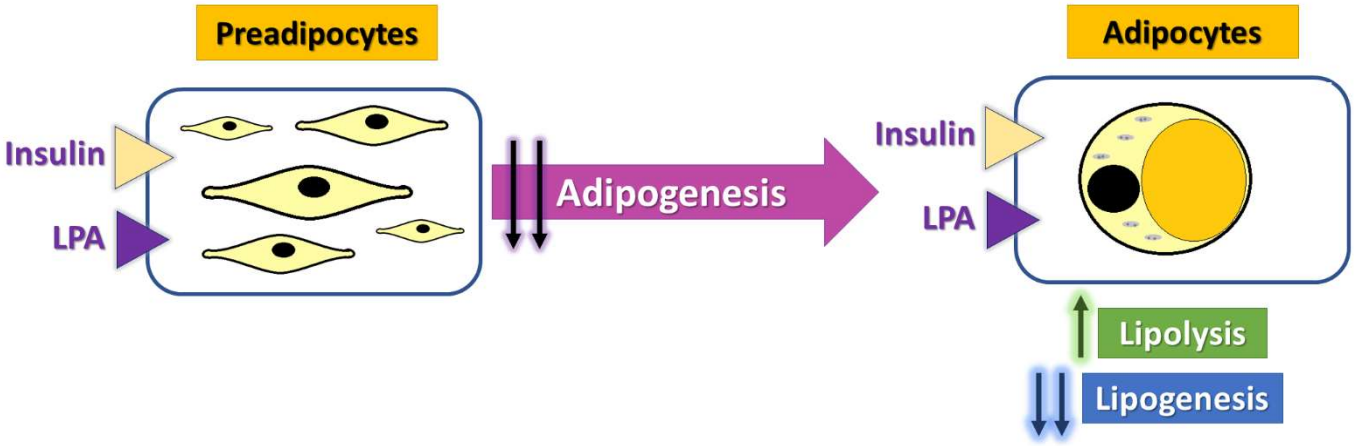

Figure 34: Low Insulin and Elevated LPA may have additive inhibitory effects on preadipocyte differentiation and adipocyte lipogenesis. LPA also induces preadipocyte proliferation.

8.2 Adipose-Specific Objectives

The overall objective of this chapter is to determine if the expression of genes and proteins involved in lipolysis, lipogenesis, and adipogenesis in *RTSAKO* adipose depots is different from *controls*.

Four adipose depots were assessed. Perirenal white adipose tissue is especially important considering its proximity to the LPA-producing kidneys in *knockout*s. Brown adipose tissue is often metabolically different from white adipose tissue due to its high mitochondria content[135]. Furthermore, two different subcutaneous white adipose depots (fat under the skin) were assessed. Inguinal white adipose tissue, located in the gluteal region, is a fatty, lubricious depot, whereas thigh adipose tissue (called subc throughout this thesis) is located in the gluteal-femoral region, and is a much more compact and distinct subcutaneous adipose tissue.

Characterization of adipose tissue will include investigation of differences in gene expression between male *RTSAKO* mice and *control* littermates at all three timepoints with regards to:

i. Adipose depot mass.
ii. Lipolysis gene expression.
iii. Lipogenesis gene expression.
iv. Adipogenesis gene expression.

8.3 Results and Discussion

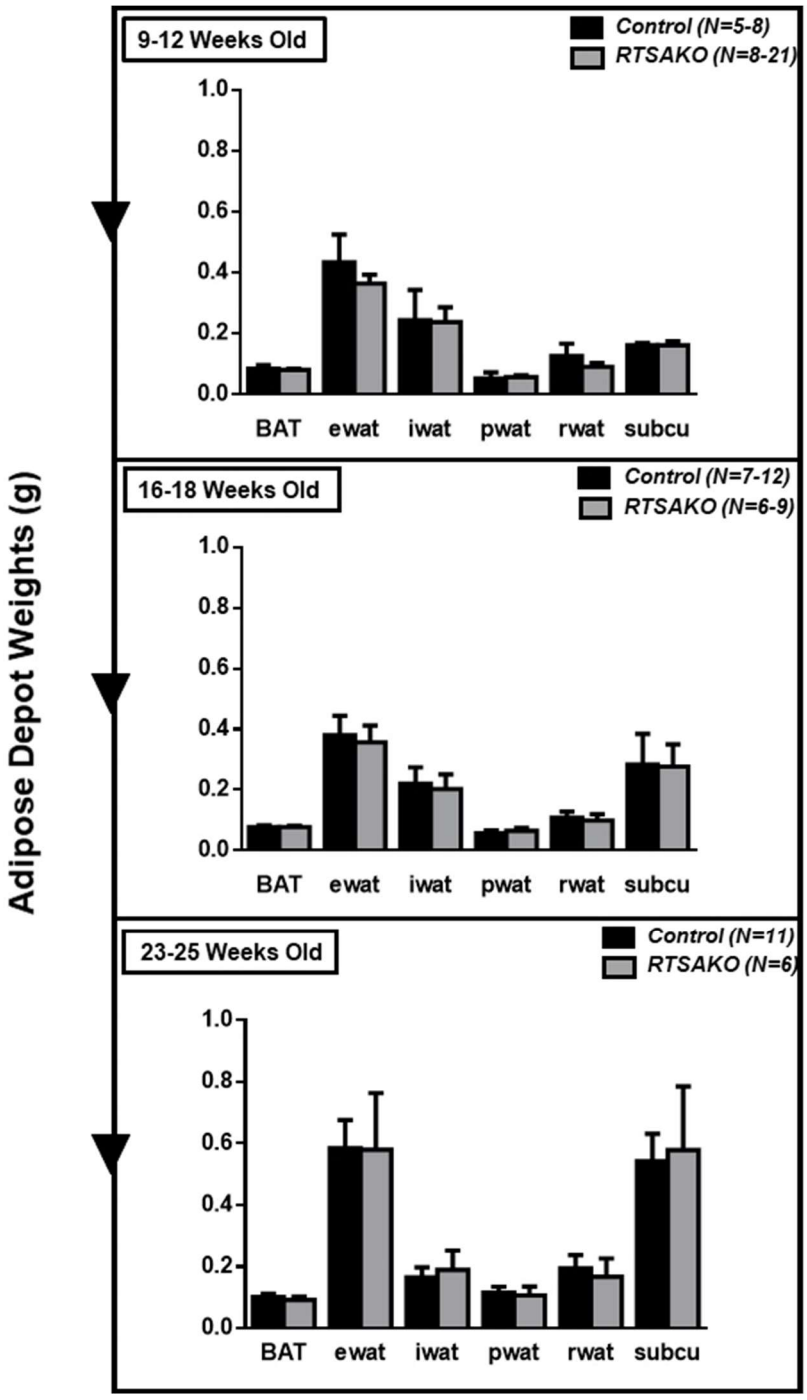

Figure 35: Adipose Depot Weights of Male Mice.

No significant differences were seen in the weights of adipose depots in knockouts and controls across the different age cohorts (top to bottom). (N=5-21).

BAT = brown adipose tissue, ewat = epididymal wat, iwat = inguinal wat

pwat = perirenal wat, rwat = retroperitoneal wat, subcu = subcutaneous wat

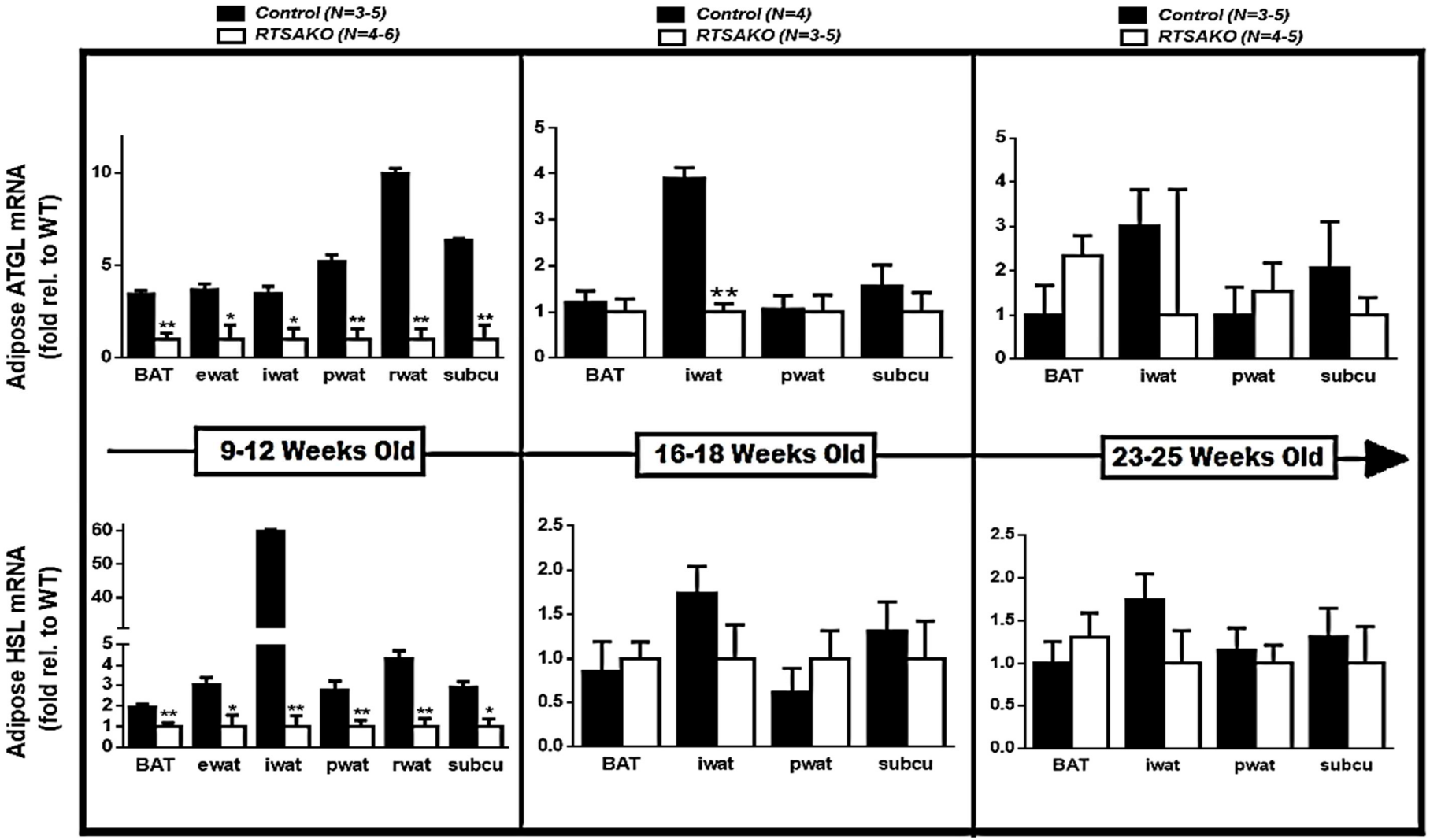

Figure 36: Expression of Lipolysis Regulating Genes in the Adipose Depots of Male Mice.

*Before onset of glucose intolerance, knockout mice showed significantly lower Atgl and Hsl expression in all adipose depots (left). Atgl expression was significantly lower in knockout iwat at onset (middle) relative to controls, but all other depots showed no significant difference. No significant differences were observed after chronic exposure to dysglycemia (right). *P<0.05, **P<0.01; (N=3-6).*

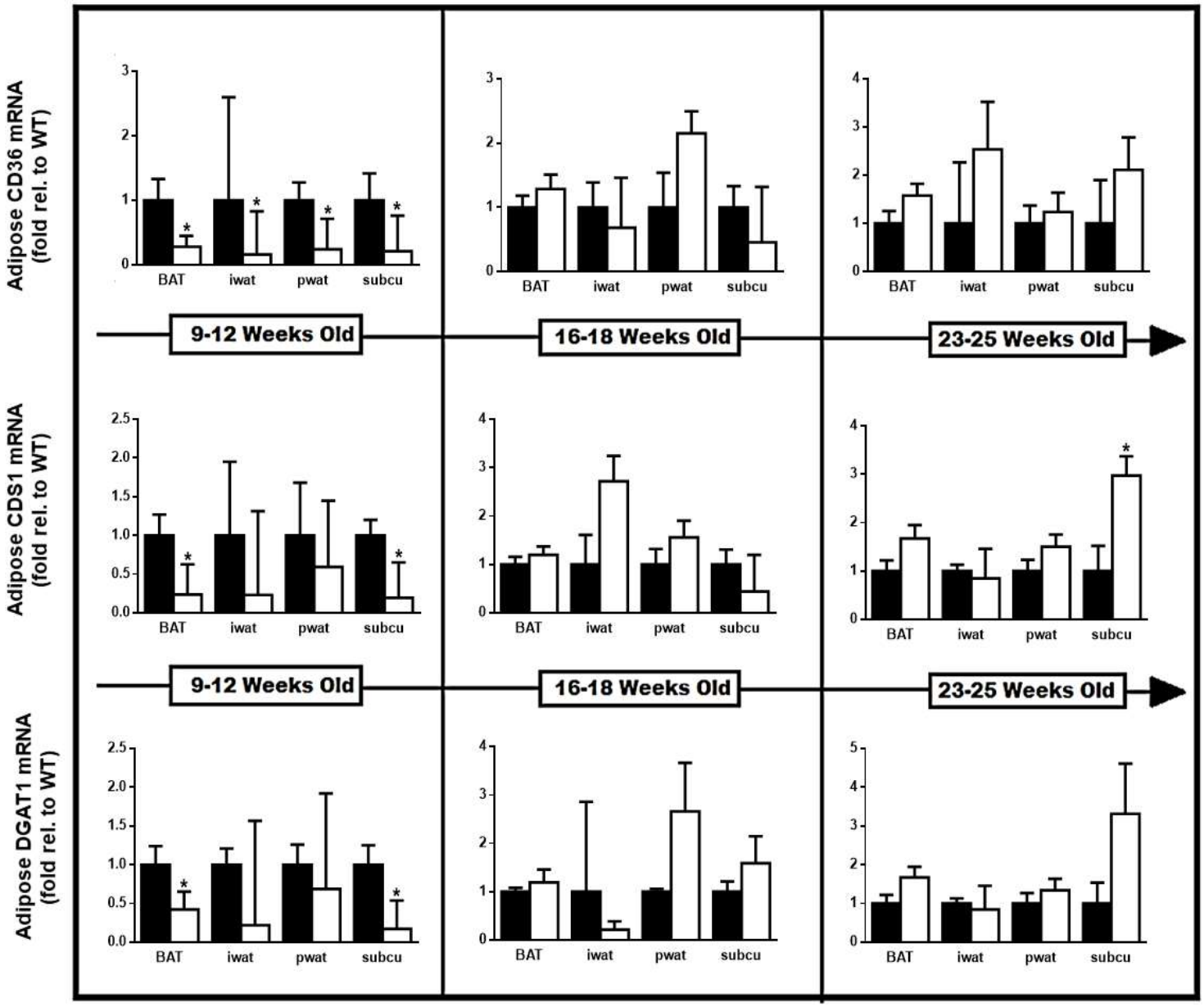

Figure 37: Expression of Lipogenesis Regulating Genes in the Adipose Depots of Male Mice: *Cd36*, *Cds1*, and *Dgat1*.

Before onset of dysglycemia (top left), knockout mice showed significantly lower expression of Cd36 in all depots, but no difference at, or after, onset (top row, middle and right). Cds1and Dgat1 expression was significantly lower in BAT and subc before onset, and Cds1 was significantly higher in subc after chronic exposure, but otherwise no differences were observed in knockouts relative to controls in the remaining depots at the time points assessed. P<0.05; (N=3-5).

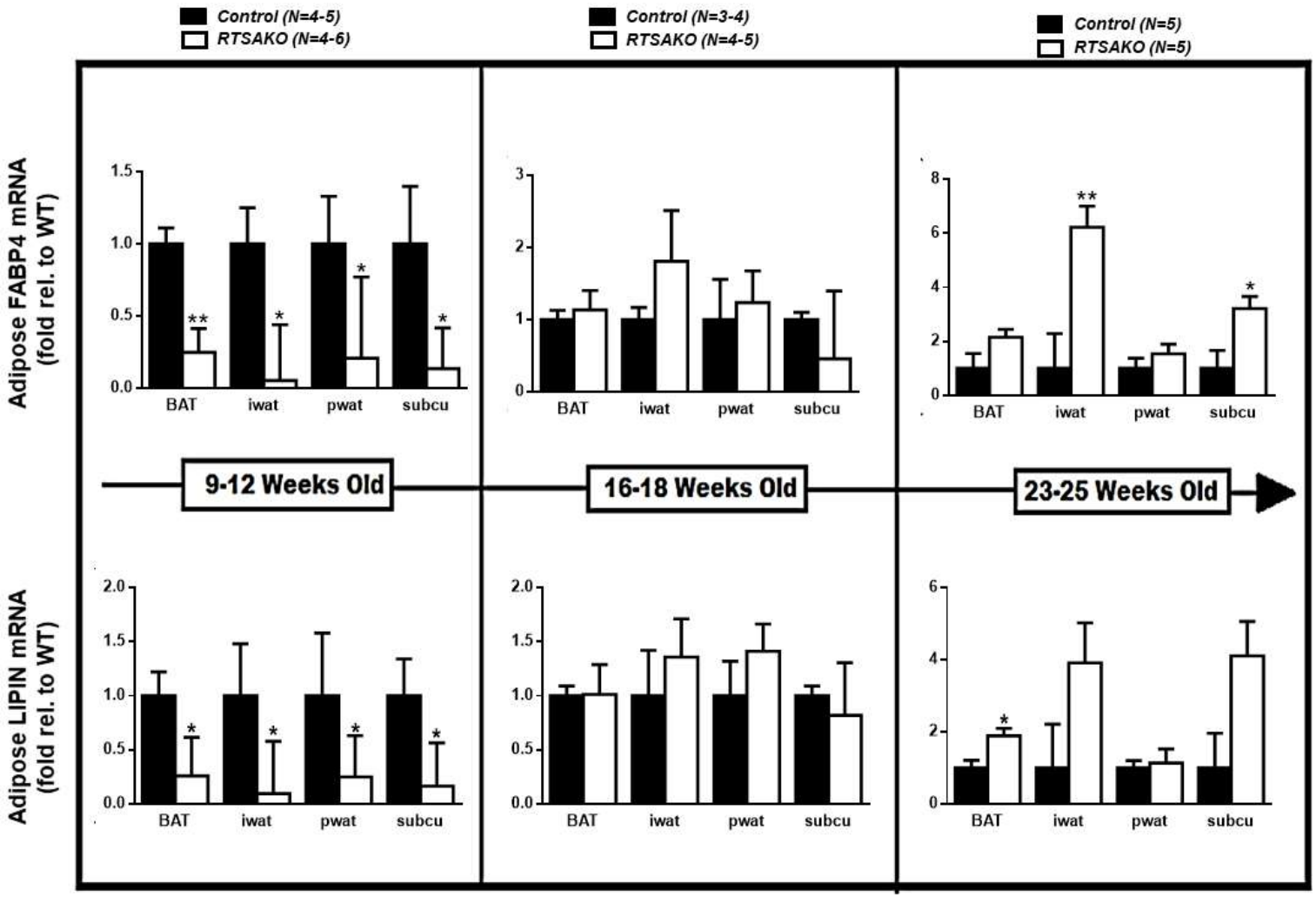

Figure 38: Expression of Lipogenesis Regulating Genes in the Adipose Depots of Male Mice: *Fabp4* and *Lipin*

*Both Fabp4 and Lipin expression were significantly lower in all knockout adipose depots relative to control littermates before dysglycemia onset. No significant differences were observed at the time of onset. After chronic exposure to dysglycemia, knockout iwat and subc showed significantly higher Fabp4 expression and higher BAT Lipin expression relative to controls. Otherwise no significant differences were observed in the other depots over the course of dysglycemia progression. *P<0.05; **P<0.01 (N=3-6).*

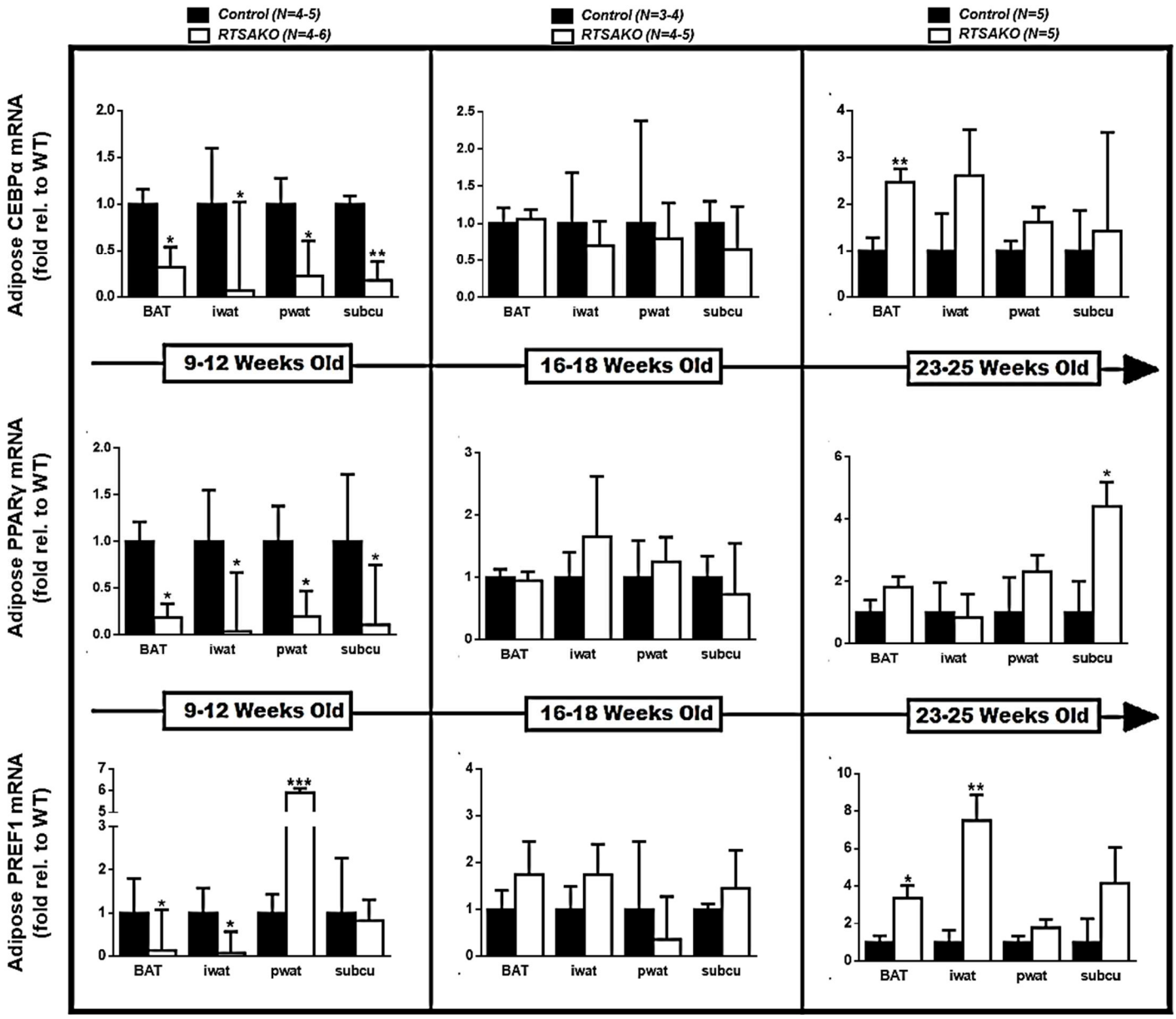

Figure 39: Expression of Adipogenesis Regulating Genes in the Adipose Depots of Male Mice: *Cebpα*, *Pparγ*, and *Pref1*.

*Before onset of glucose intolerance (left), knockout mice showed significantly lower expression of Cebpα and Pparγ in all depots assessed. Pref1 is significantly lower in BAT and inguinal WAT, however, there is a more than five-fold higher Pref1 expression in knockout pwat relative to controls at this time point. During onset (middle) no significant differences were observed in the genes assessed. After chronic exposure (right) Cebpα was significantly higher in BAT and Pparγ in subcutaneous WAT. In addition, both BAT and iwat showed significantly higher Pref1 expression in knockouts relative to controls. All other genes in the depots assessed showed no significant difference. *P<0.05; **P<0.01; ***P<0.0001; (N=3-5).*

No differences were observed in adipose depots mass

Adipose depot mass is an excellent indicator of dysregulated adipocyte metabolism. Adipose tissue is involved in the onset and progression of various metabolic disorders, and obesity directly correlates with several comorbidities[130,133,136]. The adipose organ is the largest site of lipid storage in the body, and plays an important role in endocrine homeostasis[130]. Adipose tissue is divided into regional depots that have unique cellular size, function, and organization. The fat distribution within these depots plays an important role in moderating the associated risk of excess adiposity for metabolic disease, where excess visceral fat (pwat, rwat, ewat) tends to increase risk, while storage of excess TAG in subcutaneous adipose tissue mass (subc, iwat) has been shown to be protective against diabetes and cardiovascular diseases[130]. Increased lipolysis in the visceral depots increases exposure of surrounding organs to elevations in plasma NEFAs, which can initiate ectopic lipid storage and steatosis in important metabolic tissues (i.e. renal steatosis and hepatosteatosis). Excess lipogenesis and increased preadipocyte differentiation is a characteristic of obesity, which also increases risk of developing various metabolic disorders.

Based on the previously identified *RTSAKO* phenotype, whereby dysglycemia is accompanied by low circulating insulin and elevated LPA (at 16-18 weeks), I predicted that differences in adipose tissue depot size may be observed compared to *control* littermates. However, *RTSAKO* mice present with no differences in adipose depots weights relative to *controls* at any of the time points measured (Figure 35). It is possible that adipose tissue depot masses may have stayed the same, but metabolic- and differentiation-based changes may have occurred. Since LPA has been shown to increase preadipocyte proliferation, any expected reductions in mass from inhibited differentiation and lipogenesis could be masked because of increased cell number. Therefore, although number of mature adipocytes and the TAG content per adipocyte is decreased, the number of preadipocytes present could have increased, and so the mass may remain the same. Thus, preliminary assessments of lipolysis, lipogenesis, and adipogenesis were required in follow-up to determine if metabolic, proliferative, or developmental changes were present.

Adipose depot lipolytic gene expression was not elevated in *knockout*s despite low insulinemia, but was significantly lower at 9-12 weeks of age, prior to dysglycemia

Since low insulin causes lipolytic gene and protein induction, I hypothesized that at 9-12 weeks no differences in expression would be observed, but that by the time of dysglycemic onset, impaired insulin secretion would cause higher lipolytic expression in *knockouts* relative to *control*s. Interestingly, at 9-12 weeks of age, *RTSAKO* mice have significantly lower *Atgl* and *Hsl* expression in all adipose depots assessed (Figure 36). At 16-18wks, significantly lower *Atgl* expression was observed in the inguinal white adipose tissue of *knockouts* relative to *controls*. No significant differences were observed otherwise between *knockouts* and *controls* in the expression of adipose tissue lipolysis enzymes at 16-18 and 23-25 weeks of age. The absence of elevated *Atgl* and *Hsl*

expression in *knockouts* despite low insulin could potentially explain the lack of elevated circulating NEFAs observed by others in our lab (data not shown).

Lipogenesis gene expression was lower in all depots at 9-12 weeks, but significantly higher in subcutaneous depots by 23-25 weeks of age

Low insulin, coupled with elevated LPA, should additively inhibit lipogenesis in mature adipocytes and cause reduced adipose depots mass in *knockout*s relative to *control*. Lipogenic gene expression is already inhibited at 9-12 weeks of age, prior to the manifestation of dysglycemia. *Cd36*, *Fabp4*, and *Lipin*, expression were significantly lower in the four depots assessed in *knockouts* relative to *controls* (Figure 37, 38). Furthermore, *Cds1* and *Dgat1* were also significantly lower in the BAT and subcutaneous WAT of *knockouts* at this time point (Figure 37). Humoral measures at this time point were not yet available, but collection of these data could help elucidate this phenomenon. By 16-18wks, no significant differences in the expression of lipogenesis genes were observed in any of the adipose depots studied in the two groups.

However, by 23-25weeks of age, lipogenesis gene expression was significantly higher in BAT and gluteofemoral (subc and iwat) adipose depots of *knockouts* relative to *controls*. *RTSAKO* BAT showed higher expression of *Lipin*, the enzyme responsible for the dephosphorylation of phosphatidic acid into DAG, in *knockouts* relative to *controls* (Figure 38). Overexpression of *Atx* has been shown to cause an increase in brown adipose tissue mass, although whether high *Lipin* is because of elevated LPA remains unknown[137]. Additionally, subcutaneous WAT showed significantly more *Cds1*, while both subcutaneous and inguinal WAT showed a 3-fold and 6-fold higher *Fabp4* expression in *knockouts*, respectively (Figure 37, 38). This is of particular interest because *Fabp4* transcriptional regulation is highly induced during adipogenesis, especially by increased NEFAs, insulin, and PPARγ nuclear receptor agonists[138]. Typically, insulin acts to induce the expression of genes involved in lipogenesis regulation, but the observed differences showed higher lipogenic gene expression in subcutaneous fat of *knockouts* and so cannot be explained by attenuated insulin-signaling.

Another explanation for the higher lipogenic gene expression observed in subcutaneous fat of *knockouts* could be attributed to elevations in plasma LPA. Although LPA has been shown to act antagonistically on adipogenesis, it has also been found to be a putative ligand for the nuclear receptor PPARγ, and could potentially upregulate the transcription of various pro-lipogenic and adipogenic genes[92]. However, for this stimulation to occur, LPA must be transported intracellularly, and this is unlikely since adipocytes have considerable amounts of membrane ectolipid phosphate phosphorylases, which deactivate LPA and would prevent its successful use intracellularly[92].

***Knockout*s exhibit differences in expression of adipocyte differentiation genes**

Adipose tissue contains a substantial reservoir of preadipocytes that can differentiate into mature adipocytes capable of lipid storage. Preadipocytes show an induction of proadipogenic gene expression during differentiation, and once differentiated, typically show increased lipogenic gene expression since lipid synthesis and storage is a major function of mature adipocytes. The three main adipogenesis-regulating genes assessed in these adipose depots are *Cebpα*, *Pparγ*, and *Pref1* (Figure 39). CEBPα is a terminal adipocyte differentiation protein and signals the successful commitment of preadipocyte transition into a mature adipocyte[139]. PPARγ is a nuclear receptor that is regulated by various factors, including fatty acids, cholesterol, insulin, LPA[140], and other intracellular regulatory proteins, like SREBPs[110], to profoundly regulate the induction of preadipocyte differentiation, followed by adipocyte stimulation of lipid metabolism towards lipid synthesis. Finally, PREF1, unlike the previous two proteins, is anti-adipogenic and is regulated by pro-adipogenic CEBPα and PPARγ, where decreased PREF1 leads to upregulations in these pro-differentiation factors, and vice versa[141].

Unexpectedly, at 9-12 weeks of age, gene expression differences in *knockout* mice relative to *controls* were largely, but not entirely, indicative of significantly lower adipogenesis in various adipose depots (Figure 39). Expression of *Cebpα* was consistently and significantly lower in all adipose depots of *knockouts* in comparison to *controls*. This could be explained by increased sensitivity to insulin in this cohort, as *Cebpα* is repressed by insulin action. *Cebpα* is also repressed by the action of another pro-adipogenic factor, PPARγ[139,141]. However, *Pparγ* expression was also significantly attenuated in all *RTSAKO* depots at this time point, suggesting that it was not responsible for decreased *Cebpα* expression (Figure 39). Finally, *RTSAKO* pwat presented with a 6-fold higher expression of anti-adipogenic *Pref1*. This significant induction of antiadipogenic *Pref1* in *knockouts* solely in the pwat could be related to the proximity of this adipose depot to the kidneys. LPA has been shown to significantly reduce the expression of adipogenic *Pparγ*[93,140]. As suggested by the lack of dysglycemia, the proximity of perirenal adipose tissue to the surface and vasculature of the kidney could imply that early secretion of LPA acts on this depot, in particular, to stop differentiation prior to reaching levels that cause systemwide physiological change.

LPA has been shown to inhibit adipogenesis in a dose-dependent manner, with maximal inhibition at 0.1μM LPA[92]. Time-course measures of LPA at 9-12, 16-18, and 23-25 weeks of age are currently underway to better understand the physiological levels of this molecule in *knockout*s alongside the progression of dysglycemia. The presence of significant anti-adipogenic differences in gene expression in the adipose of *knockout*s at the earliest time point could potentially be explained by LPA. Although LPA is likely not elevated enough to induce dysglycemia, perhaps systemic concentrations at this time-point are sensitive enough to affect adipose tissue. By 16-18 weeks of age, no differences in adipogenic gene expression were observed between *knockouts* and *control*s (Figure 39). The lack of inhibited adipogenic gene expression, despite high LPA and low insulin, both factors

that negatively regulate differentiation, could suggest that *RTSAKO* mice have adapted to chronic LPA exposure (especially if differences at 9-12wks were LPA-induced). Since LPA has been found to increase preadipocyte proliferation, perhaps the increased number of preadipocytes masks any differences in adipogenic gene expression, since precursor cells still possess these factors at lower levels, but not enough to proceed to adipocyte differentiation. This masking is, however, unlikely, since all gene expression was normalized to housekeeping genes, and the copies per undifferentiated cell are much lower than per differentiated cell.

At 23-25wks of age, there appears to be a significantly higher *Cebpα* expression, but a 3-fold higher *Pref1* expression in *knockout* brown adipose tissue in comparison to *controls* (Figure 39). Studies of LPA on brown preadipocytes by Hölmstrom and colleagues, found that LPA inhibits the differentiation of brown preadipocytes into mature adipocytes similar to observations in white adipose tissue[92,128]. *Cebpα* is often expressed as an end-stage differentiation protein whereas *Pref1* acts to inhibit adipogenesis, and both act antagonistically on one another. The high *Cebpα* could be attributed to already committed cells solidifying differentiation or the increased number of preadipocytes, in lieu of *Pref1* inhibition of adipogenesis by uncommitted preadipocytes. In addition, subcutaneous WAT shows a 4-fold higher *Pparγ* expression and inguinal wat showed a 7-fold higher *Pref1* expression in *knockout*s relative to *control*s.

Overall, findings presented in the adipose tissue were not homogenous, which was to be expected considering the metabolic distinctiveness of each adipose depot. Some significant differences could be attributed to attenuated insulin, whereas some may be a consequence of chronic LPA exposure. Put simply, there may be competing effects present (i.e. increased terminal adipocyte differentiation of some cells, but decreased commitment to differentiation by others, likely from an imbalance in the number of cell types) in the heterogeneric population of cells that make up the adipose tissue.

The lack of differences in adipose depot size and adipogenic gene expression at the time of dysglycemic onset and progression, suggest that this *knockout* model is adapting to changes in low insulin and LPA to prevent dyslipidemia. However, the unexpected differences in gene expression at 9-12 weeks of age is indicative of an overall inhibition of differentiation, and likely increase in pre-adipocyte proliferation, in *knockout*s relative to *control*s (since both lipolysis and lipogenesis are down, can be attributed to lack of mature adipocytes). The lack of depot size difference, and adaptive gene expression at later time points, may be a result of increased preadipocyte cell number. Therefore, proliferation and cell number in these depots should be assessed. In addition, observation of these mice over the course of aging (past 25 wks) could shed light on any future changes in adiposity in *RTSAKOs* relative to *controls*.

Chapter 9: General Integrated Discussion

The *RTSAKO* model suggests the kidneys play an important role in glucose homeostasis, likely through renal-organ crosstalk. Prior work already established that dysregulated lipid metabolism at the level of the renal-tubules led to the onset of dysglycemia, impaired insulin secretion, and elevated LPA on a systemic level. Communication between tissues may cause adaptive and maladaptive differences in organ gene and protein expression in an attempt to stabilize the metabolic imbalance manifested from the ablation of renal-tubule *Atgl*. Since dysglycemia manifests at about 16-18 weeks of age in *RTSAKO*s, it is expected that the greatest differences will manifest at this point and progress over the course of time. Figure 40 illustrates the renal-organ pathway for communication that likely causes the onset of systemic glucose intolerance, with emphasis on the three organs studied. *RTSAKO* mice only differ from their control littermates in that the *Atgl* gene is cleaved in the renal-tubule cells, dysregulating renal lipid metabolism. Despite this singular variation in the cell type of one organ, systemic impairments in glucose disposal are observed, and suggest dysregulated glucose metabolism is a result of communication through renal-lipid signaling to important glucose-regulating organs. Renal-signaling causing impaired glucose disposal can be direct through LPA (Figure 40 red arrows) or indirect (Figure 40 blue arrows) through LPA-mediated impaired insulin secretion.

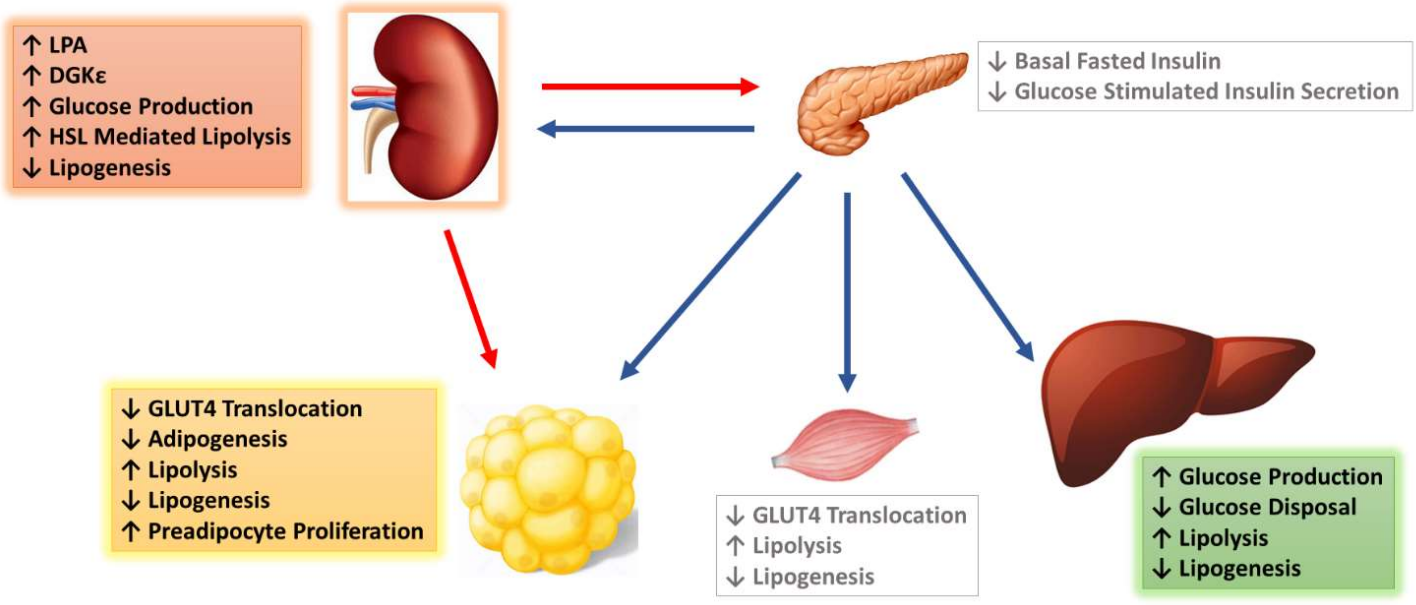

Figure 40: RTSAKO Gene and Protein Expression are Mediated through Renal-Organ Crosstalk

In order to best discuss the organ interactions that constitute *RTSAKO* metabolism, the observed expression differences in the kidneys, liver, and adipose tissue must be assessed holistically at each individual time point. This allows for a time-frame assessment of the impacts and ramifications of renal-tubule *Atgl* ablation, prior to (9-12 wks), during (16-18wks) and after chronic exposure (23-25 wks) to dysglycemia. By using control littermates as a baseline measure, observed variations in *knockout* expression can be defined as either adaptive (normalizing) or maladaptive (aggravating) to overall metabolic homeostasis. The ensuing sections present summaries of significant differences in gene and protein expression observed in all three tissues at each time point (Figure 41-43) followed by a holistic analysis of these findings. The aim of this integrated discussion is to address the final objective of this thesis, which is the impact of these differences on systemic metabolism through renal-organ cross talk.

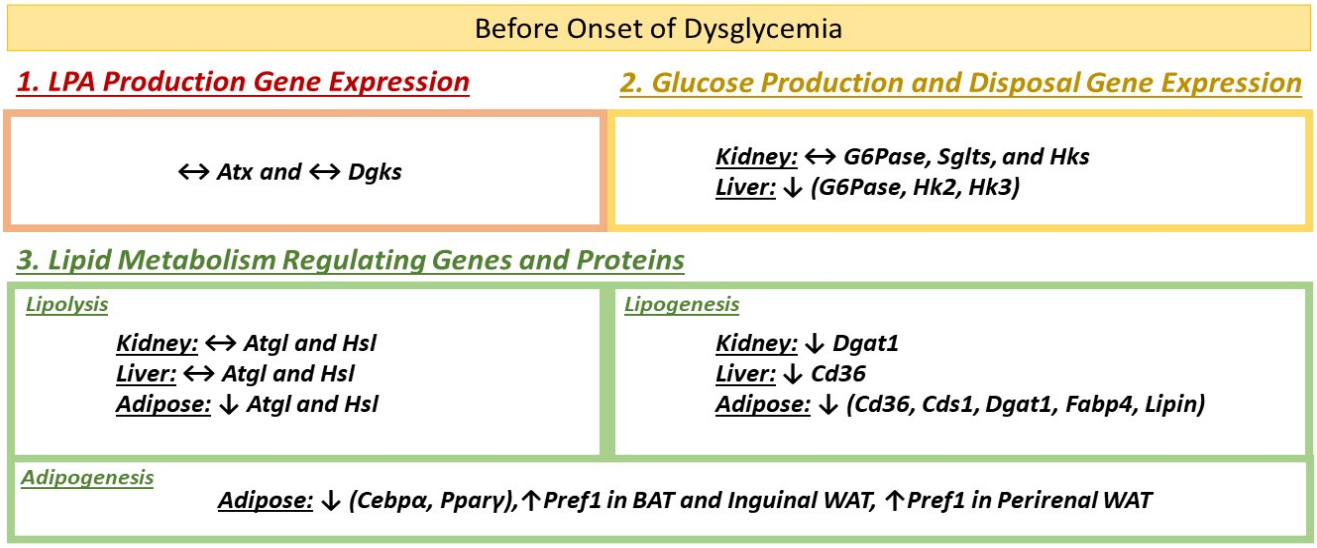

Figure 41: Summary of Significant Differences in RTSAKO Expression at 9-12 weeks of age

Before any apparent variations in glucose disposal become apparent, *RTSAKO* mice show signs of adaptive differences in gene expression that likely delay the onset of dysglycemia. Despite the ablation of renal-tubule *Atgl*, the expression of both *Atgl* and *Hsl* do not show any significant differences relative to unaltered *controls*. This could be a result of compensatory *Atgl* expression in surrounding renal cells. TAG accumulation at this time point is likely not significantly higher than *control* littermates, although lipid extractions would confirm this. In addition, the expression of LPA synthesizers was not high, and could indicate LPA levels have yet to be significantly elevated, although humoral measures are required for confirmation. However, elevations may be occurring, but not at levels that would cause significant systemwide

effects. There are signs of potential LPA-mediated activity. Liver gene expression shows significantly lower expression of *G6pase, Hk2,* and *Hk3,* and could indicate increased insulin sensitivity in *knockouts*, which could be an adaptive response to early attenuations in insulin secretion. In addition, all tissues show significantly lower lipogenic gene expression, which potentially could also be attributed to slight decreases in insulin secretion caused by renal-pancreatic signaling, although this needs to be measured directly. The likelihood of early, latent, LPA-mediated effects is further supported by the significant gene expression differences observed in adipose tissue. Significantly attenuated adipogenesis alongside no variations in depot size can realistically be explained by decreased adipocyte differentiation coupled with increased preadipocyte proliferation mediated by LPA. The lack of dysglycemia at this time point, despite signs of these slight elevations, could be attributed to the potential increased insulin sensitivity at the liver and the increased amount of glucose required to sustain enhanced preadipocyte proliferation. Therefore, despite the absence of systemic dysglycemia at this age, *RTSAKO* mice show evidence of gene expression adaptation at the liver and adipose, potentially in response to renal-LPA mediated signaling, that could be protective and delay dysglycemic onset.

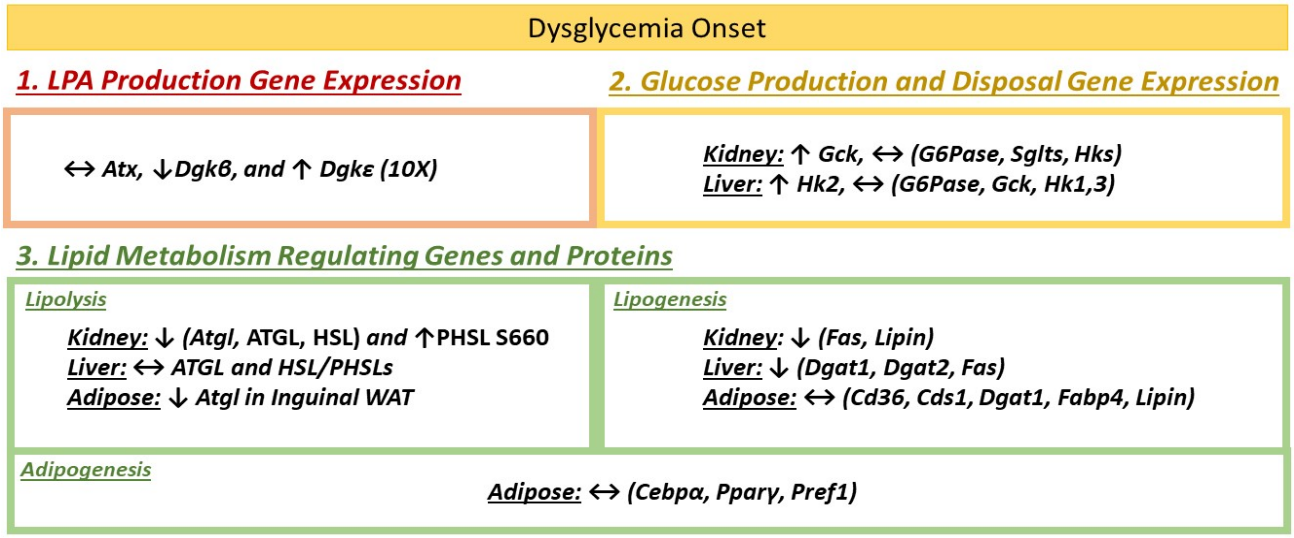

Figure 42: Summary of Significant Differences in RTSAKO Expression at 16-18 weeks of age

By 16-18 weeks, *RTSAKO*s no longer show adaptive differences in gene expression that could sustain normoglycemia. However, it is possible that prior adaptations in insulin sensitivity delay significant variations in the expression of glucose regulators in the kidneys and liver. Despite dysglycemia and low insulin, there were no notable differences in the expression of insulin-regulated *G6pase* or *Gck* in the kidney and liver relative to *controls*. If insulin sensitivity

is improved at 9-12 weeks by increased insulin receptor substrate (IRS) expression, then the significant attenuations in circulating insulin observed by 16-18 weeks may not necessarily induce significant variability in the expression of *G6pase* and *Gck* relative to control levels. Nevertheless, it appears that impairments in insulin secretion were sufficient enough to cause significantly lower lipogenic gene expression in the kidneys and liver, and potentially also in adipose.

Attributing the differences observed in the three tissues to renally-derived LPA signaling is much more likely at this time point, since prior findings have confirmed elevated LPA and its causative role in inducing dysglycemia at 16wks. This is further supported by the significantly high expression of the LPA synthesizer *Dgkε* and the shift in renal lipid-regulator expression towards HSL-mediated lipolysis. Therefore, renal-LPA crosstalk at this time point causes significantly lower lipogenic gene expression in the kidneys, livers, and potentially the adipose tissue, but no significant differences in glucose regulator gene expression, despite apparent dysglycemia, which could be conceivably explained by adaptive increases in insulin sensitivity.

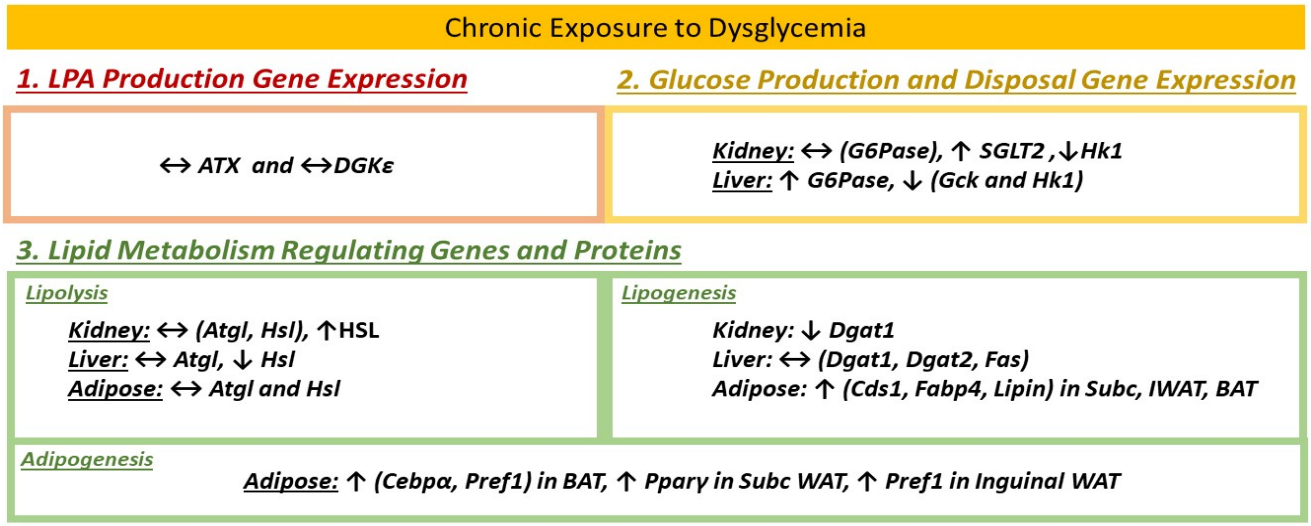

Figure 43: Summary of Significant Differences in RTSAKO Expression at 23-25 weeks of age

After 5-9 weeks of chronic exposure to renal-LPA signaling, *RTSAKO* mice begin to show signs of significant maladaptive differences in expression that could mediate the progression of dysglycemia and related pathologies. *Knockout* kidneys and livers display significantly higher glucose producing gene expression (*Sglt2* and *G6pase*) and lower glucose disposal gene expression (*Gck* and *Hks*) in comparison to *controls*. This would cause a net movement of glucose extracellularly, and enhance hyperglycemia. Furthermore, *knockout*

kidneys continue to express pro-HSL-mediated renal lipolysis, which likely continues to cause the production of renal-LPA. Although humoral measures of LPA and insulin were not conducted at this time point, glucose-regulator expression patterns are indicative of significantly attenuated insulin. Despite this, hepatic lipid-regulating gene expression shows maladaptive responses to low insulin, as *Hsl* expression is significantly lower than *controls* and lipogenesis expression is no longer significantly attenuated at this time point. This unexpected finding could be indicative of the initiation of hepatosteatosis, which is the potentially pathological accumulation of lipid in hepatocytes often comorbid with hyperglycemia. Finally, subcutaneous adipose depots present with significant pro-lipogenic and adipogenic gene expression, and could suggest an adaptive response to hyperglycemia since subcutaneous adipose tissue has been shown to be protective against hyperglycemia.

In conclusion, for the most part, *knockout* expression differences at 9-12 weeks of age appear adaptive, as *RTSAKO* mice are able to efficiently dispose of glucose, and express kidney *Atgl* and *Hsl* at levels indistinguishable from their *control* littermates, despite renal-*Atgl* ablation. These early adaptations may be protective against detrimental differences in gene expression at 16-18 weeks of age, although dysglycemia onset has begun. However, chronic exposure to renal--LPA and the consequences associated with this renal-organ mediated crosstalk eventually leads to maladaptive differences in expression that could contribute to the worsening of glucose intolerance and associated comorbidities in *RTSAKOs* in comparison to normoglycemic *controls* (Figure 44). Assessments at later time points could reveal significant steatosis, lipotoxicity, and inflammation in the kidneys and liver in response to sustained hyperglycemia and impaired insulin secretion, as well as significant differences in adiposity.

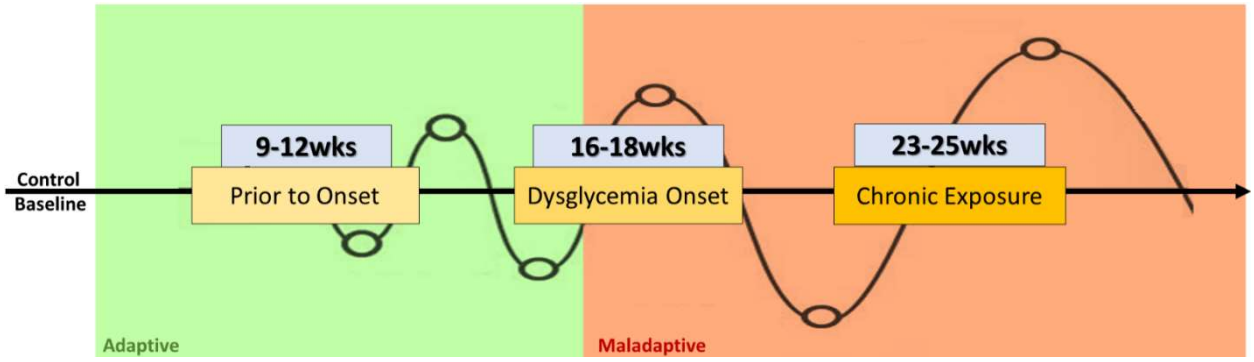

Figure 44: Differences in RTSAKO expression are represented by deviation from baseline. Baseline is defined as expression patterns observed in normoglycemic, unaltered, controls.

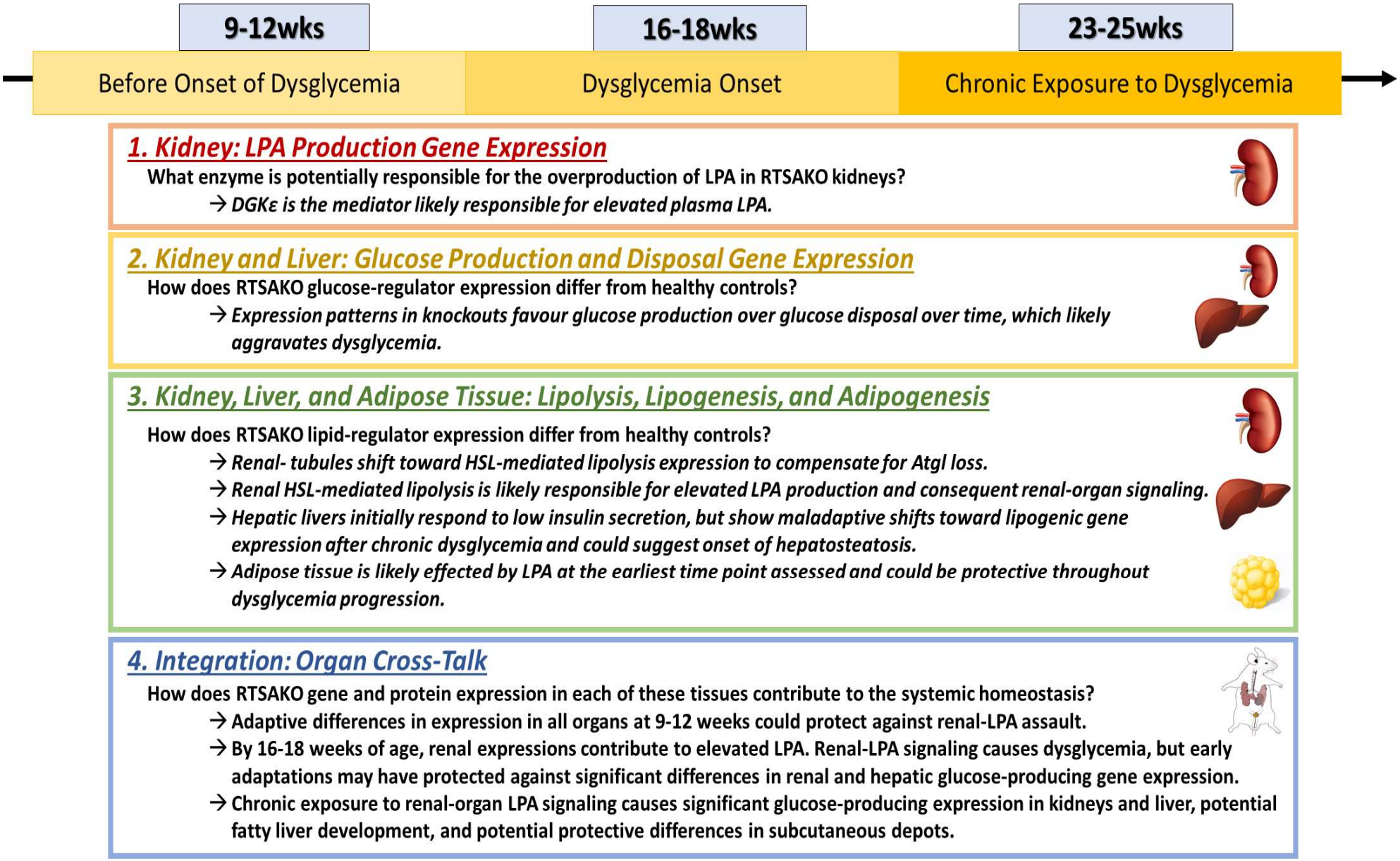

Figure 45: Summary of Findings in the Characterization of Kidney, Liver, and Adipose Tissue of RTSAKO Males.

Chapter 10: Future Directions and Conclusions

Thus far, efforts in characterizing *RTSAKO* mice have determined that by 16-18 weeks of age, dysglycemic onset occurs, and is likely a result of LPA-mediated impaired insulin secretion. Furthermore, *RTSAKO* mice present with significant adaptive gene and protein changes that act to stabilize renal metabolism prior to dysglycemic onset, but once dysglycemia is established, shifts towards maladaptive expression profiles contribute to metabolic pathology. Of the greatest importance in *RTSAKO* mice is understanding the impact of renal-tubule *Atgl* ablation in mediating the effects observed. Although the findings in this thesis significantly contribute to the elucidation of the *RTSAKO* phenotype and the manner through which dysglycemia progresses, much remains to be completed.

Investigation of the kidneys determined no significant differences in the expression of glucose and lipid mediators, except for lower *Dgat1* expression, prior to the onset of dysglycemia. However, at the time of onset (16-18wks) and with the chronic progression of dysglycemia (23-25 wks), findings determined from *knockout* gene and protein expression suggest a compensatory shift towards HSL-mediated lipolysis with the loss of available ATGL and accumulation of TAG. This would possibly result in the accumulation of MAG, which can act as a substrate for DGKε, and mediate the elevations in LPA. However, to confirm this theory, the abundance of MAG in *RTSAKO* kidneys must be assessed, as well as the conversion of MAG into LPA. This can be done by lipid extraction and separation using TLC to determine if renal MAG concentrations are significantly higher in *knockouts* relative to *controls*. Furthermore, MAG tracer studies can be employed to confirm conversion into LPA, by measuring renal conversion of labeled MAG to tracer-labeled LPA. In addition, findings in this thesis proposed DGKε to be the kinase responsible for this conversion, since *knockouts* have a ten-fold higher expression at the time of dysglycemia onset in comparison to *controls*. However, by 23-25 wks of age, expression was no longer different and could be explained by the constitutive action of the enzyme. This is supported by studies showing DGKε is constitutively active and implicated in the development of fibrotic kidneys[109]. Western blotting of this protein at the three time points could indicate rising abundance. Immunoblotting results were intended to be included in this thesis, however the DGKε antibody is uncommon, and receipt was delayed as it was backordered by months. Others will therefore complete this work. Abundance does not confirm mediation, and so chronic treatment with a pharmacological inhibitor could determine if LPA production is

attenuated in *knockouts*. This experiment is supported by a study conducted by Zhang et al., where inhibition of DGKε attenuated Huntington diseases toxicity and introduced an avenue for innovative therapies[142]. Confirmation of the role of DGKε in the induction of early-onset dysglycemia in humans could lead to a groundbreaking, novel, therapeutic target for CKD and new-onset diabetes.

Liver analyses showed lower *G6Pase* expression in *knockouts* relative to *controls* at 9-12 weeks of age and may suggest increased insulin sensitivity at this time point. Glucose and insulin tolerance tests conducted by prior investigators determined that at 9 weeks of age, *RTSAKO*s show more efficient glucose disposal in response to intraperitoneal insulin injection, although not reaching significance. Since *G6Pase* expression and regulation in hepatocytes is tightly regulated by insulin signaling, immunoblot assessment of IRS abundance and phosphorylation at this time point, as well as at later time points, should be conducted. Immunoblotting at 16 weeks showed much higher abundance of active IRS1 in *knockout* livers relative to *controls*, but my findings were preliminary in a small group of mice (*N=2*) and would require follow-up (data not shown). Investigations of IRS abundance could clarify adaptive differences in insulin sensitivity in *RTSAKO* livers, that may help *knockouts* mitigate the severity of dysglycemia. Despite glucose intolerance onset and low circulating insulin at 16-18 weeks of age, differences in glucose-regulator gene expression do not manifest until 23-25 weeks. By 23-25 weeks, however, this adaptation can apparently no longer protect against impairments in insulin secretion as observed by the significantly higher *G6Pase* and lower *Gck* expression that could aggravate hyperglycemia.

In addition, variability in the expression of lipid-regulators in *knockout* livers suggest the initiation of hepatosteatosis. At 16-18 weeks of age, *knockout* livers apparently respond to low levels of insulin by showing lower lipogenic gene expression in comparison to *controls*, as expected. However, at 23-25 weeks of age, this difference was no longer apparent, which is unexpected with low insulin. Levels of insulin at this time point were not measured, but differences in glucose regulator gene expression suggest chronically low levels. The lack of attenuated lipogenesis may suggest the early stages of fatty liver development. NAFLD is associated with hyperglycemia and often comorbid with CKD and T2DM[129,143]. Assessment of livers at a later time point could confirm lipid accumulation and hepatosteatosis onset. TLC can be used to determine elevations in the lipid content of *knockout* livers in comparison to healthy, *control* littermates.

Assessments of adipose tissue lipid regulators demonstrated a very interesting and unexpected finding. Despite the absence of dysglycemia at 9-12 weeks of age, the greatest variation in gene expression from *control* baseline occurred at this time point. Significantly low expression of lipolysis and lipogenesis indicated significantly attenuated preadipocyte differentiation. Inhibition of adipogenesis at this time point is supported by the significantly lower expression of pro-adipogenic factors CEBPα and PPARγ in all adipose depots. This significant attenuation could be caused by elevated LPA or attenuated insulin, however plasma measures of these factors at 9-12 weeks of age would need to be determined. It is unlikely that the difference observed in adipose tissue is attributed to low insulin, since the kidneys and livers showed no sign of insulin-mediated differences in expression at this time point. Measures of LPA may also prove to be insignificant between the two groups, since LPA-mediated impairments in insulin secretion have yet to manifest and LPA synthesizer expression shows no significant differences at this time point. However, the six-fold higher expression in anti-adipogenic *Pref1* in the perirenal adipose tissue that flanks the kidneys, may suggest that even slight increases in LPA secretion can significantly alter adipose tissue expression, but not yet cause significant systematic effects. This is supported by a study conducted by Simon and colleagues[92] that showed LPA acts to inhibit preadipocyte adipogenesis in a dose-dependent manner, with maximal inhibition at 0.1μM LPA. Sensitive measures of plasma LPA taken from vasculature exiting the kidney could aid in confirming even slight elevations in renal LPA production. Despite significantly attenuated lipolysis, lipogenesis, and adipogenesis in all *RTSAKO* adipose depots at this time point, no differences in depots weights were observed. The lack of difference in depots mass could be attributed to induced preadipocyte proliferation by LPA. The expression of proliferation factors like KI67 and proliferating cell nuclear antigen (PCNA) can be measured in knockout depots relative to *controls* to confirm increased preadipocyte proliferation. Furthermore, histology of depots can also be used to show more, smaller, preadipocytes and less, larger, mature adipocytes in *knockout* cross-sections versus *controls*. Another measure that can be utilized is simple DNA quantification, since proliferation requires consistent duplication of genetic material and would show higher DNA concentrations per mg of adipose in *knockouts* relative to *controls*.

Additionally, GLUT4 is the rate-limiting step in glucose metabolism at the level of the adipose tissue and skeletal muscle[144]. As a result, the expression and function of GLUT4 isoforms are of particular interest in *knockouts* since GLUT4 is tightly regulated by insulin at the mRNA and protein levels[144]. Enhanced metabolic demand is often associated with adaptive

increases in GLUT4 expression, however the occurrence of T2DM, aging, obesity, and metabolic syndrome, often presents with dysregulation of GLUT4 expression and function[144]. Therefore, gene and protein expression of GLUT4 in the different adipose depots of mice could shed light on metabolic differences between the depots at the different time point studied.

Although the pancreas and skeletal muscle play integral roles in the regulation of glucose metabolism, completion of assessments in these two tissues were beyond the time constraints of this thesis and will be completed by others in our laboratory. The most important question to be addressed in the pancreas, is whether inhibition of LPA action would restore low fasting basal insulin to levels comparable to normoglycemic, normoinsulinemic, *controls*. This can be determined by treating *knockout* mice with an LPA inhibitor to confirm if LPA inhibition restores normoinsulinemia, since inhibition has already been shown to restore glucose disposal.

Skeletal muscle is the largest sink of glucose disposal in the body and requires further analysis in *RTSAKO* mice[144]. Assessment of GLUT4 expression in muscle at the three time points explored could indicate significant differences in the transcriptional regulation of this transporter. Since GLUT4 is positively regulated by insulin[144], low circulating levels may cause significantly lower expression in *knockouts*, impairing glucose entry into the skeletal muscle. Since the skeletal muscle is the primary glucose disposal site, this can significantly contribute to the dysglycemia characteristic of *knockouts*. Therefore, GLUT4 gene expression (qPCR) and protein abundance (immunoblotting) levels in *knockouts* in comparison to normoglycemic *controls* at the three time points can further aid in the characterization of the dysglycemic phenotype, and the contributions of important metabolic tissues, present in *RTSAKO*s.

The primary focus of the *RTSAKO* project thus far has been exploration of the dysglycemic phenotype present in males. However, female *knockouts* do not present with glucose intolerance at the same time-point. The sexual dimorphism in this model is especially important, as sex differences are similarly observed in the diagnosis of T2DM in humans[145]. Obesity, the predominant risk-factor in the onset of diabetes, is more common in women. Despite this, men at a lower relative age and body mass are more frequently diagnosed with diabetes then women[145]. There are many explanations for the delayed onset of diabetes in females relative to males, such as differences in sex hormones, body fat distribution, and in the case of humans, differences based on culture, socioeconomic status, and lifestyle[145]. Assessments of females at a later time point may reveal delayed dysglycemic onset in *knockouts* and requires

further study. Investigations could narrow down the biological factors that mediate the delayed onset of renal-steatosis-induced dysglycemia in females.

Since aging is an important correlative factor in the development of metabolic syndromes, studying aging *RTSAKO* mice could aid in understanding the impact of renal steatosis on the progression of dysglycemia in the elderly. Aging populations have the highest risk of developing chronic kidney disease and diabetes, as well as the worst prognosis in comparison to other groups[14]. Studies have shown that comorbidity of these conditions doubles mortality rates in the elderly, and so understanding the relationship between dysregulated kidney metabolism and dysglycemia in aging *RTSAKO* mice could elucidate mechanisms through which these rates can be ameliorated [14].

The greatest restriction in the progression of this research is the number of mice available for testing, which is the reason for the variability in sample size per experiment. A typical female mouse can birth between 5-10 litters per year, with each litter consisting of an average of 4 pups for good breeders[146]. Furthermore, gestation periods usually last 3 weeks, and mice must be aged-out before sacrifice at each time-point[146]. In addition, pups acquired are either *knockouts* or *controls*, and since genotype is randomly assigned at conception, attaining equal number of mice for each group is not always possible. Finally, not all mice birthed are used for experimentation since breeders are required. Female breeders can last 7-8 months, however using younger females increases breeding success[146]. Therefore, female and male breeders must be replaced every few months or once litter numbers start to decline (sexual maturation occurs ~6wks)[146].

In conclusion, this thesis aimed to characterize a series of gene and protein differences in the kidneys, livers, and adipose tissue of *RTSAKO* mice relative to their *control* littermates in order to better elucidate the phenotype associated with genetically induced kidney steatosis. Analysis at various time points aimed to better understand the progression of new-onset glucose intolerance in response to renal-tubule *Atgl*-ablation. Further investigations into the phenotype of female mice, as well as aging *RTSAKO* mice, are currently underway as separate projects. Data from this thesis will lay a foundation for continued investigation of the *RTSAKO* phenotype.

This thesis explored differences in gene expression and protein abundance in *knockouts* relative to normoglycemic *controls*, with the goal of characterizing the kidneys, livers, and adipose tissue, with an emphasis on illuminating the development of the dysglycemic phenotype in *RTSAKO*s. These findings are important preliminary steps in the complete characterization of this model and help inform future directions in this project.

References

1. Russo, G. T. *et al.* Diabetic kidney disease in the elderly: Prevalence and clinical correlates. *BMC Geriatr.* **18,** 1–11 (2018).
2. Ayodele, O. E. & Alebiosu, C. O. Burden of Chronic Kidney Disease: An International Perspective. *Adv. Chronic Kidney Dis.* **17,** 215–224 (2010).
3. Ritz, E., Rychlik, I., Locatelli, F. & Halimi, S. End-stage renal failure in type 2 diabetes: A medical catastrophe of worldwide dimensions. *Am. J. Kidney Dis.* **34,** 795–808 (1999).
4. Ettinger, S. Diabetic Nephropathy, Chronic Kidney Disease. *Nutr. Pathophysiol. Obes. its Comorbidities* 161–189 (2017). doi:10.1016/B978-0-12-803013-4.00007-7
5. Taylor, E. Facing the facts. *Airl. Bus.* **34,** 32–33 (2018).
6. Goldmannová, D. *et al.* Adipocytokines and new onset diabetes mellitus after transplantation. *J. Appl. Biomed.* (2018). doi:10.1016/j.jab.2018.05.005
7. Lim, C. C. *et al.* New onset Diabetes Mellitus among Patients with Glomerular diseases. *Intern. Med. J.* (2018). doi:10.1111/imj.13964
8. Juan Khong, M. & Chong, C. P. Prevention and management of new-onset diabetes mellitus in kidney transplantation. *Neth. J. Med.* **72,** 127–134 (2014).
9. Simonson, D. C. *Insulin Resistance and the Metabolic Syndrome in Chronic Renal Disease*. *Textbook of Nephro-Endocrinology* (Elsevier Inc., 2018). doi:10.1016/B978-0-12-803247-3.00015-5
10. Meyer, C. & Gerich, J. E. Role of the kidney in hyperglycemia in type 2 diabetes. *Curr. Diab. Rep.* **2,** 237–241 (2002).
11. Teta, D. Insulin resistance as a therapeutic target for chronic kidney disease. *J. Ren. Nutr.* **25,** 226–229 (2015).
12. Basile, J. A new approach to glucose control in type 2 diabetes: The role of kidney sodium-glucose co-transporter 2 inhibition. *Postgrad. Med.* **123,** 38–45 (2011).
13. Mithieux, G. *et al.* of Diabetic Rats. **288,** 1–19 (2008).
14. Williams, M. E. & Stanton, R. C. Chapter 8 : Kidney Disease in Elderly Diabetic Patients. 1–5 (2009).
15. Nitta, K., Okada, K., Yanai, M. & Takahashi, S. Aging and Chronic Kidney Disease. *Kidney Blood Press. Res.* **38,** 109–120 (2013).
16. Herman-Edelstein, M., Scherzer, P., Tobar, A., Levi, M. & Gafter, U. Altered renal lipid metabolism and renal lipid accumulation in human diabetic nephropathy. *J. Lipid Res.* **55,** 561–572 (2014).
17. Bobulescu, I. A. *et al.* Triglycerides in the human kidney cortex: Relationship with body size. *PLoS One* **9,** (2014).
18. Bobulescu, I. A. Renal lipid metabolism and lipotoxicity. *Curr. Opin. Nephrol. Hypertens.* **19,** 393–402 (2010).
19. Slawik, M. & Vidal-Puig, A. J. Lipotoxicity, overnutrition and energy metabolism in aging. *Ageing Res. Rev.* **5,** 144–164 (2006).
20. Jiang, T., Liebman, S. E., Lucia, M. S., Li, J. & Levi, M. Role of altered renal lipid metabolism and the sterol regulatory element binding proteins in the pathogenesis of age-related renal disease. *Kidney Int.* **68,** 2608–2620 (2005).
21. Jiang, T., Liebman, S. E., Lucia, M. S., Phillips, C. L. & Levi, M. Calorie Restriction Modulates Renal Expression of Sterol Regulatory Element Binding Proteins, Lipid Accumulation, and Age-Related Renal Disease. *J. Am. Soc. Nephrol.* **16,** 2385–2394 (2005).
22. Wang, Z. *et al.* Regulation of renal lipid metabolism, lipid accumulation, and glomerulosclerosis in FVBdb/db mice with type 2 diabetes. *Diabetes* **54,** 2328–2335 (2005).
23. Zager, R. A., Johnson, A. C. M. & Becker, K. Acute unilateral ischemic renal injury induces progressive renal inflammation , lipid accumulation , histone modification , and " end-stage "

kidney disease. 1334–1345 (2011). doi:10.1152/ajprenal.00431.2011.
24. Jiang, T. *et al.* Diet-induced obesity in C57BL/6J mice causes increased renal lipid accumulation and glomerulosclerosis via a sterol regulatory element-binding protein-1c-dependent pathway. *J. Biol. Chem.* **280,** 32317–32325 (2005).
25. Kume, S. *et al.* Role of Altered Renal Lipid Metabolism in the Development of Renal Injury Induced by a High-Fat Diet. *J. Am. Soc. Nephrol.* **18,** 2715–2723 (2007).
26. Stemmer, K. *et al.* High-fat-diet-induced obesity causes an inflammatory and tumor-promoting microenvironment in the rat kidney. *Dis. Model. Mech.* **5,** 627–635 (2012).
27. Igarashi, P. Kidney-specific gene targeting. *J. Am. Soc. Nephrol.* **15,** 2237–2239 (2004).
28. Haemmerle, G. *et al.* Triglyceride Lipase. **211,** 734–737 (2006).
29. Marvyn, P. M., Bradley, R. M., Button, E. B., Mardian, E. B. & Duncan, R. E. Fasting upregulates adipose triglyceride lipase and hormone-sensitive lipase levels and phosphorylation in mouse kidney. *Biochem. Cell Biol.* **93,** 262–7 (2015).
30. Weinberg, J. M. Lipotoxicity. *Kidney Int.* **70,** 1560–1566 (2006).
31. Lathey, R. K., Jackson, R. E., Bodenham, A., Harper, D. & Patle, V. Original Article. **55,** 1–7 (2017).
32. Schaffer, J. E. Lipotoxicity: When tissues overeat. *Curr. Opin. Lipidol.* **14,** 281–287 (2003).
33. Luk AO, So WY, Ma RC, Kong AP, Ozaki R, Ng VS, Yu LW, Lau WW, Yang X, Chow FC, Chan JC, T. P. H. K. D. R. Chronic Kidney Disease in 5 , 829 Patients A 5-year prospective analysis of the Hong Kong Diabetes Registry. *Diabetes Care* **31,** 2357–2361 (2008).
34. Virchow, R. Cellular pathology. As based upon physiological and pathological histology. *Philadelphia J. B. Lippincott* (1863). doi:10.5962/bhl.title.32770
35. Irazabal, M. V. & Eirin, A. Role of Renal Sinus Adipose Tissue in Obesity-induced Renal Injury. *EBioMedicine* **13,** 21–22 (2016).
36. Musso, G. *et al.* Fatty liver and chronic kidney disease: Novel mechanistic insights and therapeutic opportunities. *Diabetes Care* **39,** 1830–1845 (2016).
37. De Vries, A. P. J. *et al.* Fatty kidney: Emerging role of ectopic lipid in obesity-related renal disease. *Lancet Diabetes Endocrinol.* **2,** 417–426 (2014).
38. Cho, K. hyang, Kim, H. ju, Kamanna, V. S. & Vaziri, N. D. Niacin improves renal lipid metabolism and slows progression in chronic kidney disease. *Biochim. Biophys. Acta - Gen. Subj.* **1800,** 6–15 (2010).
39. Ahmadian, M. *et al.* Desnutrin/ATGL is regulated by AMPK and is required for a brown adipose phenotype. *Cell Metab.* (2011). doi:10.1016/j.cmet.2011.05.002
40. Attané, C. *et al.* A beta cell ATGL-lipolysis/adipose tissue axis controls energy homeostasis and body weight via insulin secretion in mice. *Diabetologia* (2016). doi:10.1007/s00125-016-4105-2
41. Peyot, M.-L. *et al.* Adipose Triglyceride Lipase Is Implicated in Fuel- and Non-fuel-stimulated Insulin Secretion. *J. Biol. Chem.* (2009). doi:10.1074/jbc.M109.006650
42. Duncan, R. E. & Jaworski, K. Triglycerol metabolism in adipose tissue. **2,** 229–237 (2009).
43. Duncan, R. E., Ahmadian, M., Jaworski, K., Sarkadi-Nagy, E. & Sul, H. S. Regulation of Lipolysis in Adipocytes. *Annu. Rev. Nutr.* **27,** 79–101 (2007).
44. Ahmadian, M., Wang, Y. & Sul, H. S. Lipolysis in adipocytes. *Int. J. Biochem. Cell Biol.* **42,** 555–559 (2010).
45. Eichmann, T. O. *et al.* Studies on the substrate and stereo/regioselectivity of adipose triglyceride lipase, hormone-sensitive lipase, and diacylglycerol-O- acyltransferases. *J. Biol. Chem.* **287,** 41446–41457 (2012).
46. Ahmadian, M. *et al.* Adipose overexpression of desnutrin promotes fatty acid use and attenuates diet-induced obesity. *Diabetes* (2009). doi:10.2337/db08-1644
47. Saltiel, A. R. & Kahn, C. R. Insulin signalling and the regulation of glucose and lipid metabolism. *Nature* **414,** 799–806 (2001).
48. Ali, A. T., Hochfeld, W. E., Myburgh, R. & Pepper, M. S. Adipocyte and adipogenesis. *Eur. J. Cell Biol.* **92,** 229–236 (2013).

49. Gustafson, B., Hedjazifar, S., Gogg, S., Hammarstedt, A. & Smith, U. Insulin resistance and impaired adipogenesis. *Trends Endocrinol. Metab.* **26,** 193–200 (2015).
50. Noguchi, K., Herr, D., Mutoh, T. & Chun, J. Lysophosphatidic acid (LPA) and its receptors. *Curr. Opin. Pharmacol.* **9,** 15–23 (2009).
51. Choi, J. W. *et al.* LPA Receptors: Subtypes and Biological Actions. *Annu. Rev. Pharmacol. Toxicol.* **50,** 157–186 (2010).
52. Yanagida, K. *et al.* Identification and characterization of a novel lysophosphatidic acid receptor, p2y5/LPA6. *J. Biol. Chem.* **284,** 17731–17741 (2009).
53. Ishii, I., Fukushima, N., Ye, X. & Chun, J. Lysophospholipid Receptors: Signaling and Biology. *Annu. Rev. Biochem.* **73,** 321–354 (2004).
54. Anliker, B. & Chun, J. Lysophospholipid G protein-coupled receptors. *J. Biol. Chem.* **279,** 20555–20558 (2004).
55. Mutoh, T., Rivera, R. & Chun, J. Insights into the pharmacological relevance of lysophospholipid receptors. *Br. J. Pharmacol.* **165,** 829–844 (2012).
56. Yung, Y. C., Stoddard, N. C. & Chun, J. *LPA receptor signaling: pharmacology, physiology, and pathophysiology*. *Journal of Lipid Research* **55,** (2014).
57. Rancoule, C. *et al.* Lysophosphatidic acid impairs glucose homeostasis and inhibits insulin secretion in high-fat diet obese mice. *Diabetologia* (2013). doi:10.1007/s00125-013-2891-3
58. Rancoule, C. *et al.* Depot-specific regulation of autotaxin with obesity in human adipose tissue. *J. Physiol. Biochem.* **68,** 635–644 (2012).
59. Rancoule, C. *et al.* Involvement of autotaxin/lysophosphatidic acid signaling in obesity and impaired glucose homeostasis. *Biochimie* **96,** 140–143 (2014).
60. Mirzoyan, K. *et al.* Increased urinary lysophosphatidic acid in mouse with subtotal nephrectomy: potential involvement in chronic kidney disease. *J. Physiol. Biochem.* **72,** 803–812 (2016).
61. Cersosimo, E., Garlick, P. & Ferretti, J. Renal substrate metabolism and gluconeogenesis during hypoglycemia in humans. *Diabetes* **49,** 1186–1193 (2000).
62. Silverthorn, D. U. *Human Physiology an integrated approach*. *Journal of Chemical Information and Modeling* **53,** (2013).
63. Gerich, J. E. Role of the kidney in normal glucose homeostasis and in the hyperglycaemia of diabetes mellitus: Therapeutic implications. *Diabet. Med.* **27,** 136–142 (2010).
64. van Schaftingen, E. & Gerin, I. The glucose-6-phosphatase system. *Biochem. J.* **362,** 513–32 (2002).
65. Meyer, C., Dostou, J., Nadkarni, V. & Gerich, J. Effects of physiological hyperinsulinemia on systemic, renal, and hepatic substrate metabolism. *Am. J. Physiol.* **275,** F915-21 (1998).
66. Meyer, C., Woerle, H. J., Dostou, J. M., Welle, S. L. & Gerich, J. E. Abnormal renal, hepatic, and muscle glucose metabolism following glucose ingestion in type 2 diabetes. *Am. J. Physiol. Metab.* **287,** E1049–E1056 (2004).
67. Cersosimo, E., Garlick, P. & Ferretti, J. Insulin regulation of renal glucose metabolism in humans. *Am. J. Physiol. Metab.* **276,** E78–E84 (1999).
68. Wilson, J. E. Isozymes of mammalian hexokinase: structure, subcellular localization and metabolic function. *J. Exp. Biol.* **206,** 2049–2057 (2003).
69. Smith, J. A., Stallons, L. J. & Schnellmann, R. G. Renal cortical hexokinase and pentose phosphate pathway activation through the EGFR/Akt signaling pathway in endotoxin-induced acute kidney injury. *AJP Ren. Physiol.* **307,** F435–F444 (2014).
70. John, S., Weiss, J. N. & Ribalet, B. Subcellular localization of hexokinases I and II directs the metabolic fate of glucose. *PLoS One* **6,** (2011).
71. Roberts, D. J. & Miyamoto, S. Hexokinase II integrates energy metabolism and cellular protection: Akting on mitochondria and TORCing to autophagy. *Cell Death Differ.* **22,** 248–257 (2015).
72. Wang, R. *et al.* Differential expressed genes of change in glucose metabolism in the liver of GCK knockout mice. *Gene* **516,** 248–254 (2013).

73. Mitrakou, A. Kidney: Its impact on glucose homeostasis and hormonal regulation. *Diabetes Res. Clin. Pract.* **93,** S66–S72 (2011).
74. Guebre-Egziabher, F. *et al.* Ectopic lipid accumulation: A potential cause for metabolic disturbances and a contributor to the alteration of kidney function. *Biochimie* **95,** 1971–1979 (2013).
75. Sears, B. & Perry, M. The role of fatty acids in insulin resistance. *Lipids Health Dis.* **14,** 1–9 (2015).
76. Rancoule, C. *et al.* Lysophosphatidic acid impairs glucose homeostasis and inhibits insulin secretion in high-fat diet obese mice. *Diabetologia* **56,** 1394–1402 (2013).
77. Yea, K. *et al.* Lysophosphatidic acid regulates blood glucose by stimulating myotube and adipocyte glucose uptake. *J. Mol. Med.* **86,** 211–220 (2008).
78. Jaworski, K., Sarkadi-Nagy, E., Duncan, R. E., Ahmadian, M. & Sul, H. S. Regulation of Triglyceride Metabolism.IV. Hormonal regulation of lipolysis in adipose tissue. *Am. J. Physiol. Liver Physiol.* (2007). doi:10.1152/ajpgi.00554.2006
79. Voet, D., Voet, J. & Pratt, C. *Fundamentals of Biochemistry: Life At The Molecular Level*. (Wiley and Sons, 2013).
80. KENNEDY, E. P. & WEISS, S. B. The function of cytidine coenzymes in the biosynthesis of phospholipides. *J. Biol. Chem.* (1956).
81. SMITH, S. W., WEISS, S. B. & KENNEDY, E. P. The enzymatic dephosphorylation of phosphatidic acids. *J. Biol. Chem.* (1957).
82. Carman, G. M. & Han, G.-S. Phosphatidic acid phosphatase, a key enzyme in the regulation of lipid synthesis. *J. Biol. Chem.* (2009). doi:10.1074/jbc.R800059200
83. Kume, K. & Shimizu, T. cDNA cloning and expression of murine 1-acyl-sn-glycerol-3-phosphate acyltransferase. *Biochem. Biophys. Res. Commun.* (1997). doi:10.1006/bbrc.1997.7214
84. Kuge, O. & Nishijima, M. Phosphatidylserine synthase I and II of mammalian cells. *Biochimica et Biophysica Acta - Lipids and Lipid Metabolism* (1997). doi:10.1016/S0005-2760(97)00137-9
85. Jin, K., Norris, K. & Vaziri, N. D. Dysregulation of hepatic fatty acid metabolism in chronic kidney disease. *Nephrol. Dial. Transplant.* **28,** 313–320 (2013).
86. Blue, M. L., Williams, D. L., Zucker, S., Khan, S. A. & Blum, C. B. Apolipoprotein E synthesis in human kidney, adrenal gland, and liver. *Proc. Natl. Acad. Sci. U. S. A.* (1983). doi:10.1073/pnas.80.1.283
87. Ruiz, R. *et al.* Sterol regulatory element-binding protein-1 (SREBP-1) is required to regulate glycogen synthesis and gluconeogenic gene expression in mouse liver. *J. Biol. Chem.* (2014). doi:10.1074/jbc.M113.541110
88. Ferry, G. *et al.* Autotaxin is released from adipocytes, catalyzes lysophosphatidic acid synthesis, and activates preadipocyte proliferation. Up-regulated expression with adipocyte differentiation and obesity. *J. Biol. Chem.* **278,** 18162–18169 (2003).
89. D'Souza, K., Paramel, G. V. & Kienesberger, P. C. Lysophosphatidic acid signaling in obesity and insulin resistance. *Nutrients* **10,** 10–15 (2018).
90. Dusaulcy, R. *et al.* Altered food consumption in mice lacking lysophosphatidic acid receptor-1. *J. Physiol. Biochem.* **65,** 345–350 (2009).
91. Boucher, J. *et al.* Potential involvement of adipocyte insulin resistance in obesity-associated up-regulation of adipocyte lysophospholipase D/autotaxin expression. *Diabetologia* **48,** 569–577 (2005).
92. Simon, M. F. *et al.* Lysophosphatidic acid inhibits adipocyte differentiation via lysophosphatidic acid 1 receptor-dependent down-regulation of peroxisome proliferator-activated receptor γ2. *J. Biol. Chem.* **280,** 14656–14662 (2005).
93. Nobusue, H., Kondo, D., Yamamoto, M. & Kano, K. Effects of lysophosphatidic acid on the in vitro proliferation and differentiation of a novel porcine preadipocyte cell line. *Comp. Biochem. Physiol. - B Biochem. Mol. Biol.* **157,** 401–407 (2010).
94. Abu El-Asrar, A. M. *et al.* Expression of lysophosphatidic acid, autotaxin and acylglycerol kinase

as biomarkers in diabetic retinopathy. *Acta Diabetol.* (2013). doi:10.1007/s00592-012-0422-1
95. Klemm, D. J. *et al.* Insulin-induced adipocyte differentiation: Activation of CREB rescues adipogenesis from the arrest caused by inhibition of prenylation. *J. Biol. Chem.* (2001). doi:10.1074/jbc.M103382200
96. Valet, P. *et al.* Alpha2-adrenergic receptor-mediated release of lysophosphatidic acid by adipocytes. A paracrine signal for preadipocyte growth. *J. Clin. Invest.* **101,** 1431–1438 (1998).
97. Accili, D. & Taylor, S. I. Targeted inactivation of the insulin receptor gene in mouse 3T3-L1 fibroblasts via homologous recombination. *Proc. Natl. Acad. Sci.* (1991). doi:10.1073/pnas.88.11.4708
98. Rosen, E. D. The transcriptional basis of adipocyte development. in *Prostaglandins Leukotrienes and Essential Fatty Acids* (2005). doi:10.1016/j.plefa.2005.04.004
99. Takeda, H. *et al.* PI 3-kinase gamma and protein kinase C-zeta mediate RAS-independent activation of MAP kinase by a Gi protein-coupled receptor. *EMBO J.* (1999). doi:10.1093/emboj/18.2.386
100. Ishii, I., Fukushima, N., Ye, X. & Chun, J. L YSOPHOSPHOLIPID R ECEPTORS : Signaling and Biology. *Annu. Rev. Biochem.* (2004). doi:10.1146/annurev.biochem.73.011303.073731
101. Chun, J., Hla, T., Lynch, K. R., Spiegel, S. & Moolenaar, W. H. International Union of Basic and Clinical Pharmacology. LXXVIII. Lysophospholipid Receptor Nomenclature. *Pharmacol. Rev.* (2010). doi:10.1124/pr.110.003111
102. Pagès, C., Simon, M.-F., Valet, P. & Saulnier-Blache, J. S. Lysophosphatidic acid synthesis and release. *Prostaglandins Other Lipid Mediat.* **64,** 1–10 (2001).
103. Aoki, J., Inoue, A. & Okudaira, S. Two pathways for lysophosphatidic acid production. *Biochim. Biophys. Acta - Mol. Cell Biol. Lipids* **1781,** 513–518 (2008).
104. Xu, A. *et al.* Overexpression of autotaxin is associated with human renal cell carcinoma and bladder carcinoma and their progression. *Med. Oncol.* **33,** 1–8 (2016).
105. Shimizu, M. *et al.* Serum Autotaxin Levels Are Associated with Proteinuria and Kidney Lesions in Japanese Type 2 Diabetic Patients with Biopsy-proven Diabetic Nephropathy. *Intern. Med.* **55,** 215–221 (2016).
106. Sato, Y. *et al.* Distinct 1-monoacylglycerol and 2-monoacylglycerol kinase activities of diacylglycerol kinase isozymes. *Biochim. Biophys. Acta - Proteins Proteomics* **1864,** 1170–1176 (2016).
107. Abu El-Asrar, A. M. *et al.* Expression of lysophosphatidic acid, autotaxin and acylglycerol kinase as biomarkers in diabetic retinopathy. *Acta Diabetol.* **50,** 363–371 (2013).
108. Jaworski, K., Sarkadi-Nagy, E., Duncan, R. E., Ahmadian, M. & Sul, H. S. Regulation of Triglyceride Metabolism.IV. Hormonal regulation of lipolysis in adipose tissue. *Am. J. Physiol. Liver Physiol.* **293,** G1–G4 (2007).
109. Ozaltin, F. *et al.* DGKE Variants Cause a Glomerular Microangiopathy That Mimics Membranoproliferative GN. *J. Am. Soc. Nephrol.* **24,** 377–384 (2013).
110. Tang, T. *et al.* Desnutrin/ATGL activates PPARδ to promote mitochondrial function for insulin secretion in islet β cells. *Cell Metab.* (2013). doi:10.1016/j.cmet.2013.10.012
111. Sackmann-Sala, L., Berryman, D. E., Munn, R. D., Lubbers, E. R. & Kopchick, J. J. Heterogeneity among white adipose tissue depots in male C57BL/6J mice. *Obesity* (2012). doi:10.1038/oby.2011.235
112. Rodriguez-Lazaro, D. & Hernandez, M. Real-time PCR in Food Science: Introduction. *Curr. Issues Mol. Biol.* (2013).
113. Reid, B. N. *et al.* Hepatic overexpression of hormone-sensitive lipase and adipose triglyceride lipase promotes fatty acid oxidation, stimulates direct release of free fatty acids, and ameliorates steatosis. *J. Biol. Chem.* **283,** 13087–13099 (2008).
114. Igarashi, P. *et al.* Ksp-cadherin gene promoter. II. Kidney-specific activity in transgenic mice. *Am. J. Physiol.* (1999).
115. Mubbunu, L., Bowa, K., Petrenko, V. & Silitongo, M. Correlation of Internal Organ Weights with

Body Weight and Body Height in Normal Adult Zambians : A Case Study of Ndola Teaching Hospital. **2018,** (2018).
116. Bryson, J. M., Coy, P. E., Gottlob, K., Hay, N. & Brooks Robey, R. Increased hexokinase activity, of either ectopic or endogenous origin, protects renal epithelial cells against acute oxidant-induced cell death. *J. Biol. Chem.* **277,** 11392–11400 (2002).
117. Gaidhu, M. P. *et al.* Prolonged AICAR-induced AMP-kinase activation promotes energy dissipation in white adipocytes: novel mechanisms integrating HSL and ATGL. *J. Lipid Res.* **50,** 704–715 (2009).
118. Daval, M. *et al.* Anti-lipolytic action of AMP-activated protein kinase in rodent adipocytes. *J. Biol. Chem.* **280,** 25250–25257 (2005).
119. Yen, C.-L. E., Stone, S. J., Koliwad, S., Harris, C. & Farese, R. V. *Thematic Review Series: Glycerolipids.* DGAT enzymes and triacylglycerol biosynthesis. *J. Lipid Res.* **49,** 2283–2301 (2008).
120. Sul, H. S., Latasa, M., Moon, Y. & Kim, K. Symposium : The Role of Long Chain Fatty Acyl-CoAs as Signaling Molecules in Cellular Metabolism Regulation of the Fatty Acid Synthase Promoter by Insulin 1 , 2. 315–320 (2000).
121. Manmontri, B. *et al.* Glucocorticoids and cyclic AMP selectively increase hepatic lipin-1 expression, and insulin acts antagonistically. *J. Lipid Res.* **49,** 1056–1067 (2008).
122. Reue, K. & Dwyer, J. R. Lipin proteins and metabolic homeostasis. *J. Lipid Res.* **50,** S109–S114 (2009).
123. Harris, T. E. *et al.* Insulin controls subcellular localization and multisite phosphorylation of the phosphatidic acid phosphatase, lipin 1. *J. Biol. Chem.* **282,** 277–286 (2007).
124. Zhang, P., O'Loughlin, L., Brindley, D. N. & Reue, K. Regulation of lipin-1 gene expression by glucocorticoids during adipogenesis. *J. Lipid Res.* **49,** 1519–1528 (2008).
125. Clark, J. M. & Diehl, A. M. Hepatic steatosis and type 2 diabetes mellitus. *Curr Diab Rep* **2,** 210–215 (2002).
126. Sheedfar, F. *et al.* Increased hepatic CD36 expression with age is associated with enhanced susceptibility to nonalcoholic fatty liver disease. *Aging (Albany. NY).* **6,** 281–295 (2014).
127. Kershaw, E. E. *et al.* Adipose triglyceride lipase: function, regulation by insulin, and comparison with adiponutrin. *Diabetes* **55,** 148–57 (2006).
128. Holmström, T. E. *et al.* Non-transactivational, dual pathways for LPA-induced Erk1/2 activation in primary cultures of brown pre-adipocytes. *Exp. Cell Res.* **316,** 2664–2675 (2010).
129. Bhatt, H. B. & Smith, R. J. Fatty liver disease in diabetes mellitus. *Hepatobiliary Surg. Nutr.* **4,** 101–8 (2015).
130. Bjørndal, B., Burri, L., Staalesen, V., Skorve, J. & Berge, R. K. Different adipose depots: Their role in the development of metabolic syndrome and mitochondrial response to hypolipidemic agents. *J. Obes.* **2011,** (2011).
131. Wronska, A. *et al.* White Adipose Tissue Depot-Specific Activity of Lipogenic Enzymes in Response to Fasting and Refeeding in Young and Old Rats. *Gerontology* **61,** 448–455 (2015).
132. Villena, J. A., Roy, S., Sarkadi-Nagy, E., Kim, K. H. & Hei, S. S. Desnutrin, an adipocyte gene encoding a novel patatin domain-containing protein, is induced by fasting and glucocorticoids: Ectopic expression of desnutrin increases triglyceride hydrolysis. *J. Biol. Chem.* (2004). doi:10.1074/jbc.M403855200
133. Passaro, A. *et al.* Gene expression regional differences in human subcutaneous adipose tissue. *BMC Genomics* **18,** 1–11 (2017).
134. Pagès, C. *et al.* LPA as a paracrine mediator of adipocyte growth and function. *Ann. N. Y. Acad. Sci.* **905,** 159–164 (2000).
135. Cinti, S. The adipose organ. *Prostaglandins Leukot. Essent. Fat. Acids* **73,** 9–15 (2005).
136. Ix, J. H. & Sharma, K. Mechanisms Linking Obesity, Chronic Kidney Disease, and Fatty Liver Disease: The Roles of Fetuin-A, Adiponectin, and AMPK. *J. Am. Soc. Nephrol.* **21,** 406–412 (2010).

137. Dusaulcy, R. *et al.* Adipose-specific disruption of autotaxin enhances nutritional fattening and reduces plasma lysophosphatidic acid. *J. Lipid Res.* **52,** 1247–1255 (2011).
138. Furuhashi, M., Saitoh, S., Shimamoto, K. & Miura, T. Fatty acid-binding protein 4 (FABP4): Pathophysiological insights and potent clinical biomarker of metabolic and cardiovascular diseases. *Clin. Med. Insights Cardiol.* **2014,** 23–33 (2014).
139. Ramji, D. P. & Foka, P. CCAAT/enhancer-binding proteins: structure, function and regulation. *Biochem. J.* **365,** 561–75 (2002).
140. McIntyre, T. M. *et al.* Identification of an intracellular receptor for lysophosphatidic acid (LPA): LPA is a transcellular PPAR agonist. *Proc. Natl. Acad. Sci.* **100,** 131–136 (2003).
141. Wang, Y., Kim, K.-A., Kim, J.-H. & Sul, H. S. Pref-1, a Preadipocyte Secreted Factor That Inhibits Adipogenesis. *Jounal Nutr.* **136,** 2953–2956 (2006).
142. Zhang, N. *et al.* Inhibition of lipid signaling enzyme diacylglycerol kinase ε attenuates mutant huntingtin toxicity. *J. Biol. Chem.* **287,** 21204–21213 (2012).
143. Musso, G. *et al.* Emerging Liver-Kidney Interactions in Nonalcoholic Fatty Liver Disease. *Trends Mol. Med.* **21,** 645–662 (2015).
144. Karnieli, E. & Armoni, M. Transcriptional regulation of the insulin-responsive glucose transporter GLUT4 gene: from physiology to pathology. *Am. J. Physiol. Metab.* **295,** E38–E45 (2008).
145. Kautzky-Willer, A., Harreiter, J. & Pacini, G. Sex and gender differences in risk, pathophysiology and complications of type 2 diabetes mellitus. *Endocr. Rev.* **37,** 278–316 (2016).
146. Manual, R. Breeding Strategies for Maintaining Colonies of Laboratory Mice. *Jackson Labs* (2007).